1-1-2012

Fracture Energy, Fatigue and Creep Properties of Engineered Cementitious Composites Incorporating Fly Ash/Slag with Different Aggregates

Mohamed A. Sherir
Ryerson University

FRACTURE ENERGY, FATIGUE AND CREEP PROPERTIES OF ENGINEERED CEMENTITIOUS COMPOSITES INCORPORATING FLY ASH/SLAG WITH DIFFERENT AGGREGATES

By

Mohamed A A Sherir

B.Sc. Degree in Civil Engineering, Islamic University of Gaza, Gaza 2001

A Thesis

Presented to Ryerson University

In the partial fulfillment of the degree of

Master of Applied Science

(Civil Engineering)

Toronto, Ontario, Canada, 2012

AUTHOR'S DECLARATION

I hereby declare that I am the sole author of this thesis.

I authorize Ryerson University to lend this thesis to other institutions or individuals for the purpose of scholarly research.

I further authorize Ryerson University to reproduce thus project or by photocopying or by other means, in total or in part, at the request of other institutions or other individuals for the purpose of scholarly research.

FRACTURE ENERGY, FATIGUE AND CREEP PROPERTIES OF ENGINEERED CEMENTITIOUS COMPOSITES INCORPORATING FLY ASH/SLAG WITH DIFFERENT AGGREGATES

Mohamed A A Sherir

Master of Applied Science, Civil Engineering

Ryerson University, Toronto, Canada, 2012

ABSTRACT

This thesis investigates the influence of microsilica sand and local crushed sand, and different supplementary cementing materials on the mechanical properties of engineered cementitious composites (ECCs). ECC is a special type of high performance fiber reinforced cementitious composite with high ductility which exhibits strain-hardening and multiple-cracking behaviours in tension. The use of local aggregates in ECC production can lower its cost to mitigate the obstacles of wider commercial use.

The experimental results showed that multiple-cracking behaviour was developed under fatigue loading for fly ash ECC (FA-ECC) mixtures, and the number of cracks was lower at both lower fatigue stress level and higher fatigue number of cycles. FA-ECC mixtures with silica sand exhibited higher deflection evolution under fatigue loading than FA-ECC mixtures with crushed sand. Based on the experimental results on link slab specimens, both FA-ECC mixtures with silica and crushed sands exhibited almost the same creep behaviour.

Acknowledgments

I would like to express my deepest gratitude to my supervisors, Dr. Mohamed Lachemi and Dr. Khandaker M. Anwar Hossain, for their guidance, support and patience during the development of this thesis. During my years at Ryerson they have been there for me without hesitation.

I would like to thank Dr. Hossain for willingness to always help along with patience, kind words, inspiration and belief in me, which pulled me through this thesis. His countless proof readings, corrections and support made this document possible.

This research project was funded by the Ministry of Transportation of Ontario Highway Infrastructure Innovations Funding Program. Their collaboration and financial support are highly appreciated. From the Ministry of Transportation of Ontario, we would like to thank Hanna Schell, David Rhead and Clifford Lam.

Thanks and appreciations to our industrial partners for their guidance, support and in-kind donations throughout the duration of this research project. We would like to thank Lafarge Canada and St. Marys Cement for their support. Special thanks for Dr. Abdurrahmaan Lotfy and Mr. Wafiq Taha for their assistance.

This research work was conducted at the Concrete Materials Laboratory and Structural Laboratory of Ryerson University's Department of Civil Engineering. The support received from many people at Ryerson made this project successful. We would like to thank, all lab technologists for their assistance and support.

I would like to thank my parents for their support during this project. I am grateful for their care and love.

Finally, special gratitude goes to my beloved wife, Heba Abuzour. Without her constant love and sacrifice, my success would not be possible.

Dedicated To My Wife & My Children

Table of Contents

List of Figures

List of Tables

LIST OF SYMBOLS/ABBREVIATIONS

ECC	Engineered cementitious composite
SCC	Self-consolidating concrete
HPFRCC	High performance fiber reinforced cementitious composites
FRC	Fiber reinforced concrete
F	Fly ash class F
CI	Fly ash class CI
SL	Slag
C	Portland cement
SS	Silica sand
CS	Crushed sand
SCMs	Supplementary cementing materials
A/B	Aggregate to binder ratio,
PVA	Polyvinyl alcohol fiber
PE	Polyethylene fiber
HRWRA	High range water reducing admixture
SP	Superplasticizer
σ_o	Maximum fiber-bridging capacity
σ_{fc}	First cracking strength
δ_o	Crack opening corresponding to σ_0
δ_{ss}	Steady-state flat-crack propagation
$\sigma(\delta)$	Fiber bridging relationship
J_{tip}	Crack tip matrix toughness (fracture energy of the matrix)
$J_{b'}$	Complementary energy
K_m	Matrix fracture toughness
G_F	Fracture energy
E_m	Young's modulus
$\int_0^{\delta_{max}} F(\delta)d\delta$	Area under the curve
A_{lig}	Cross-sectional area of the ligament, above the notch
MOR	Flexural strength (modulus of rupture)
LVDT	Linear variable displacement transducer
T_{50}	Time flow of workability
FA-ECC	ECC mixture incorporating fly ash
SL-ECC	ECC mixture incorporating slag
S-N Curve	Fatigue stress to fatigue life number of cycles relationship

CHAPTER ONE

INTRODUCTION

1.1 General

For decades, normal cementitious materials have proven to be a suitable material in infrastructure constructions and have been successfully implemented in numerous projects around the world. However, the deteriorating condition of the infrastructure in North America and elsewhere due to inherently brittle failure resulting from tensile and impact loading in such cementitious materials has motivated authorities and researchers to seek new technology for enhancement of concrete material properties. Therefore, polymeric fibers were employed as a reinforcing material in cementitious materials. The main use of fiber in cementitious materials is for the sake of enhancing the resistance and toughness in tension and shear. The contribution of fiber reinforcement to construction materials can be traced back to the beginning of human civilisation when horsehair or straw were mixed into the mud for bricks and straw mats were used for housing construction in the Far East 4000 years ago. Modern fiber reinforced cementitious materials have been analysed since 1960's (Gao and Zijl, 2005).

In the last decade, a new type of composite called Engineered Cementitious Composite (ECC) has been developed. ECC is a special type of high performance fiber-reinforced cementitious composite featuring high ductility and damage tolerance under mechanical loading, including tensile and shear loadings (Li, 1997; Li et al., 2001; Li, 2003). By employing micromechanics-based material optimization, tensile strain capacity in excess of 3% under uniaxial tensile loading can be attained with only 2% fiber content by volume (Li, 1997; Lin and Li, 1997; Lin et al., 1999). The characteristic strain hardening after matrix first cracking is accompanied by sequential development of multiple microcracking and the tensile strain capacity is 300-500 times greater than that of normal concrete. The formation of multiple micro cracking is necessary to achieve high composite tensile ductility. Even at ultimate load, the crack width remains on the order of 50 to 80 micrometer. This tight crack

width is self-controlled and, whether the composite is used in combination with conventional reinforcement or not, it is a material characteristic independent of rebar reinforcement ratio.

In contrast, normal concrete and fiber reinforced concrete (FRC) rely on steel reinforcement for crack width control. By suppressing cracks in the presence of large imposed structural deformations, ECC can offer structural durability improvements in addition to water-tightness and other serviceability enhancements. These properties, together with a relative ease of production including self-consolidation casting (Kong et al., 2003a; Kong et al., 2003b) and shotcreting (Kim et al., 2003), make ECCs suitable for various civil engineering applications. Currently, self-consolidating ECC is emerging in full scale structural applications (Lepech and Li, 2007). The ingredients and mix proportions of ECC are optimized through micromechanics based material design theory to satisfy strength and energy criteria to attain high composite tensile ductility (Li, 1997; Li et al., 2001; Li, 2003; Yang and Li, 2006). The type, size and amount of fiber, matrix ingredients and interface characteristics are tailored for multiple cracking and controlled crack width in ECCs.

Aggregates typically occupy an important volume fraction in conventional concrete, and thus have important effects on different aspects of material properties. In addition to their role as economic filler, aggregates help to control dimensional stability of cement-based materials, which may be considered to consist of a framework of cement paste with relatively large shrinkage movements restrained by aggregates. However, the presence of coarse aggregates in a paste tends to increase the tortuosity of the fracture path, and lead to a tough matrix which delays crack initiation and prevents steady-state flat-crack propagation in ECC, resulting in loss of tensile ductility. Moreover, the introduction of aggregates with a particle size larger than the average fiber spacing leads to balling and greater interaction of fibers between the large aggregate particles, and the effect becomes more pronounced as the maximum size of aggregate particles increase. Therefore, an increase in aggregate size makes it more difficult to achieve a uniform dispersion of fibers. The greater the size of aggregates, the more clumping and interaction of fibers would occur. Therefore, the size of the aggregates is expected to have a significant influence on the properties of composite. Hence, in spite of positive effects of aggregates on dimensional stability and economy of

fiber reinforced cement composites, there are limits on aggregate size beyond which problems with fiber dispersability, fresh mix workability and matrix toughness may start to damage the composite material performance characteristics.

Therefore, instead of coarse aggregate, standard ECC incorporates fine aggregate with an aggregate to binder ratio (A/B) of 0.36 to maintain adequate stiffness and volume stability (Li et al., 1995). The binder system is defined as the total amount of cementitious material, i.e. cement and SCMs, generally FA, in ECC. The silica sand has a maximum grain size of 250 μm and a mean size of 110 μm. Another purpose of using fine silica sand is to obtain the optimum gradation of particles to produce good workability (Fischer and Li, 2003).

Due to environmental and economic reasons, there is a growing trend to use industrial wastes or by-products as supplementary materials or admixtures in the production of cementitious composite. Among the various supplementary materials, FA and SL are the most commonly available SCMs. Because of several potential benefits, fly ash and slag have increasingly found use in high performance concrete in the last few decades (Mehta, 1985).

In the past few decades, substitution of SCMs, such as FA and SL, has been of great interest and gradually applied to practical applications of ECC (Kim et al., 2004a; Kim et al., 2007; Wang and Li, 2007; Yang et al., 2007; Zhou et al., 2009). FA is a by-product of the coal power plant, whereas SL is a by-product in the manufacture of pig iron. Both of these waste materials from industrial processes are usually available in large quantities and at a fraction of the price of cement. The absence of coarse aggregate in ECC results in a higher cement content. Partial replacement using FA or SL reduces the environmental burden. Further, it has been found that incorporating high amount of FA, especially Class F fly ash, can reduce the matrix toughness and improve the robustness of ECC in terms of tensile ductility. Additionally, un-hydrated FA particles with small particle size and smooth spherical shape serve as filler particles resulting in higher compactness of the fiber/matrix interface transition zone that leads to a higher frictional bonding. This aids in reducing the steady-state crack width beneficial for long-term durability (Lepech and Li, 2005a; Lepech and Li, 2005b; Wang and Li, 2007; Yang et al., 2007) of the structure.

Since the increase in aggregate size leads to an increase in the matrix toughness while the use of SCMs leads to reduce the matrix toughness, locally available aggregate could successfully be used in conjunction with high volume SCMs in the production of ECC. Very limited information is currently available in the published literature revealing the influence of aggregate size on the performance (ductility and mechanical behaviour) of ECC. Accordingly, one of the current research goals is to design a new class of ECCs with a matrix incorporating locally available aggregates that can show similar mechanical properties compared to standard ECC mixtures containing microsilica sand.

1.2 Research Significance

Rehabilitation of bridge structures damaged by continuous wear, as well as time-dependent and environmental effects is a major concern for a large number of reinforced concrete and prestressed concrete bridge structures. Every year, in North America, billions of dollars are spent to repair and maintenance bridges. As bridge structures ages, cost of repairs and maintenance magnifies. The poor durability of concrete bridges throughout Canada is an increasingly large concern for highway transportation authorities. With decreasing budget allocations for infrastructure maintenance, rehabilitation, and replacement, the need for greater durability is apparent. The leaking expansion joints are a major source of deterioration of multi-span bridges in Canada. Expansion joints can be replaced by flexible link slabs made with ECC forming a joint less multi-span bridge and hence, solving the problem of premature deterioration (Caner and Zia, 1998; Hossain et al., 2012b).

The use of ECC and its application to link slab in bridge construction is an emerging technology and still, very little research has been conducted (Caner and Zia, 1998). Research studies showed significant enhancement of ductility and crack width control in ECC link slabs confirming that the use of ECC can be effective in extending the service life of bridge deck systems. Lack of research studies especially in Canada warrants extensive research investigations on various aspects such as: optimization of ECC mix design parameters, short/long term mechanical/durability properties of ECC and structural performance of ECC based link slab. The full understanding of the behaviour of ECC material is very important for this new technology to be adopted in bridge and other types of structures.

1.3 Research Objectives and Scope

The main objective of the current research is to explore the development of greener ECCs and analyze the mechanical properties (such as compressive and flexural strengths, fracture energy, fatigue loading performance and creep behavior) of ECCs for construction with particular reference to link slab applications in bridge decks.

The study explores experimental methods and testing procedures for mechanical properties of ECC and other concretes. The effect of mix design parameters such as size/type of aggregate namely silica sand (SS) and local crushed sand (CS), and amount/type of supplementary cementing materials (SCMs) such as (FA class CI, FA class F and SL) content on ECC properties mentioned above is analysed based on extensive experiments to identify/select best ECC mixtures for link slab applications.

Consequently, the best ECC mix design is employed to cast small-scale model link slab specimens to evaluate the performance under sustained loading (long-term creep) compared to its conventional self-consolidating concrete counterpart. Such test results facilitate to develop guidelines for ECC mix proportioning and testing methods. Such guidelines will help local concrete industry to select and manufacture cost-effective and greener ECC mixes especially for link slab applications.

1.4 Thesis outline

Chapter 1 introduces engineered cementitious composite (ECC) in general and describes objectives, scope and significance of the research. In Chapter 2, the background of ECC, the role of materials in ECC (fibers and pozzolanic materials such as FA class CI, F and SL) mechanical properties, applications and the cost of ECC are discussed. In Chapter 3, the experimental program, materials properties and tests on mechanical properties of ECC are discussed. The results of the experimental studies are presented and discussed in Chapter 4. The conclusions of the research and recommendations for future research studies are presented in Chapter 5.

CHAPTER TWO

LITERATURE REVIEW AND BACKGROUND

2.1 Introduction

Civil infrastructure including buildings, bridges, roadways, tunnels, dams and airfield pavements, may be subjected to multi-hazards such as earthquakes, fires, storm surges, winds, projectiles and blast loading. Protection from catastrophic failures of infrastructure due to such extreme loadings cannot be assured even though with many decades of research in structural design and materials development. This is illustrated by events such as the 1995 Alfred Murrah Federal Building bombing, the 1994 Northridge Earthquake in California and the 2005 Hurricane Katrina in the Gulf of Mexico.

The development of high-strength concrete over the last several decades has given hope for stronger structures. However, there is also increasing aknowlegment that when a certain level of compressive strength is reached, the failure of a structure or structural element will be dominated by brittle fracture in tension. This recognition has led to an expansion of materials property development towards tensile ductility in recent years. This development may provide a rational basis to support the construction of new infrastructure and the rehabilitation of existing infrastructure for enhanced against multi-hazards.

As a result, the need to develop cost-effective high ductility cementitious materials suitable for structural applications is essential. In the last several years, many investigations have been done to a composite material known as Engineered Cementitious Composites (ECC). In many respects, this material has characteristics similar to medium to high strength concrete but with different development approach (Li, 2011; Li and Kanda, 1998).

The design approach behind ECC is significantly different from that behind ultra high strength concrete. The most fundamental principle of designing ultra high strength concrete is the tight packing of particles, leaving as little void as possible in the hardened composite.

This approach results in a delay of cracks growing when the material has defects and extends the strength and stiffness of the concrete. This delay in crack initiation is a result of both smaller defect sizes and higher essential matrix toughness, in accordance with fracture mechanics. However, once a crack grows, its propagation is unstable and results in a high composite brittleness. The addition of fibers reduces this brittleness, making the material usable in a structural member. On the other hand, this class of material shows tension softening responses when tested under uniaxial tensile loading, with a strain capacity no more than 0.2 percent.

ECC is designed based on the micromechanics of crack initiation, fiber bridging and steady-state flat-crack propagation (Maalej and Li, 1994; Lin and Li, 1997; Li et al., 2002) in a brittle matrix reinforced with randomly distributed short fibers. By carefully allowing cracks to form at a tensile stress just below the fiber-bridging capacity (for example, before fiber-bridging capacity is exhausted via fiber pull-out or rupture), and by controlling the crack width through the crack propagation mode (flat-crack versus Griffith-type crack), ECC has the ability to undergo tensile strain hardening response accompanied with non-catastrophic damage in the form of multiple crack formation.

2.2 Engineered Cementitious Composite (ECC)

As a special type of High Performance Fiber Reinforced Cementitious Composites (HPFRCC), ECC is a fiber reinforced cement based composite material (Li, 1998; Li, 2003; Li et al., 2001) that has been systematically engineered to achieve high ductility under tensile and shear loading. The most distinctive characteristic separating ECC from conventional concrete and fiber reinforced concrete (FRC) is an ultimate tensile strain capacity between 3 to 5%, depending on the specific ECC mixture. This strain capacity is realized through the formation of many closely spaced micro cracks, allowing for a strain capacity over 300 times than that of normal concrete. These cracks, which carry increasing load after formation, allow the material to exhibit strain hardening, similar to many ductile metals.

Although the components of ECC may be similar to FRC, the distinctive ECC characteristic of strain hardening through micro cracking is achieved through micromechanical tailoring of

the components (i.e. cement, aggregate, and fibers) (Li, 1998; Lin et al., 1999), along with the control of the interfacial properties between components. Fracture properties of the cementitious matrix are carefully controlled through mix proportions. Fiber properties, such as strength, modulus of elasticity, and aspect ratio have been customized for use in ECC. The interfacial properties between fiber and matrix have also been optimized in cooperation with the manufacturer for use in this material. Typical mix proportions of ECC using a polyvinyl alcohol (PVA) fiber are given in Table 2.1. All proportions are given with materials in the dry state.

Table 2.1 Engineered cementitious composite typical mix design proportions (Nawy, 2008)

Cement	Fly Ash	Sand	Water	(HRWRA)*	Fiber (Vol. %)
1.0	1.2	0.8	0.56	0.012	0.02

* High-Range Water Reducer Admixture

While most HPFRCCs rely on a high fiber volume to achieve high performance, ECC uses low amounts, typically 2% by volume, of short, discontinuous fiber which is greater than the calculated critical fiber content required to achieve strain hardening. This low fiber volume along with the common components, allows flexibility in construction execution. Various fiber types have been used in the production of ECC. Typical ECC mixtures use polyvinyl alcohol (PVA). The PVA fiber is surface coated by an oil agent (1.2% by weight) to reduce the fiber/matrix interfacial bonding. The mix design described in Table 2.1 has been experimentally demonstrated in a broad range of investigations to consistently produce good ECC fresh and hardened properties. Adaptations of this reference mix have been used in various construction projects. Full-scale production of ECC was carried out in Japan (Kunieda and Rokugo, 2006) and in the United States (Lepech and Li, 2007). Experience in concrete ready-mix plants suggests the charging sequence of raw material shown in Table 2.2.

Table 2.2 Material charging sequence into ready-mix trucks (Nawy, 2008)

Activity No.	Activity	Elapsed Time (min)
1	Charge all sand.	2
2	Charge approximately 90–95% of mixing water, all HRWR, all hydration stabilizers.	2
3	Charge all fly ash.	2
4	Charge all cement.	2
5	Charge remaining mixing water to wash drum fins.	4
6	Mix at high RPM for 5 minutes or until material is homogenous.	5
7	Charge fibers.	2
8	Mix at high RPM for 5 minutes or until material is homogenous.	5
	Total	24

Currently, ECC is designed for several types of engineered applications, other than ECC large-scale on site construction applications, ECC is designed for high-early-strength ECC applications that require rapid strength gain to quickly reopened transportation to the motorist public (Wang and Li, 2006a), Lightweight ECC applications to minimize the dead load of structural members (Wang and Li, 2003), Green ECC applications to maximize material greenness and infrastructure sustainability (Lepech et al., 2007; Li et al., 2004) and Self-healing ECC applications to heal cracks after experiencing damages (Li and Yang, 2007; Yang et al., 2005). Although the design of ECC is involved in different types of construction applications, the development of ECC is still evolving and even broader ranges of ECC properties beyond those which have developed in the literature can be expected in the future as the need arises.

Figure 2.1 shows a typical uniaxial tensile stress-strain curve of ECC containing 2% PVA fiber (Weimann and Li, 2003). The characteristic strain hardening after first cracking is accompanied by multiple micro cracking. The crack width development during inelastic straining is also shown in Figure 2.1. Even at ultimate load, the crack width remains less than about 80 μm. Unlike normal concrete or FRC, the steady-state crack width is an intrinsic material property, independent of loading (tension, bending, or shear) and steel reinforcement type and amount. This observation has important implications in service life, economics, and architectural aesthetics. In short, where steel reinforcement is used to control

crack width in concrete, such steel reinforcement can be completely eliminated in ECC. Under severe bending loads, an ECC beam deforms similar to a ductile metal plate through plastic deformation (Figure 2.2), hence the nickname of ECC is “bendable concrete” (Li, 2011). In compression, ECC materials exhibit compressive strengths similar to high strength concrete (e.g. greater than 60 MPa) (Lepech and Li, 2007).

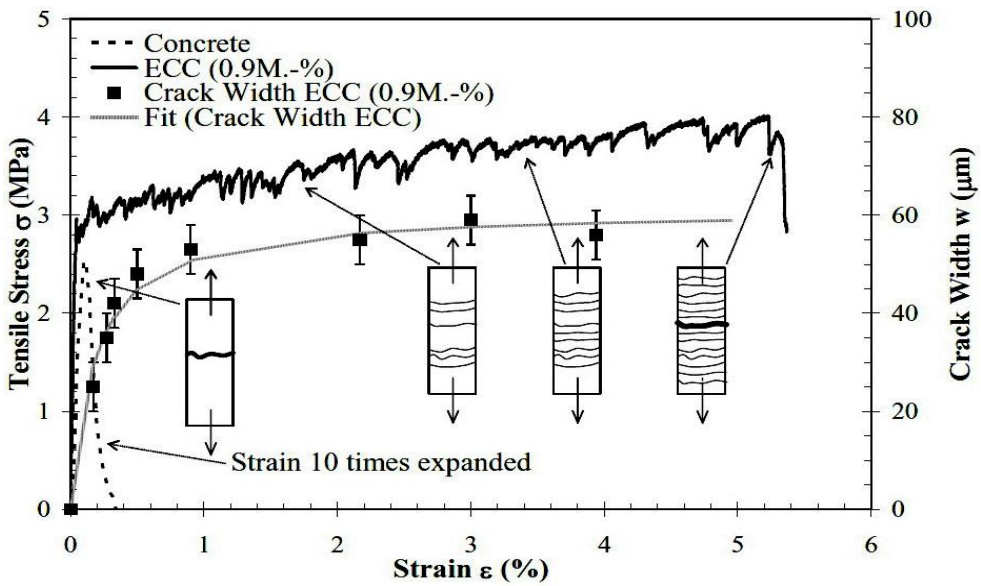

Figure 2.1 Typical tensile stress-strain curve and crack width development of ECC (Weimann and Li, 2003)

Figure 2.2 Extreme flexing capabilities of ECC under a large bending load (Li, 2011)

2.3 ECC Material Design Considerations

To understand the fundamental mechanisms governing strain hardening ECC behavior versus tension softening FRC behavior, it is necessary to recognize the load bearing and energy absorption roles of fiber bridging. Kanda and Li (1998) suggested two important complementary requirements to achieve strain hardening ECC behavior. The first is first cracking stress criterion which defined as strength criterion and the second is steady-state cracking criterion which defined as fracture energy criterion. Both conditions are necessary for multiple cracking and expressed as shown in Equation 2.1;

Strength criterion

$$\sigma_0 > \sigma_{fc} \tag{2.1a}$$

Fracture energy criterion

$$J_b^{'} = \sigma_o \delta_o - \int_0^{\delta_o} \sigma(\delta) d\delta \geq J_{tip} \approx \frac{K_m^2}{E_m} \tag{2.1b}$$

where σ_{fc} and σ_0 are the first cracking strength and maximum fiber-bridging capacity on each potential crack plane; δ_0 is the crack opening corresponding to σ_0 in the fiber bridging relationship $\sigma(\delta)$, which goes through a maximum; J_{tip} and $J_{b'}$ are the crack tip matrix toughness and the complementary energy of the fiber-bridging relation, respectively; and K_m and E_m are the matrix fracture toughness and Young's modulus, respectively (Nawy, 2008).

As shown in Figure 2.3, the strength criterion (Equation 2.1a) ensures the initiation of micro cracks from initial flaw sites in the composite before the tensile load exceeds the maximum fiber-bridging capacity. Ensuring that the maximum fiber-bridging capacities on existing crack planes remain higher than the first matrix cracking strength of potential new crack planes allows additional cracks to form; otherwise, saturated multiple cracking would not be attained, and sparsely spaced cracks will result, limiting the tensile ductility.

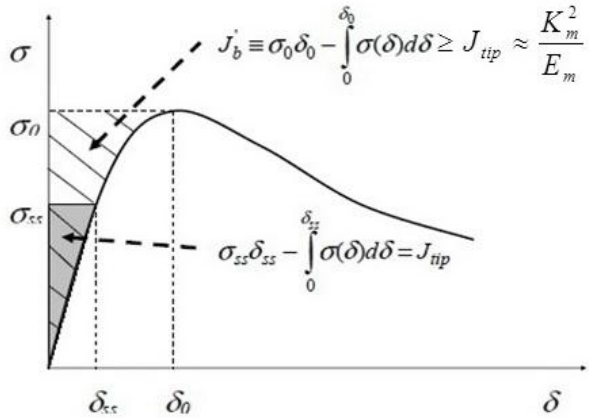

Figure 2.3 Typical σ(δ) curve for tensile strain-hardening composite (Yang and Li, 2006)

The fracture energy criterion (Equation 2.1b) prescribes the mode of crack propagation once initiated. The normal form of Griffith-type cracks is not favorable to multiple cracking. This is because the crack opening in Griffith-type cracks always widen during propagation as in typical tension softening fiber reinforced cementitious materials. The only means of preventing this is by altering the Griffith-type crack propagation mode to a steady-state flat-crack propagation mode (δ_{ss}), as in the case of ECC materials. In ECC case, the crack extends while the crack opening remains constant at any location regardless of the length of the crack. In this manner, δ_{ss} stays below δ_0 along the entire crack line. During flat-crack propagation, energy is exchanged between external applied loading and energy absorbed by the fiber-bridging process in the opening of the crack which leads to the enforcement of energy balance results in (Equation 2.1b). Violation of Equation 2.1b results in fracture localization, as in the case of FRC, and terminates the multiple crack process.

It should be noted that both parts of Equation 2.1 have been arranged so the left-hand sides of the inequality sign contain terms that pertain to fiber and interface properties, while the right-hand sides contain terms that pertain to matrix properties, all of which are measurable physical properties. This observation emphasizes the usefulness of Equation 2.1 to aid in the fiber, matrix, and interface selection or tailoring process to arrive at viable compositions of ECCs (Nawy, 2008).

It could be concluded that the strength and energy criteria must be considered to ensure adequate initiation of multiple cracks, and that cracks initiated propagate in the steady-state flat-cracking mode, in order to achieve saturated multiple cracking so that a robust ductile composite is assured (Yang and Li, 2006).

Once an ECC mixture is selected which sufficiently meets the two above criteria, the formation of multiple steady-state cracks, and strain hardening performance, can be realized. However, in addition to forming these cracks, the material must be designed to show crack widths below than 100 μm threshold limit which is usually prescribed (Reinhardt and Jooss, 2003; Sahmaran et al., 2009). In order to let ECC material exhibits multiple cracking and strain hardening performance, maximum crack opening δ_o should be kept below the 100 μm threshold limit.

2.4 The Role of Materials in ECC

The development of ECC from FRC was made by tailoring the properties of fibers, matrix, and interface between fiber and matrix. The way to tailor matrix and interface in ECC is to optimise the materials used in the mix, such as fibers, supplementary cementitious materials as cement replacement, and graded sand content resulting in the development of the matrix and fiber/matrix interface. Therefore, the composite failure type will convert from brittle to ductile failure. The roles of fibers, cement replacement materials are very important in ECC behaviour and will be introduced below.

2.4.1 The Role of Fiber in ECC

The high cost of high performance fiber such as polyethylene (PE) fiber limits the commercial applications. The relatively higher strength and higher modulus of Poly vinyl alcohol (PVA) fiber than those of other low cost fibers, such as Nylon and polypropylene fibers, showed PVA fiber to be most suitable alternative for ECC.

The most important role of fiber mixed into brittle matrix is to enhance its toughness, which needs the fiber to carry tensile load after the matrix has cracked. This process can occur

through fiber-bridging function which is the basic property of fiber reinforced material. Fiber-bridging provides closing traction to a crack and transfers stresses across the crack (JCI-DFRCC Committee, 2003). Lower chemical bonding between fiber and matrix, is always preferable to outweigh the chemical bond easily. Once the low chemical bond is overcome, not all resistance will be lost, which enabling fiber/matrix slippage accompanied with continuing transfer stresses through fibers to slowdown the effect of external loads applied and to maintain equilibrium between transferred stresses and external loads (JCI-DFRCC Committee, 2003; Gao and Zijl, 2005).

2.4.2 Pozzolanic Material

The Greeks, pre-400BC, followed by the Romans, were the first civilisations to use pozzolanas in lime mortars. The Romans used not only crushed pottery, bricks and tiles that formed the first artificial pozzolanas, but also found that some volcanic soils were excellent for producing a hydraulic mortar when mixed with lime. A hydraulic mortar or concrete is one which will set and harden under water. One such soil was found close to the town of Pozzuoli, near Naples in Italy-hence the name pozzolana or pozzolan.

More recently, over 100,000 tonnes of pozzolana was used in the construction of the Los Angeles aqueduct from 1910 to 1912. Since then, pozzolanas have been used in the construction of many mass concrete and marine structures such as dams and harbours, particularly in Europe, North America and Japan (Ruskulis and Otto, 2005).

According to ASTM C 618 (2012) , a more formal definition describes pozzolana as “a siliceous or siliceous and aluminous material, which in itself possesses little or no cementitious value but will, in finely divided form and in the presence of moisture, chemically react with calcium hydroxide at ordinary temperatures to form compounds possessing cementitious properties” (Neville, 2002). In simple words, a pozzolana is a material which, when combined with calcium hydroxide, exhibits cementitious properties. Pozzolanic materials are supplementary cementitious materials (SCMs) and commonly used as an addition to Portland cement concrete mixtures. Some of the most used materials are ground granulated blast furnace slag (hereafter denoted as slag), fly ash, condensed silica

fume, volcanic materials, rice husk ash, metakaolin etc. (Hossain, 2005; 2003; 2004; 2012a; Hassan et al., 2012; Karahan et al., 2012). When properly used as a portion of the cementitious material, these pozzolanic admixtures can improve the properties of the fresh and hardened concrete and in some cases reduce the material cost of concrete. Although several types of supplementary cementitious materials exist, the focus of this review will be on the two types used in this study, namely slag and fly ash. A brief overview of the history, properties, and the role of slag and fly ash as well in ECC is presented in the following sections.

2.4.2.1 Fly Ash

Fly ash, known also as pulverized fuel ash, is probably the pozzolana in greatest use globally today. In 1976, it was estimated that some 30 million tonnes were used annually and that the annual increase in usage was about ten per cent. It is the residue from the combustion of pulverized coal in power stations and is essentially a waste material (Ruskulis and Otto, 2005). During combustion process the fused material cools and solidifies to form the spherical fly ash particles. Typical particle size of fly ash is around 20 microns but may range from one micron up to as large as 100 microns. Specific surface of fly ash is usually between 250-600 m^2/kg. The high specific surface of the fly ash means that the material is readily available for reaction with calcium hydroxide (Neville, 2002).

According to the American Society for Testing and Materials (ASTM), there are two classes of fly ash (Table 2.3), high calcium class C, which is normally produced from sub-bituminous coals and low calcium class F, which is normally produced from bituminous coals. Class C fly ashes differ from class F fly ashes in that they are self-hardening even without the presence of cement (ASTM C 618, 2012).

Table 2.3 Specifications for fly ash (ASTM C 618, 2012)

Class of Ash	ASTM Specification
Class C	$SiO_2 + Al_2O_3 + Fe_2O_3 > 50\%$
Class F	$SiO_2 + Al_2O_3 + Fe_2O_3 > 70\%$

The use of fly ash in ECC mixtures as a cement replacement provided a reduction of fiber/matrix interfacial bond and then result in reduction of crack tip toughness. Peled and Shah (2003) reported that FA enhance fiber pull-out but reduce the composite strength, the composite flexural stress may reduce 50% when 70% cement was replace by fly ash (Peled and Shah, 2003). Furthermore, it is revealed that a high volume of fly ash tends to reduce fiber/matrix interface bond and matrix toughness in favor of attaining high tensile strain capacity (Wang and Li, 2007; Sahmaran et al., 2009). Micromechanics analysis indicates that the increase of fiber/matrix interface frictional bond in high volume fly ash ECCs mixtures is responsible for the tight crack width and show a robustness improvement by achieving more saturated multiple cracking (Yang et al., 2007).

2.4.2.2 Granulated Blastfurnace Slag (Slag)

Slag has been used as a partial replacement for Portland cement in concrete projects in the United States for over a century. Earlier usage of slag cement in Europe and elsewhere demonstrates that long-term concrete performance is enhanced in many ways. Based on these early experiences, modern designers have found that these improved durability characteristics help further reduce life-cycle costs, lower maintenance costs and makes concrete more sustainable.

Slag is a waste product in the manufacture of pig iron, about 300 kg of slag being produced for each tonne of pig iron. Chemically, slag is a mixture of lime, silica and alumina which has the same oxides that make up Portland cement but not in the same proportions. Slag can produce a cementitious material in different ways. Firstly, slag can be used together with limestone as a raw material. When slag mixed with limestone powder as partial replacement for Portland cement, limestone is usually considered as an inert filler material. The incorporation of limestone powder with Portland cement has many advantages on early compressive strength, durability and workability (Zhou et al., 2009). Secondly, grinding slag to an appropriate fineness and then used on its own as a cementitious material. Thirdly and as in the most countries, by mixing both Portland cement and slag together resulted in Portland blastfurnace cement (Neville, 2002). When slag mixed with Portland cement, it

accelerates the hydration of Portland cement and reacts with the calcium hydroxide, one of the hydration products of Portland cement. Although the addition of slag results in a lower strength at early ages, the replacement of Portland cement by slag, up to 70%, does not have any negative effect on the compressive strength of concrete after 28 days. The addition of slag can improve the durability of concrete and results in a more homogeneous fiber distribution, because slag particles provide a driving force for fiber dispersion.

It is found that the contribution of optimized range of slag ECC mixture proportions to fiber dispersion outweigh the side-effect of decreased potential for saturated multiple cracking, including a slight increase in matrix fracture toughness and fiber/matrix bond strength (Kim et al., 2007). The use of limestone powder and slag together as cement replacement in ECC mixtures exhibits high tensile strain capacity of 3.3%, a tight crack width of 57 μm and a moderate compressive strength of 38 MPa (Zhou et al., 2009). Compressive strength development of slag concrete shows slower initial strength development for up to about 3 days, but will increase noticeably more than normal concrete after seven days. The rapid strength development of slag concrete makes it advantageous for structural applications (Alexander et al., 2003).

2.5 Mechanical Properties of ECC

2.5.1 Fatigue Flexure

Although there are many studies reporting the improvement in mechanical properties and the failure mechanisms of ECCs under static loading conditions, there have been very few studies that reveal its properties and failure mechanisms under fatigue loading conditions. The first attempt to investigate fatigue behavior and properties of ECC was done by Matsumoto (1998). There were mainly two objectives of the research since ECC has never been tested under fatigue loading. First, the failure mode and its associated mechanisms of ECC in fatigue had to be identified. Second, fatigue strength and life had to be measured and the results were compared to plain concrete and fiber reinforced concrete in the conventional stress to number of cycles (S-N) diagram. According to macroscopic and microscopic observations, the test results confirmed that polyethylene fiber ECC mixtures (PE-ECC)

exhibited multiple crack formation even under fatigue loading, but failed by major crack fracture due to fiber fatigue rupture. Furthermore, there were not enough data for constructing a S-N curve of PE-ECC because only one specimen at each load level was tested. In addition, Suthiwarapirak et al. (2004) investigated the flexural fatigue characteristics of shotcreted ECC repair materials containing PVA fibers. The test results exhibited a unique fatigue stress–life relationship that is represented by a bilinear function on a semi-logarithmic scale which is similar in shape of metal fatigue fracture. The failure mechanism of ECCs involved the development of multiple cracks, and the number of cracks was higher when the fatigue stress level was higher (Suthiwarapirak et al., 2004). Similar advantages in the fatigue resistance of ECC have also been found in comparison to polymer cement mortars (Suthiwarapirak et al., 2002). The performance of ECC has been investigated in high fatigue scenarios, such as rigid pavement overlay rehabilitation. In these overlay applications; reflective cracking through the new overlay is of greatest concern. Existing cracks and locally reduced load capacity in the substrate pavement can result in flexural fatigue within the overlay structure. To evaluate ECC performance as a rigid pavement overlay material, both ECC/concrete and concrete/concrete overlay specimens were tested in flexural fatigue (Zhang and Li, 2002). Test results show that the load capacity of ECC/concrete overlay specimens was double that of concrete/concrete overlay specimens, the deformability of ECC/concrete specimens was significantly higher, and the fatigue life was extended by several orders of magnitude. Further, the micro cracking deformation mechanism of ECC effectively eliminated reflective cracking. Qian and Li (2008) investigated the performance of jointed ECC pavement material as an alternative to jointed normal plain concrete pavement material (JPCP). While JPCP has been extensively used in highway construction due to the wide availability of concrete materials, brittle fracture failure due to repeated loadings remains the major limitation to its durability and service life. Test results showed that the use of ECC materials as an alternate to normal pavement materials arrested such failure mode and greatly enhances its long term durability performance. The ECC specimens totally eliminate the single fracture mode in concrete by developing extensive micro cracks under flexural fatigue loading. Moreover, fatigue resistance of ECC for repair of viaducts subjected to train loading was studied by Inaguma et

al. (2005). In fatigue-prone concrete infrastructure, the application of ECC materials may be able to significantly lengthen service-life, reduce maintenance events, and life cycle costs.

2.5.2 Long-term Creep

The performance of ECC material has been investigated by Rouse and Billington (2007) to study the ability of using such materials in hinge regions of segmentally precast, post-tensioned concrete bridge piers. In such applications, the ECC segments would be subjected to considerable long-term compressive loads. It was expected that large creep strains are likely to occur due to the post-tensioning and because the ECC contains no coarse aggregate. Therefore, a series of experiments on ECC specimens, as well as similar specimens without fibers, were conducted to provide information about shrinkage and creep of the material. Based on the experimental results, it was found that the ECC material developed greater creep strains than a similar cementitious mixture without fiber reinforcement. Crack openings on the surface of shrinkage specimens without fibers were found to be over 2.5 times that of the corresponding specimens with fibers (ECC). Furthermore, the addition of fine aggregate in ECC can significantly reduce creep and shrinkage of the material. Similar larger response in creep strains of concrete specimens reinforced with small amounts of steel or polypropylene fibers have been found in comparison to specimens without fibers (Balaguru and Ramakrishnan, 1988; Houde et al., 1987).

2.5.3 Fracture Energy

Since there is no information for fracture energy experiments that have been conducted on ECC material in the published literature, the author used the general information for fracture energy available to the normal concrete.

The development of fracture mechanics for concrete was slow as compared to other structural materials. Linear elastic fracture mechanics theory was developed in 1920 by A.A. Griffith, but it was not until 1961 that the first experimental research in concrete was conducted by (Kaplan, 1961). Fracture mechanics had been applied successfully to design metallic and brittle materials for many years; however, comparatively few applications were

found for concrete. This trend continued up until the middle of 1970s when major advances were finally made. Throughout the last two decades, intensive research has been performed and applications of fracture mechanics in the design of beams, anchorage, and large dams are becoming more common. When compared to other structural theories, fracture mechanics is not yet as mature a theory (Mehta and Monteiro, 2006).

In the field of fracture mechanics, two parameters, G_F and K_m, are very important. G_F, called the fracture energy, is defined as the amount of energy required to create a crack of one unit of area while K_m, called the fracture toughness, is defined as a measure of the magnitude of the stress concentration which exists in front of the crack tip when the crack starts to propagate (Mehta and Monteiro, 2006). Fracture energy G_F and fracture toughness K_m have been found to be fracture mechanics parameters which are material properties to describe the resisting properties of concrete to cracking.

The first experimental research on fracture mechanics of concrete was performed by (Kaplan, 1961). Experimental test results indicated that the fracture toughness increases with increasing aggregate volume, maximum aggregate size and roughness of the aggregate while the toughness decreases with increasing water/cement ratio and increasing air content. One of the problems encountered in the early stages of this research was that, instead of being a material property, the value of the fracture toughness, K_m, was strongly influenced by the size of the specimen tested. It soon became apparent that fracture mechanics measurements should not be made on small concrete specimens. To overcome this problem, the fracture energy of concrete G_F is generally determined experimentally by using a notched specimen loaded in flexure, according to RILEM Recommendation TC-50 FMC (Mehta and Monteiro, 2006). The value of G_F is obtained by computing the area under the load deflection relationship and dividing it by the net cross section of the specimen above the notch. This method is called the direct method for determining the fracture energy and it allows much smaller specimens to be used in the fracture energy tests (Bazant, 1979).

2.6 Applications of ECC

To illustrate the performance of ECC in real world applications, a number of recent/ongoing projects involving the use of ECC are briefly highlighted.

Members made of ECC in combination with steel plates provide higher flexural resistance with a thinner cross section than normal steel-concrete members. Figure 2.4 shows the Mihara Bridge in Hokkaido, Japan with a bridge length of 972 m and central span of 340 m (Mitamura et al., 2005). In 2004, half the depth of the asphalt overlay on the steel deck of this bridge was replaced with 40 mm thick ECC to increase the load bearing capacity and stiffness of the decks while reducing the stress generated, thereby improving the fatigue resistance of the stiffener for the steel deck. This became necessary because the requirements for fatigue resistance in the standard specifications were revised while the bridge was under construction. The bridge was opened to traffic in 2005. The steel-reinforced road bed contains nearly 800 m^3 of ECC material. The tensile ductility and tight crack control behavior of ECC led to a 40% reduction in material used during construction.

Figure 2.4 Overview of Mihara Bridge (Mitamura et al., 2005)

Figure 2.5 shows the repair of the Mitaka Dam in Hiroshima-Prefecture, Japan in 2003 (Kojima et al., 2004). This dam is over 60 years old, with a severely damaged concrete surface. Cracks, spalling, and water leakage were concerns that prompted the use of ECC as

a water-tight cover layer. This 20 mm layer was applied by spraying the ECC material directly onto approximately 600 m^2 of the upstream dam surface.

Figure 2.5 Spray repair of the Mitaka Dam with ECC for water-proofing (Kojima et al., 2004)

A gravity concrete retaining wall in Gifu, Japan measuring approximately 18 m in width and 5 m in height was constructed in the 1970s. It was repaired using ECC in 2003 (Rokugo et al., 2005) as shown in Figure 2.6. Ordinary Portland cement could not be used due to the severity of the cracking in the original structure, which would have caused reflective cracking. ECC was intended to minimize this danger; after one year only micro cracks of tolerable width were observed. Cracking was harder to observe 24 months after repair compared to 12 months after, being hidden by dirt accumulated on the surface.

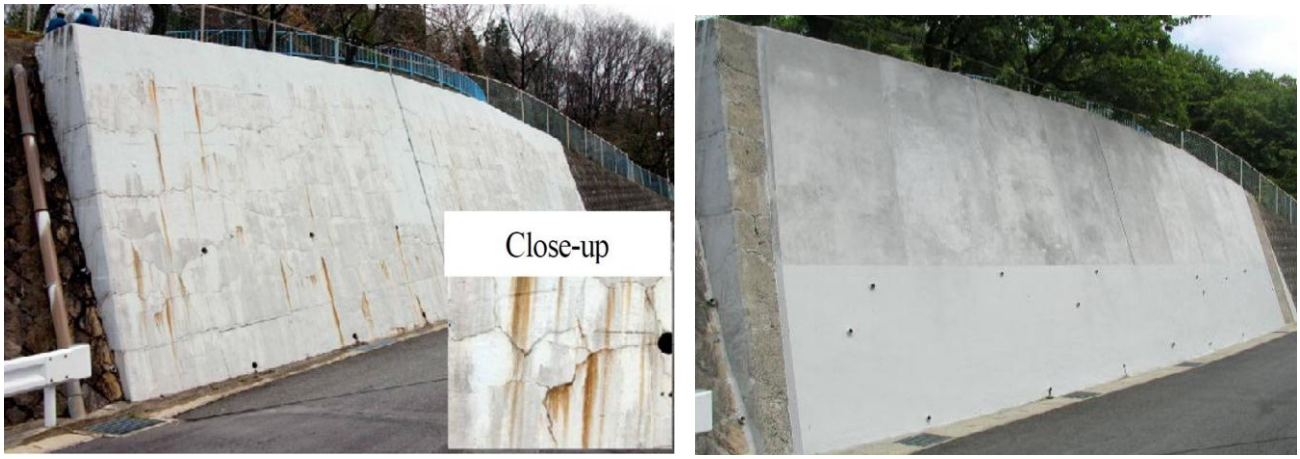

(a) Before repair (b) After repair

Figure 2.6 Surface repair of concrete retaining wall (Rokugo et al., 2005)

As one of the first field applications of ECC in the USA, an ECC patch repair Figure 2.7(a) placed on the deck of the Curtis Road Bridge in Michigan, US in 2002. A complete summary of this work has been outlined by Li and Lepech (2004). During this work, one small section of a deteriorated bridge deck was repaired with ECC while the remaining portion was repaired with a commercial concrete patching material commonly used by the Michigan Department of Transportation (MDOT). This repair scenario allowed for a unique ECC/concrete comparison subjected to identical environmental and traffic loads. As of the time of this writing, ECC patch and surrounding concrete have experienced almost three full winter freeze-thaw cycles. This bridge is traveled by heavily loaded 11-axle trucks. Figure 2.7(b) shows the monitored maximum crack width as a function of age. It reveals that the crack width in the ECC patch remains almost at a constantly low level, around 50 μm, while the maximum crack width in the surrounding concrete is significantly higher at the same age. The last data point at 780 days after repair indicates a maximum crack width of 3.8 mm in the concrete.

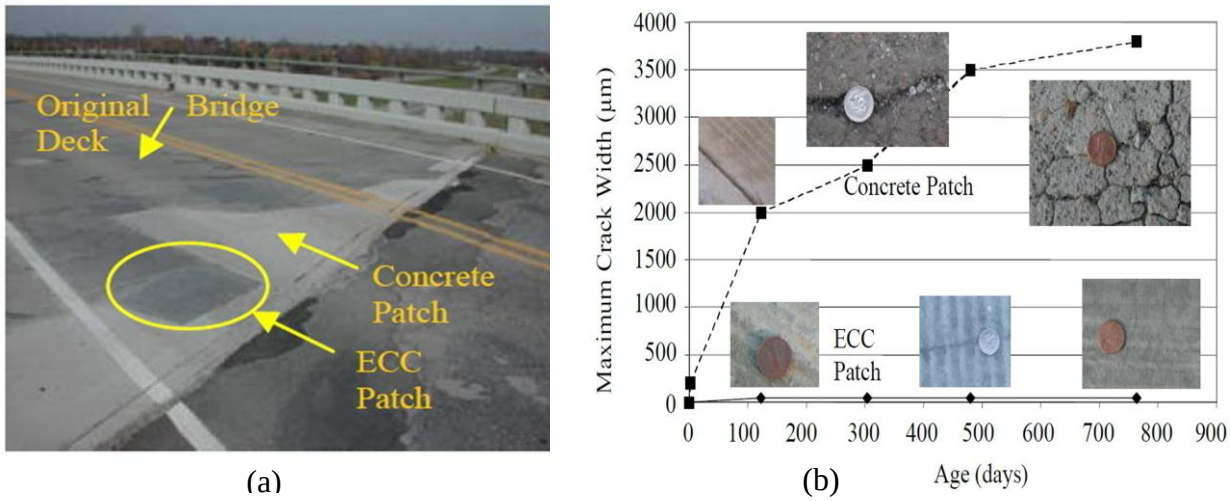

(a) (b)

Figure 2.7 (a) Patch repair on a bridge deck. (b) Crack width development in concrete patch and ECC patch over time (Li and Lepech, 2004)

In addition to bridge deck patching repairs, the most recent field application of ECC in the US is with a bridge "link slab" completed in cooperation with MDOT on Grove Street Bridge in Southeast Michigan in 2005 as shown in Figure 2.8 (Lepech and Li, 2007). The objective was to eliminate the maintenance requirements associated with typical bridge deck expansion joints. In this project, about 32 m^3 of ECC were cast in place using standard ready-mix concrete trucks to build the first ECC link slab in US. With a strain capacity exceeding 2%, these composites can be used to replace traditional steel expansion devices and can fully accommodate the thermal deformations of adjacent bridge spans. This ECC link slab design was adopted in 2006 in the highway segment that extends from Bolzano to the Austrian border bridge in north Italy.

Also in Japan ECC has been used in structural applications as coupling beams (Maruta et al., 2005) within high rise concrete construction. Due to the high energy absorption capacity of steel reinforced ECC material, the application of this material in coupling beams which connect adjacent core walls is very advantageous for high rise buildings in seismic regions. The recent development of precast ECC coupling beam elements by Kajima Corporation in Japan can be easily integrated into current seismic construction practices. Currently two high-rise buildings in Tokyo, Japan have been built integrating ECC coupling beams, Figure 2.9.

(a) During construction (b) After construction

Figure 2.8 ECC link slab on Grove Street Bridge, Michigan, USA (Lepech and Li, 2007)

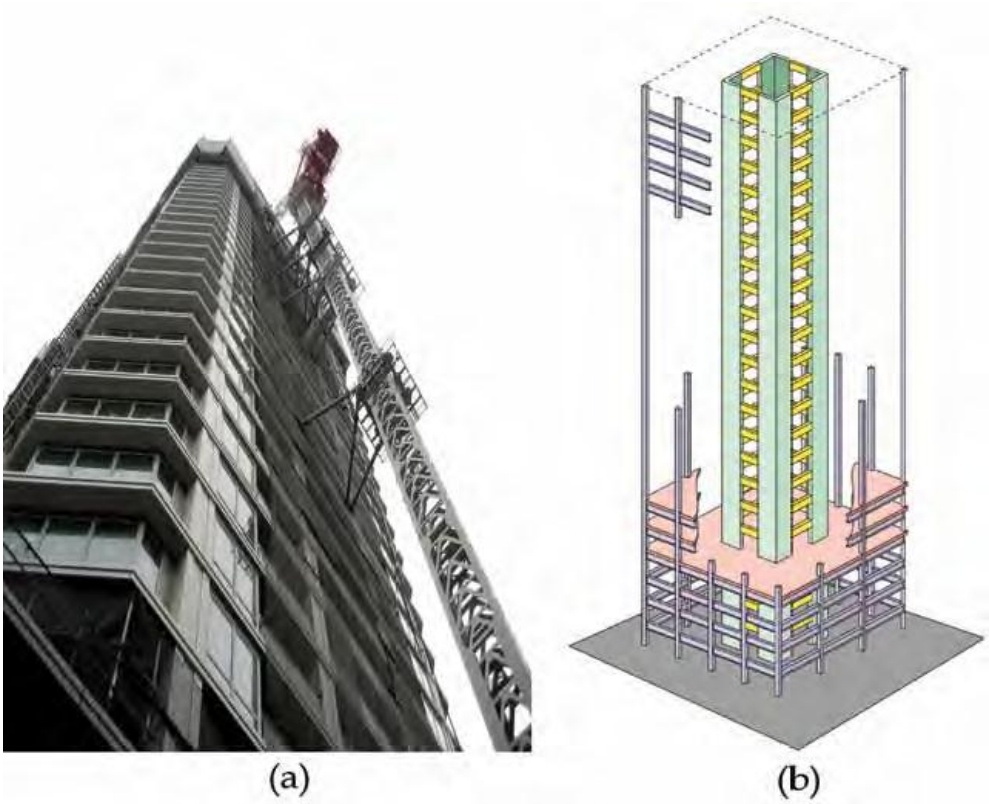

Figure 2.9 (a) The Nabeaure Tower in Yokohoma, Japan under construction, it uses precast ECC coupling beams in building core for seismic resistance and (b) Schematics showing coupling beams (in yellow) on each floor (Maruta et al., 2005).

2.7 Link Slab Bridge Decks

2.7.1 General

It was common practice before the 1970's to design multiple-span bridges as single-span structures, which were simply supported on piers and then connected by mechanical joints or paved-over joints at the pier locations Figure 2.10. While this system provided a simple and effective structural solution, it brought along a range of maintenance issues that have compromised the durability of many of these structures. Historically, bridge joints have never performed up to design expectations (Lam et al., 2008). A mechanical joint is typically employed at the end of the simple span deck to allow deck deformations imposed by girder deflection, concrete shrinkage, and temperature variations as shown in Figure 2.11. It is well known that bridge deck joints are expensive to install and maintain. Deterioration of joint functionality due to debris accumulation can lead to severe damage in the bridge deck and substructure. The durability of beam ends, girder bearings, and supporting structures can be compromised by water leakage and flow of deicing chemicals through the joints. Figure 2.12 shows the typical damage in mechanical joints which is exemplified by cracking, spalling and disintegration of the concrete deck slab in the area adjacent to these joints. A possible approach to alleviate this problem is the elimination of mechanical deck slab joints in multi-span bridges (Kim et al., 2004b).

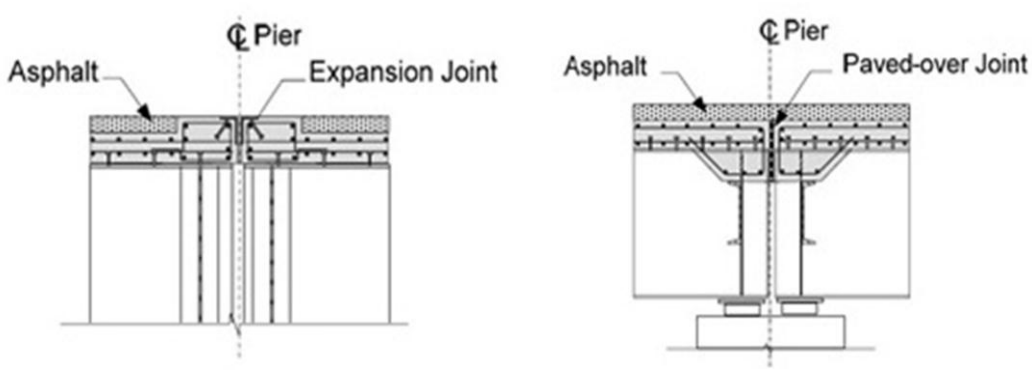

(a) Expansion joint between spans (b) Paved-over joint between spans

Figure 2.10 Common practice deck Joints in bridges with Multiple Simple Spans (Lam et al., 2008)

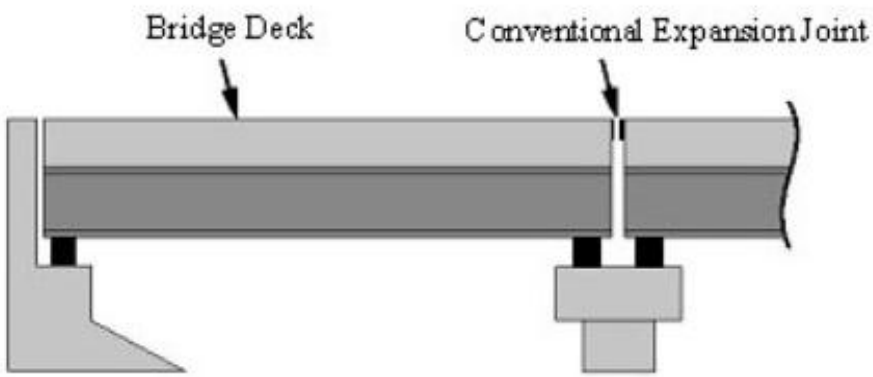

Figure 2.11 Conventional expansion joints (Li and Lepech, 2004)

Figure 2.12 Typical Corrosion Damage Caused by Leaking Deck Joints (Lam et al., 2008)

Link slabs are continuous concrete decks over simply supported steel or concrete girders at the piers. The decks undergo negative flexure as the girders deflect under live load on the spans. The negative flexure results in lateral cracking on the top surface of the deck. Presence of cracks in the top surface of the concrete deck provides a means for water to infiltrate to the reinforcing steel and cause adverse corrosion Figure 2.13 (Ho and Lukashenko, 2011).

Two systems to eliminate deck joints have been attempted in the US (Hossain, 2011). The first was by Convert the simply supported spans into a semi-continuous deck system for live

load by encasing the girder ends in a monolithic transverse concrete diaphragm that is fully connected to the girders by shear studs in order to transfer the negative moments caused by live load and other superimposed dead loads as shown in Figure 2.14. It can be seen that the modifications are extensive with major retrofitting of the steel box girders required to resist the negative moment at the pier support. As a result, the costs of this rehabilitative scheme became expensive.

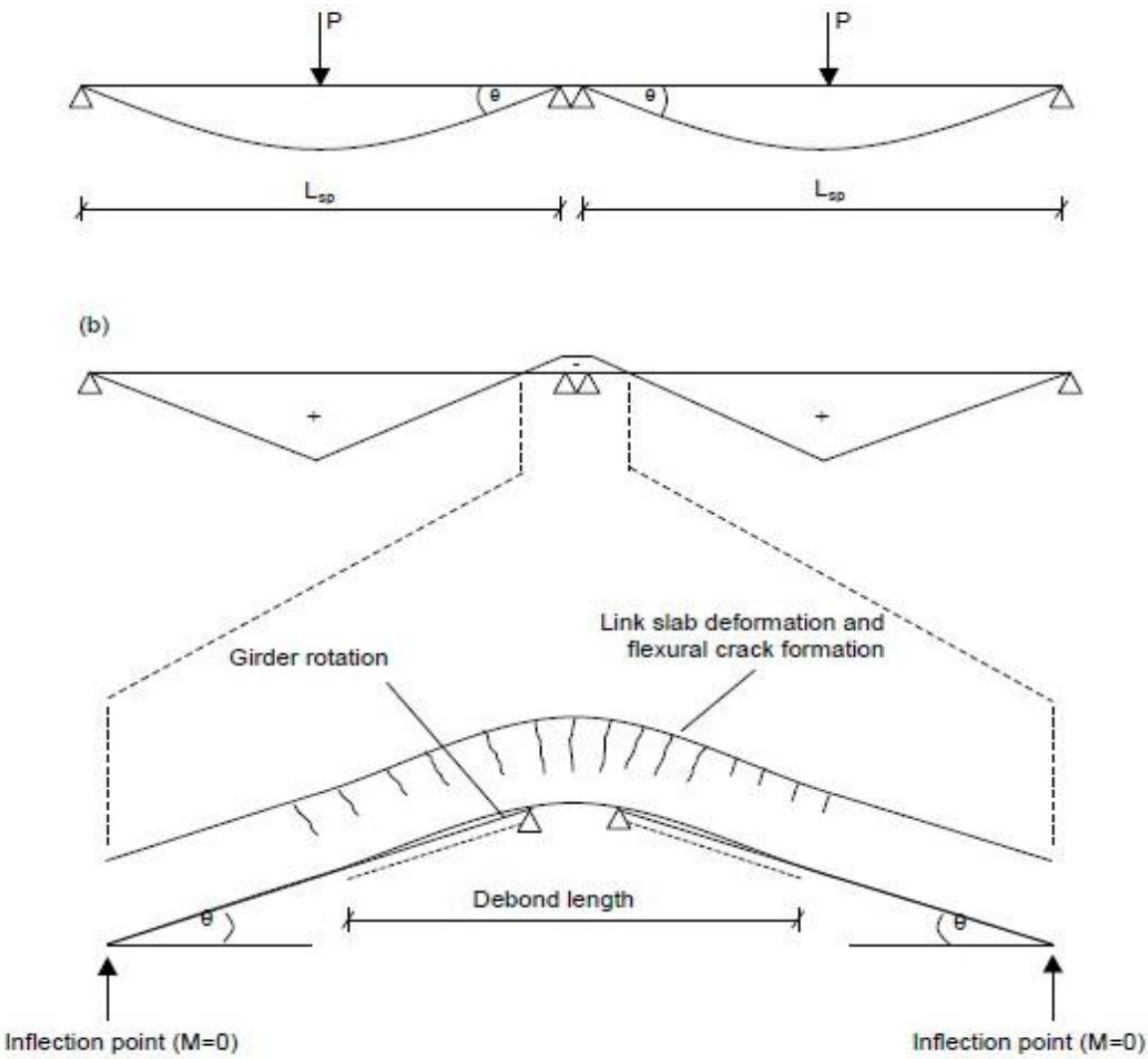

Figure 2.13 Schematics of two span bridge subjected to point load at mid span for (a) deformed shape of bridges; and (b) moment distribution on bridge span and corresponding deformed shape of link slab region (Kim et al., 2004b)

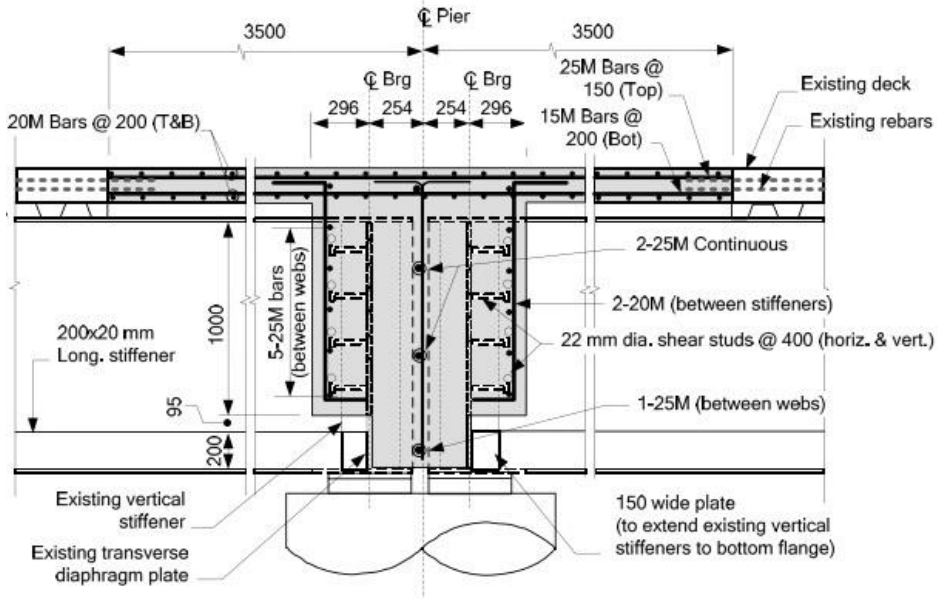

Figure 2.14 Semi-Continuous deck system details (Lam et al., 2008)

The second system that can be used to eliminate deck joints in bridges is the debonded link slab system Figure 2.15 (Lam et al., 2008). The concept of this system that is the concrete link slab is debonded from the girders for a longer length at each girder end, thereby providing the flexibility necessary to accommodate the end-rotations of the simply-supported girders. This system simplifies construction details and even does not require replacing a large area of the deck slab on both sides of the pier when rehabilitation is needed.

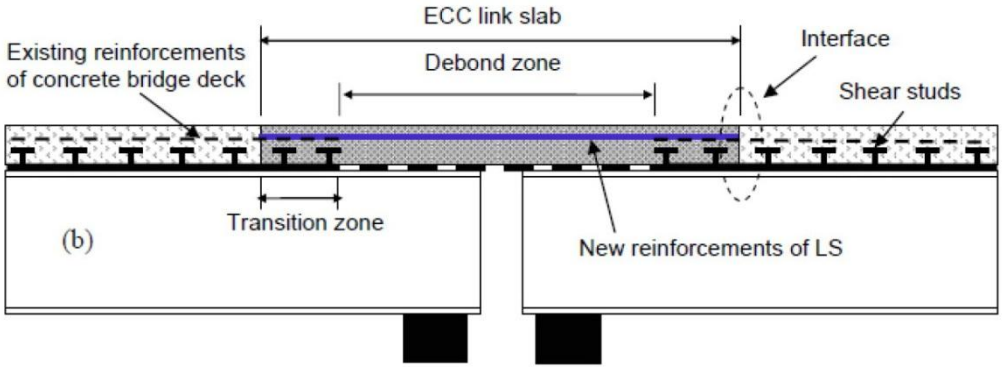

Figure 2.15 Typical flexible link slab (Lam et al., 2008)

Caner and Zia (1998) developed and experimentally analyzed the performance of jointless bridge decks and proposed design methods for the link slab. These investigations revealed

that the link slab was subjected to bending under typical traffic conditions rather than axial elongation. Tensile cracks were observed at the top of the link slab under service load conditions due to a negative bending moment. For steel girders, the measured maximum crack width was 300μm at 40% of ultimate load and 750μm at 67% of ultimate load. They also pointed out that additional tensile stress may be imposed on the link slabs due to shrinkage, creep, and temperature loading, and that crack width must be carefully controlled. The recommendation was to use epoxy coated reinforcing bars in the link slab in order to avoid reinforcement corrosion. To reduce the stiffness of the link slab, debonding of the link slab over the girder joint for a length equal to 5% of each end of the adjoining girders span was also recommended as shown in Figure 2.15.

However, normal concrete link slabs could not accommodate the large tensile strain capacity and micro-cracking behaviour. Therefore and as in the case of semi-continuous deck systems, the need for heavily steel reinforcement to keep crack widths below acceptable serviceability limits was essential. This high reinforcement ratio within concrete link slabs unnecessarily stiffens the link slabs. An additional difficulty observed with construction of concrete link slabs is their sensitivity to poor construction practices.

In recent times, ECC with its flexible processing has emerged from laboratory testing to field applications. Research studies showed significant enhancement of ductility and crack width control in ECC material (Hossain, 2011). The tensile strain hardening behavior and multiple cracking with crack widths below 100 μm provided an allowable performance level for the ECC. The compressive strength of ECC is 80 MPa at 28 days and significantly higher than anticipated 35 MPa. This indicates that the hardened properties of the ECC can meet and exceed the structural requirements of link slabs. These ECC properties will provide link slabs with significantly enhanced rotational and axial deformation capacity while controlling crack width, resulting in low permeability and reduced maintenance needs of repaired bridge deck systems with ECC link slabs. The combination of greener materials along with the extended life cycle suggests that the sustainability of highway bridges utilizing ECC link slabs will be far superior to the conventional concrete bridges (Kim et al., 2004b).

2.7.2 A Case study Application of Debonded Link Slab System in Canada

Unfortunately, the use of deboned ECC link slab systems in Canada is growing slowly due to lack of knowledge of this material even though with the knowledge of that ECC could reduce costs for maintenance and construction time. Accordingly, very shy attempts have been done throughout Canada employing the use of fiber reinforced concrete; not even ECC; compared to US and Japan.

Camlachie Road Underpass over Hwy 402 Bridge in Ontario is an example of using this new technology incorporating fiber reinforced concrete (Lam et al., 2008). This bridge was originally a two simple-spans structure, carrying Camlachie Road traffic over Highway 402, about 20 km east of Sarnia in Ontario. The deck superstructure consisted of two steel box girders with a 190 mm thick composite concrete slab cast on top. The two simply-supported spans were both 38.405 m in length and were supported on conventional abutments at the ends and a circular reinforced concrete column in the middle.

The bridge was rehabilitated in 2007, when all the expansion joints were eliminated by incorporating a debonded link slab detail at the central pier location that made the deck slab continuous over the pier, while the girders remained discontinuous.

Construction of the link slab consisted of removal of a 6.0 m wide strip of existing deck symmetrical about the pier centreline including all existing shear studs in the middle 4.0 m wide strip and replacement with a new cast-in-place link slab of matching thickness to existing deck slab, which was cast on top of the exposed girders but debonded from the top flanges over the middle 4.0 m wide segment. Figure 2.16 shows some photographs of the link slab construction. To further limit the extent and severity of any cracking in the link slab, fiber-reinforced concrete was used instead of normal concrete. The use of fiber reinforced concrete was expected to improve the crack-control performance of the link slab.

To evaluate the performance of the link slab, electrical resistance strain gauges were installed on some of the longitudinal reinforcement bars in the link slab. A behavioural load test of the structure is planned in future and no field observation is reported yet.

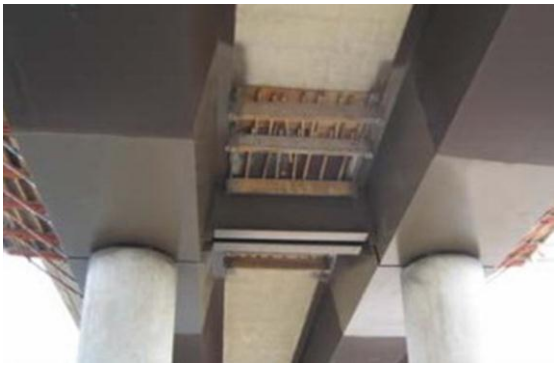

(a) Formwork at Soffit of Link Slab

(b) Concrete Pour for Link Slab

Figure 2.16 Construction of debonded Link Slab at Camlachie Road/Hwy 402 Underpass (Lam et al., 2008)

2.8 The Cost of ECC

The development of ECC has to take into consideration additional matters, such as availability of materials, standardization of the design of the mix and test methods, and, the most important issue is the cost of ECC.

The cost-benefit should be considered based on the whole structural life cycle cost. The life cycle cost includes the cost of materials, of the building, and maintenance costs. The use of ECC in construction members provides the possibility to eliminate shear reinforcement. Hence, reduction of construction cost is achieved. The durability of construction, particularly for infrastructure, which is supposed to use large volume ECC materials, is improved as it is supported by the ductility of ECC materials. Thereby, the cost of maintenance is reduced significantly. Furthermore, the higher cost of ECC materials than normal concrete is caused by the use of fiber and higher cement content. Partial substitution of cement by an industrial by-product, such as FA and slag, can reduce the cost of ECC in comparison with other HPFRCC. In addition to cement replacement and as the objective of this research, the substitution of silica sand by local crushed sand will reduce the cost of ECC significantly.

2.9 Review Conclusion

Although there are many studies reporting the improvement in mechanical properties and the failure mechanisms of ECCs under static loading conditions, there have been very few studies that reveal its properties and failure mechanisms under fatigue loading. Matsumoto (1998) was the first researcher to investigate fatigue behavior and properties of ECC under fatigue loading. The test results confirmed that polyethylene fiber ECC mixtures (PE-ECC) exhibited multiple crack formation even under fatigue loading, but failed by major crack fracture due to fiber fatigue rupture. Furthermore, the S-N curve of PE-ECC was not introduced due to lack of tested specimen numbers at each fatigue loading level. In addition, Suthiwarapirak et al. (2004) investigated the flexural fatigue characteristics of shotcreted ECC repair materials containing PVA fibers. The test results exhibited bilinear fatigue stress–life (S-N curve) relationship on a semi-logarithmic scale which was similar in shape of metal fatigue fracture. As the same results of Matsumoto (1998), the failure mechanism of ECCs involved the development of multiple cracks, and the number of cracks was higher when the fatigue stress level was higher (Suthiwarapirak et al., 2004). Similar advantages in the fatigue resistance of ECC have also been found in comparison to polymer cement mortars (Suthiwarapirak et al., 2002). The performance of ECC as rigid pavement overlay rehabilitation material under high fatigue scenarios was investigated (Zhang and Li, 2002). Reflective cracking in this kind of application through the new overlay material is a greatest concern. To evaluate the ECC performance as a rigid pavement overlay material, both ECC/concrete and concrete/concrete overlay specimens were tested in flexural fatigue. Test results show that the load capacity of ECC/concrete overlay specimens was double that of concrete/concrete overlay specimens, the deformability of ECC/concrete specimens was significantly higher, and the fatigue life was extended by several orders of magnitude. Qian and Li (2008) investigated the performance of jointed ECC pavement material as an alternative to jointed normal plain concrete pavement material (JPCP). Test results showed that the use of ECC materials arrested such failure mode and greatly enhances its long term durability performance. The ECC specimens totally eliminate the single fracture mode in concrete by developing extensive micro cracks under flexural fatigue loading. Moreover, the fatigue resistance of ECC for repair of viaducts subjected to train loading was studied by

Inaguma et al. (2005). The use of ECC material is significantly lengthen service-life, reduce maintenance events, and life cycle costs.

Rouse and Billington (2007) investigated the performance of ECC material when used in hinge regions of segmentally precast, post-tensioned concrete bridge piers. Based on the experimental results, it was found that the ECC material developed greater creep strains than a similar cementitious mixture without fiber reinforcement. Crack openings on the surface of shrinkage for specimens without fibers were found to be more than corresponding specimens with fibers. Furthermore, the addition of fine aggregate in ECC can significantly reduce creep and shrinkage of the material. Similar larger response in creep strains of concrete specimens reinforced with small amounts of steel or polypropylene fibers have been found in comparison to specimens without fibers (Balaguru and Ramakrishnan, 1988; Houde et al., 1987). No information is currently available in the published literature revealing the fracture energy property of ECC.

Due to the lack of information in the mechanical properties of ECC such as fatigue flexure, long-term creep and fracture energy properties compared to extensive researches which have been done so far on investigating stress-strain capacity, there is an urgent need for further research studies to optimize the material characteristics in order to design ECC mixes especially tailored for link slab applications. Furthermore, the need to reduce the relatively high cost of ECC is essential to overcome the obstacles which preventing wider commercial use of ECC. According to these needs, for the last few years, a very extensive research has been in progress at Ryerson University to develop greener and sustainable ECC mix designs by reducing cement and fiber contents. ECC mixtures have been developed by incorporating industrial by-products materials such as fly ash class CI, F and slag and metakaolin as replacement of cement up to 70% as well as fibers of different types and configurations. Introduction of such supplementary cementitious materials has an inevitable influence on improving strain-hardening behavior and durability of ECC. In addition to these innovation, attempts to reduce the cost of ECC, a number of commercial projects in Japan and Australia have already demonstrated that initial construction cost savings could be achieved when ECC is used, through smaller structural member size, reduced or eliminated steel

reinforcement, elimination of other structural protective systems, and/or faster construction offered by the unique fresh and hardened properties of ECC.

The present study contributes the existing knowledge of ECC by incorporating locally available crushed sand instead of silica sand and by employing different cement replacement rates up to 70%. It is well known that commercially available microsilica sand is relatively expensive and difficult to obtain when compared with commonly available sands, such as crushed sand. Therefore, the effects of microsilica sand (as a control material), locally crushed sand and different SCM/C ratio on the compressive and flexural properties, fracture energy, fatigue performance and creep as well as crack development were experimentally determined to identify/select best ECC mixtures for link slab applications. Consequently, the best ECC mix design is employed to cast small-scale model link slab specimens to evaluate the performance of ECC under sustained loading (long-term creep) compared to its self-consolidating normal concrete counterpart.

This research is a part of an extensive program evaluating the performance of ECC link slab under monotonic, fatigue and sustained loading. Overall research will lead to the development of guidelines for ECC mix proportioning and testing methods for local industry to manufacture cost-effective and greener ECC mixes especially for link slab applications.

2.10 Summary

In this chapter, the characteristics and basic micro mechanisms of ECC were presented. The role of materials and their influence on ECC, such as fibers and cement replacement materials were also introduced in this chapter. The mechanical properties of ECC such as fatigue flexure, long-term creep and fracture energy were also introduced based on available literature. A number of recent/ongoing applications of ECC were briefly introduced as well which exhibited the flexibility of ECC in real world applications, and the most important issue which is the cost-benefit relation of ECC was also presented.

CHAPTER THREE

EXPERIMENTAL PROGRAMS

3.1 Introduction

In this chapter, two groups of 6 ECC mixtures were designed and selected to study and investigate the performance of ECC. The first group incorporated silica sand and different SCMs while the second group incorporated the same SCMs but with crushed sand. Based on these two groups, four different phases of tests were carried out to investigate the influences of both type/size of aggregate and type/amount of SCMs on ECC mechanical properties.

This chapter also presents the materials and equipment used in this research, material proportions, mixing procedures and specimen preparation. All ECC mixes were mixed by using Hobart type mixer with 20-liter capacity to prepare specimens. Test procedures such as compressive strength test, three point bending test, four point bending test and long-term creep testing employed in this research to investigate the performance of ECC mixtures are presented in this chapter.

3.2 Materials

3.2.1 Cement

The cement used in all mixtures was Type GU (general use), hydraulic cement which correspond to CSA A3001-03 (previously Type 10 normal Portland cement). Chemical composition, physical and strength properties of cement are presented in Table 3.1

Table 3.1 Chemical properties of Portland cement, fly ashes and slag

Chemical composition (%)	Cement	Fly Ash (F)	Fly Ash (CI)	Slag
Calcium Oxide CaO	61.40	5.57	14.30	40.8
Silicon Dioxide SiO_2	19.60	59.5	41.57	35.4
Aluminium Oxide Al_2O_3	4.90	22.2	26.12	13.00
Ferric Oxide Fe_2O_3	3.10	3.90	8.44	0.50
Magnesium Oxide MgO	3.00	-	3.40	8.00
Sulfur Trioxide SO_3	3.60	0.19	1.55	0.10
Alkalis as Na_2O	-	2.75	0.71	0.20
Loss on ignition LOI	2.30	0.21	1.49	-
Sum (SiO_2+Al_2O_3+Fe_2O_3)	27.60	85.6	76.13	48.9
Physical properties		Fly Ash (F)	Fly Ash (CI)	Slag
Residue 45 μm(%)		9.60	17.50	1
Density (g/cm^3)		2.18	2.43	2.11
Blaine fineness (m^2/kg)		306	-	430
Physical properties		Cement		
Residue 45 μm(%)		3.00		
Density (g/cm^3)		3.15		
Blaine fineness (m^2/kg)		410		
Air Content (%)		7.79		
Initial Setting time (mins.)		113		
Compressive Strength (MPa) 1 day		19.41		
Compressive Strength (MPa) 3 day		30.35		
Compressive Strength (MPa) 28 day		41.47		

3.2.2 Supplementary Cementitious Materials (SCMs)

Class-F fly ash and Class-CI fly ash conforming to ASTM C-618 (2012) requirements obtained from Lafarge plant were used to produce eight different ECC mixes. The chemical and physical properties for both of them are given in Table 3.1

Blast furnace slag was supplied from Lafarge plant as well. It was used as a SCM to obtain four ECC mixes. The chemical and physical properties of slag are shown in Table 3.1.

3.2.3 Aggregate

According to the micromechanic based design of ECC, to achieve strain hardening behaviour, low matrix fracture toughness is required. However, with the increasing of maximum grain size of aggregate, increase in toughness of the matrix is appeared and as a result, the production of standard ECC has been restricted to the use of fine aggregate such as microsilica sand with a maximum grain size of 250 µm and a mean size of 100 µm (Li et al., 1995). Commercially available microsilica sand is relatively expensive and difficult to obtain when compared with commonly available sands (Sahmaran et al., 2009). For this purpose, two different types of fine aggregates were incorporated for ECC mixes. First is #730 Silica Sand (SS) with maximum size of 0.30 mm and second is Crushed Sand (CS) with maximum size of 1.18mm (sieve No. 16). The typical screen analysis of aggregates was conducted in accordance with (ASTM C 136, 2005) and (ASTM C 117, 2004). Their grain size distributions are tabulated in Table 3.2.

Table 3.2 Sieve analysis of silica sand and crushed sand

U.S. Sieve #	Opening (mm)	% Retained crushed sand	% Retained silica sand
16	1.18	0.00	-
20	0.841	6.0	-
30	0.60	17.50	-
40	0.42	-	0.00
50	0.30	60.0	2.20
70	0.21	-	14.70
100	0.15	90.25	47.50
140	0.105	-	28.80
200	0.074	98.75	6.40
270	0.053	-	0.40

3.2.4 High Range Water Reducing Admixture (HRWRA)

To improve the workability of ECC mixtures, ADVA® cast 575 from Grace Construction Products was used as HRWRA. ADVA® cast 575 is polycarboxylic-ether with solid content of approximately 30% and conforming to ASTM C 494 type F and (ASTM C1017 type I, 2007). The characteristics of ADVA® cast 757 are given in Table 3.3.

Table 3.3 HRWRA ADVA® cast 575

Description	Property
Color	Turkish Blue
State	Liquid
Odor	-
pH	2.7-6.5
Boiling Point	100°C
Freezing Point	0°C
Specific Gravity	1.1

3.2.5 Polyvinyl Alcohol (PVA) Fiber

Polyvinyl alcohol (PVA) fiber was used in the production of ECC mixes. PVA fiber is hydrophilic which means the tendency to interact or dissolved by water (Kim et al., 2007). Therefore, the strong bond between the matrix and fiber tends to break the fiber rather than pull it out of the matrix. This bounds the multiple cracking and leads to less or no strain hardening behaviour. To overcome this, PVA fiber is currently oil coated whereby fibers slip in the matrix, rather than break (Li et al., 2002). PVA fibers with a length of 8 mm and a diameter of 39 μm were used. The tensile strength of the PVA fiber is 1600 MPa and the density is 1,300 kg/m^3. The fiber surface is coated with 1.2% oil by weight to reduce the fiber/matrix chemical and friction bond.

3.3 Mixture Proportions

3.3.1 ECC Mix Designs

Two main groups of 12 ECC mixtures have been designed and selected. The first group was composed of 6 ECC mixtures which were produced using microsilica sand with a maximum grain size of 0.30 mm. The second group was composed of the same first group ECC mixtures but was produced using local crushed sand with maximum size of 1.18 mm. Both aggregate size and type were used to study their influence on mechanical properties of ECC. The supplementary Cementitious Materials (SCMs) used in both groups were Class-CI fly ash with calcium oxide content 14.30%, Class-F fly ash with calcium oxide content 5.57% and Slag with calcium oxide content 40.8%. These SCMs were used as Portland cement replacement at ratios of 1.2 and 2.2, respectively. Mixture proportions for both groups of ECC mixtures are given in Table 3.4. The water/binder ratio was kept in the range of 0.27 for both class CI and F fly ash and 0.30 for slag. As shown in Table 3.4, the ECC mixtures are labeled such that the ingredients are identifiable from their Mix IDs. The first letter in the mixture designations indicates the SCM type (CI = fly ash class CI, F = fly ash class F, S = slag). The numbers after the letter indicate the SCM (CI, F or S) – cement ratio and last letters represent aggregate type (SS or CS).

Table 3.4 ECC Mixture proportions

First Group-Silica Sand									
Mixture ID	Ingredients, kg/m^3							FA/C or S/C	w/b
	Water	Cement	FA	Slag	Sand	PVA	HRWRA		
CI_1.2_SS	331	570	684	-	455	26	5.4	1.2	0.27
CI_2.2_SS	327	386	847	-	448	26	4.2	2.2	0.27
F_1.2_SS	331	570	684	-	455	26	5.4	1.2	0.27
F_2.2_SS	327	386	847	-	448	26	4.2	2.2	0.27
S_1.2_SS	380	575	-	690	456	26	4.50	1.2	0.30
S_2.2_SS	379	395	-	868	455	26	3.80	2.2	0.30
Second Group-Crushed Sand									
Mixture ID	Ingredients, kg/m^3							FA/C or S/C	w/b
	Water	Cement	FA	Slag	Sand	PVA	HRWRA		
CI_1.2_CS	327	559	671	-	446	26	5.4	1.2	0.27
CI_2.2_CS	319	376	825	-	436	26	4.2	2.2	0.27
F_1.2_CS	327	559	671	-	446	26	5.4	1.2	0.27
F_2.2_CS	319	376	825	-	436	26	4.2	2.2	0.27
S_1.2_CS	380	575	-	690	456	26	4.50	1.2	0.30
S_2.2_CS	379	395	-	868	455	26	3.80	2.2	0.30

HRWRA: High range water reducing admixture, C: Cement, FA: fly ash, CI: Fly Ash class-CI, F: Fly Ash class-F, S: Slag, w/b: water to binder ratio (binder = C+SCMs)

3.3.2 SCC Mix Design

Self-consolidating concrete (SCC) was used as a control mix to evaluate the performance of ECC under sustained loading. Simultaneously, the best of ECC mix designs was employed to cast link slab specimen models compared to SCC counterpart. The compressive strength of SCC at 28 days was ranging between 60~63 MPa, modulus of elasticity was 33.59 GPa and its flexural strength value was 3 MPa at 1 mm of ultimate mid-span deflection. Except coarse and fine aggregate, all the materials for SCC mix design were the same as those of ECC mixtures. Well graded coarse sand was used as a fine aggregate and 10 mm nominal size aggregate was used as coarse aggregate. The mix design of SCC is presented in Table 3.5.

Table 3.5 SCC mix design as a control mix

Ingredients (kg)					
			Aggregate		
Water kg/m^3	Cement kg/m^3	Slag kg/m^3	Fine kg/m^3	Coarse kg/m^3	HRWRA kg/m^3
172	400	90	910	750	1850

3.3.3 Experimental Program

To investigate the performance of 12 ECC mixtures (two groups) designed and selected in the present study, four different phases of tests were carried out. The first phase was fracture energy test at 7, 28, 90 days for both ECC groups, respectively. The second phase was four-point bending test at 28, and 56 days for both ECC groups. The second part of this phase was fatigue test which was applied at 28 days only for 50000 cycles at 4 Hz cyclic loading and 55% fatigue flexural stress level. Slag mixtures have been omitted from this phase because they did not exhibit multiple cracking behaviours; a detailed discussion will be provided later; and the best ECC mix designs which have been selected from those two phases have been included in the third phase.

The author in the third phase tried to exhaust the chosen ECC mixtures as much as he could to get the optimum ECC performance by applying fatigue flexure test in two different approaches; the first approach was applying different fatigue flexural stress levels namely 40%, 55% and 70% of the average maximum stress for 50,000 cycles at 4 Hz cyclic loading and the second approach was applying different fatigue cycles namely 200,000, 300,000 and 1,000,000 cycles at 4 Hz cyclic loading and 55% fatigue stress level as well.

The best of the best ECC mixtures from the third phase have been included in the fourth phase which is the creep test. In this phase, three link slab bridge deck specimens have been casted and tested; one of them is SCC. SCC is a suitable concrete to use when casting link slab bridge dicks because heavily reinforced link slab section virtually makes it impossible to apply vibration. For this reason SCC mix was chosen as control mix for ECC specimens. The experimental program flowchart of the present study is given in Figure 3.1.

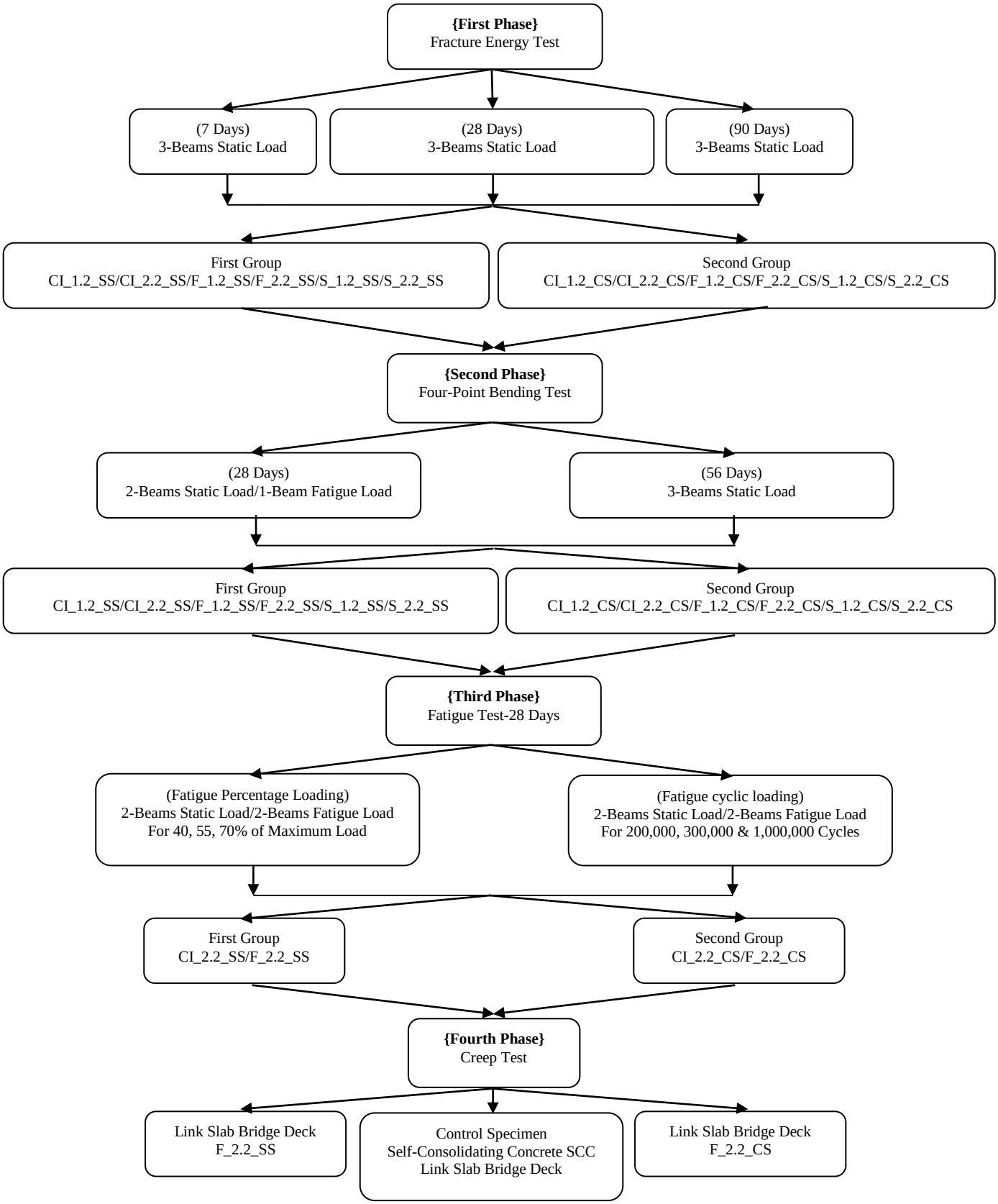

Figure 3.1 Experimental Program Flowchart

3.4 Mixing Procedure and Specimen Preparation

In this study, a Hobart type mixer with 20-liter capacity was used in preparing all ECC mixtures. All the materials of ECC mixtures were weighed separately before starting mixing. All solid materials except PVA fiber including cement, SCMs (FA or S), and aggregate were thrown into the mixer for the dry mix. After 30 seconds dry mix, 90% of water was added into the mixer. The mixer speed was then increased for another 2 minutes. The remaining 10% of water and SP were added until a consistent and uniform ECC mixture was obtained. The final step of mixing procedure was to add the PVA fiber into the mixer in two patches. The mixing was stirred for another 3 minutes. It should be noted that slight adjustment in the amount of SP in each mixture was performed to achieve better fiber dispersion and workability. Figure 3.2 shows mixing procedure by using Hobart mixer.

Mixing of Solid Ingredients

Water Addition

HRWRA Addition

Fiber Addition & Dispersion

Figure 3.2 Production of ECC by using Hobart type mixer

After the mixing was completed, the workability was assessed and recorded. Workability was measured by conventional slump test. Subsequently, the workability was assessed at three different levels, ranging between “self-compacting”, “moderated workability” and “hard to compact”. As shown in Figure 3.3(a), ECC exhibited excellent workability eliminating the need for vibration and also a small adjustment by hand was needed to get a smooth surface as shown in Figure 3.3(b).

(a) (b)

Figure 3.3 Excellent workability of ECC mixtures

At least three specimens of each ECC mixture were tested under each type of loading condition for testing ages (7, 28, 56 and 90 days). 50-mm cubic specimens were prepared for the compressive strength test at 28 days, 355×50×75 mm prism specimens were prepared for the four-point bending test at 28 and 56 days and fracture energy tests at 7, 28 and 90 days. Fatigue test applied for each type of loading conditions at 28 days only. Figure 3.1 shows the specimen preparation flowchart for each mixture investigated for a total of 276 beams. All specimens were demolded after 24 hours and moisture cured in plastic bags at 95 ± 5% relative humidity (RH), 23 ± 2 °C. The specimens were kept in the curing room until the day of testing.

3.5 Test Procedure

3.5.1 Slump Flow Test + T50 Time

This test method is used to monitor the consistency of fresh, unhardened self-consolidating concrete and its unconfined flow potential. It measures two parameters: flow spread and flow time T50 (optional). The former indicates the free, unrestricted deformability and the latter indicates the rate of deformation within a defined flow distance.

The slump test is performed by using Abrams cone with the internal upper/lower diameter equal to 100/200 mm and the height of 300 mm, as shown in Figure 3.4. The slump cone is placed on base plate of size at least 900 × 900 mm, made of steel, and clearly marked with circles of Ø200mm and Ø500mm at the centre, as shown in the figure.

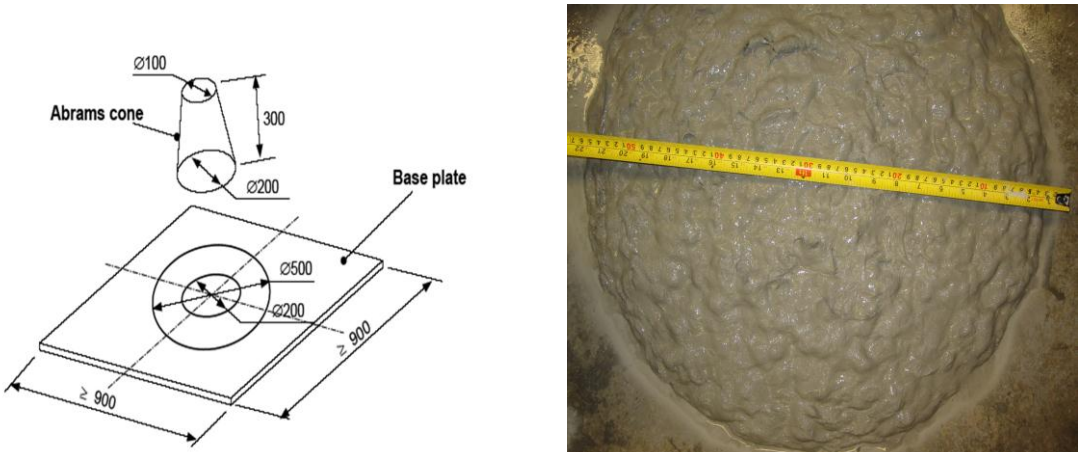

Figure 3.4 Slump flow test + T50

The cone is placed on moist base plate and then filled with concrete mix without any external compacting action such as rodding or vibrating. The cone is lift perpendicularly to the base plate in a single movement to let the concrete to be allowed to flow out freely without obstruction from the cone. A stopwatch should be started the moment the cone lost contact with the base plate. Then the stopwatch should be stopped when the front of the concrete first touches the circle of diameter 500 mm. The stopwatch reading is recorded as the T50 value. The test is completed when the concrete flow has ceased (Schutter, 2005 and ASTM C1611, 2009).

3.5.2 Compressive Strength

Performance of the hardened concrete was evaluated for all ECC mixtures by measuring compressive strength at age 28 days. Cubic samples (at least 3 specimens for each of age) of 50 mm were cast from each ECC mixture. The compression test was carried out on the cubic specimens by using a compression testing machine with a capacity of 400,000 lbs. Medium failure load; range 3 (up to 80,000lbs) was used for all cubes in accordance with (ASTM C39, 2003).

3.5.3 Fracture Energy

Fracture energy (G_F) is a mechanical property of concrete. It is defined as the amount of energy required to create a crack of one unit of area (Bazant, 1979). In order to measure the fracture energy of ECC mixtures, RILEM TC50-FMC (Fracture Mechanics of Concrete) recommendation was used. According to this test method, three prismatic samples of 355×50×75 mm size were prepared with a notch depth one-third the depth of the beam (25 mm) and thickness of approximately 3mm for each age of 7, 28 and 90 days. These samples were tested by means of three-point bending test on notched beams at a rate of 0.005 mm/sec. During the tests, the load and the mid-span deflection were recorded on a computerized data recording system. Fracture energy was computed from the area under the load-deflection curve divided by the cross-sectional ligament area. The upper limit of the deflection to be used in the area calculation was set to the displacement at which the strength had dropped to 50% of the peak value. The set-up for measuring fracture energy is presented in Figure 3.5.

Fracture energy of the specimens was calculated based on Equation (3.1):

$$G_F = \left[\int_0^{\delta_{max}} F(\delta) d\delta + (mg\delta_{max}) \right] / [(d-a)b] \quad \ldots\ldots\ldots\ldots\ldots\ldots (3.1)$$

Where:

m = the weight of the beam,

g = 9.81 m/s^2,

d = beam depth,

b = beam width,

a = notch depth,

δ_{max} = maximum deflection,

$\int_0^{\delta_{max}} F(\delta)d\delta$ = area under the curve,

(d-a)b = A_{lig} which is the cross-sectional area of the ligament (Wu et al. 2000).

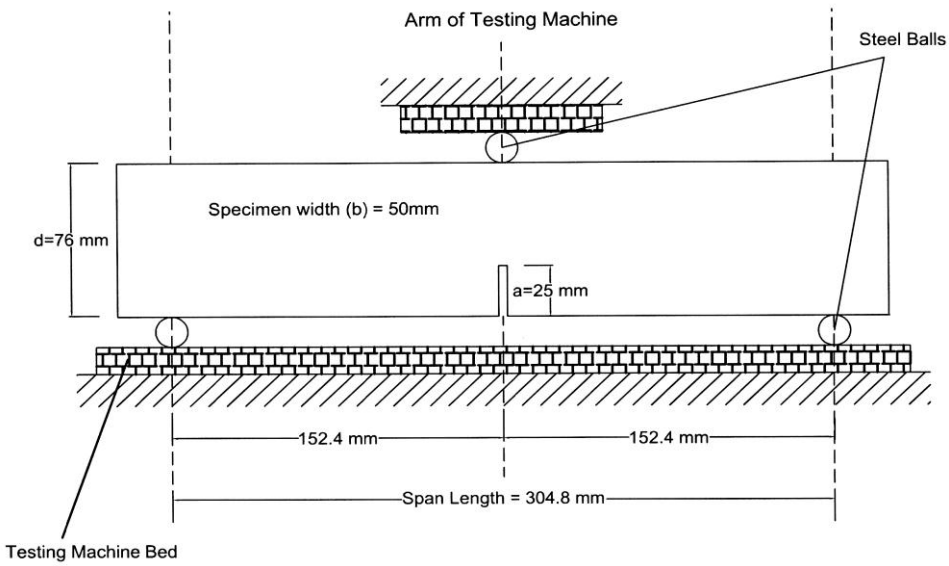

Figure 3.5 Test set-up for measuring fracture energy

3.5.4 Flexural Strength

To measure the flexural strength of ECC specimens (Modulus of rupture), three prismatic samples of 355x76x50 mm were prepared for ages 28 and 56 days. ECC samples were cleaned and sanded to obtain a flat surface for balancing the crack propagation into the samples, and then four-point bending test was performed under displacement control condition at a loading rate of 0.005 mm/s on a closed-loop controlled servo-hydraulic material test system. The span length of flexural loading was 304.8 mm with a 101.6 mm center span length. During the flexural tests, the load and the mid-span deflection were recorded on a computerized data recording system. Test setup is presented in Figure 3.6.

Flexural strength of the specimens was calculated in accordance with (ASTM C 78, 2002) as follows:

$$MOR = \frac{PL}{bd^2} \quad \ldots\ldots\ldots\ldots\ldots\ldots (3.2)$$

Where:

MOR = Flexural strength (modulus of rupture), MPa,

P = maximum applied load indicated by the testing machine, N,

L = span length, mm,

b = average width of specimen, mm, at the fracture, and

d = average depth of specimen, mm, at the fracture.

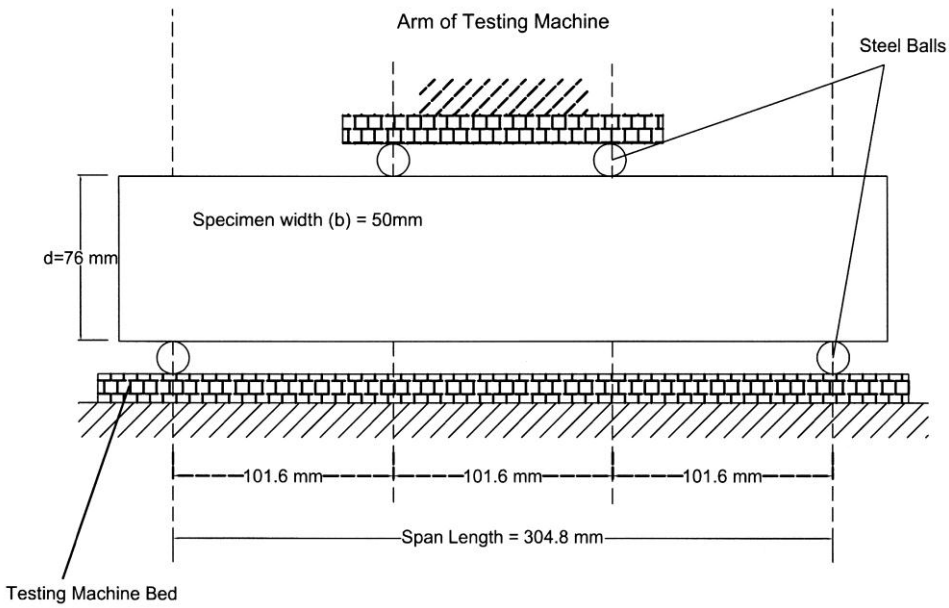

Figure 3.6 Four point bending test setup

3.5.5 Fatigue Flexure

To investigate the ECC concrete performance under fatigue flexural test, two approaches were adopted: the first was applying different fatigue stress levels and the second was applying different fatigue cyclic loading. Accordingly, four prismatic samples of 355x50x76 mm were prepared for the age of 28 days. The four-point bending test was conducted under both static and fatigue loading. Two out of four samples were prepared for static loading tests as control specimens which were carried out under displacement control conditions, while the other two samples were prepared for fatigue loading tests which were performed

under load control conditions. Specimens were simply supported on a span of 304.8 mm and subjected to two-point loads at one-third of the span as shown in Figure 3.6.

In the first approach, static flexural tests were conducted before fatigue flexural tests and were applied at the constant rate of 0.005 mm/s. The static flexural strengths were determined by averaging the flexural strength results of ECC control specimens. Based on their static flexural averages, the different maximum fatigue stress levels were determined as 40, 55 and 70% and the tests were conducted at 50,000 cycles and 4 Hz cyclic loading. In the second approach, 55% of fatigue stress level value was fixed and tests were conducted at different fatigue cycles namely 200,000, 300,000 and 1,000,000 cycles at the same 4 Hz cyclic loading as well.

Fatigue flexural tests were performed under load control conditions. The ratio between minimum and maximum flexural stress was set equal to 0.30 for all specimens in order to avoid any impact and slip of specimens during testing. At the first cycle of each specimen, load was gradually applied to the maximum stress level at 0.50kN/min static loading rate in order to avoid any sudden collapse in the specimen. The cyclic fatigue loading was then applied. During the fatigue flexural tests, the mid-span deflection evolutions were recorded on data sheet and at the end of the fatigue flexural tests; static flexural tests were conducted on the fatigued ECC specimens to calculate the fatigue residual.

3.5.6 Long-term Creep Testing

Three link slab bridge deck specimens were cast and tested under long-term creep test. One of these specimens was cast with SCC. It is widely acknowledged that SCC and ECC exhibit excellent workability eliminating the need for vibration between the reinforcing steel and moderate finish-ability in practical applications as in link slab bridge decks. For this reason SCC mix was chosen as a control mix in addition to ECC as shown in Figure 3.7.

Figure 3.7 SCC to the left and ECC to the right, excellent workability eliminating the need of vibration

The experimental investigation of ECC link slabs was conducted using a representative section (711 mm [28 in.] wide) of a link slab between the inflection points of the adjacent deck slabs (3251 mm [128 in.] long). The thickness of the slab was 230 mm [9in.]. The zero moment condition at the inflection points as well as the boundary conditions at the pier was simulated by roller supports. The two beam supports allow both rotation and longitudinal displacements for the beam. Due to limitations of the laboratory facilities, the representative section was scaled down to ¼-scale model of the prototype shown in Figure 3.8.

The casting procedure of the link slab bridge deck specimens was followed the general field practice. The bridge deck part was cast initially and left for setting. After 24 hours the link

slab zone was cast with different ECC mixtures or SCC depending on the case. The specimens were cured for 28 days at the laboratory temperature while covered with the burlap. The relative humidity (RH) and the temperature of the laboratory were 45±5% and 24±2°C, respectively.

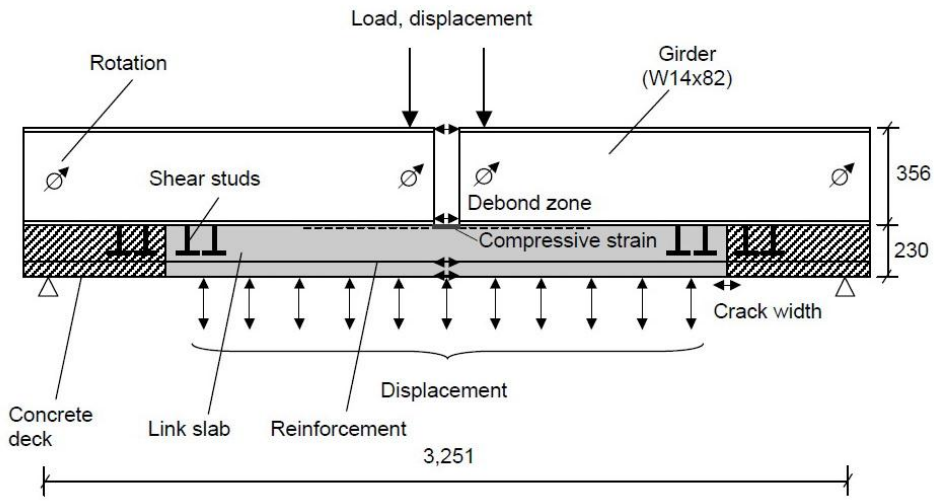

Figure 3.8 Representative section of link slab, dimensions in mm (Kim et al., 2004b)

Static loading tests were performed on similar precast specimens to those prepared for long-term creep testing to evaluate their ultimate load capacity. A percentage of the measured capacity was then used for the long-term creep testing. According to ACI committee 215 recommendations in creep loading, low levels of sustained stress increase the static strength, whereas high levels of sustained stress resulted in increased micro cracking and failure in some cases (ACI Committee Report 215, 1997). Consistently, the level of the applied sustained load was 25% of the ultimate static load capacity of bridge deck specimens.

It should be noted that the static loading were performed on link slab specimens in an inverted condition to represent the actual loading and support conditions. Therefore, the design of creep test setup should follow the same loading inverted system of static loading as well.

To prepare the specimens for long-term creep test, wide boards of wood with dimensions 900 x 620 x 20 mm were fastened with 50 x 100 mm wood lumbers in both directions. The

wood boards have clamped with steel I section of the link slab bridge deck specimens. According to the static loading test results, the load value of F_2.2_SS specimen was 10.50 kN which is the same value as in F_2.2_CS specimen compared to 4 kN for SCC specimen. To apply 25% of the ultimate static load for all of them, interlock bricks were used to apply uniformly distributed load on the wood boards. Figure 3.9 shows the test setup of the long-term creep test.

Figure 3.9 Test setup of long-term creep test

The instrumentation and measuring system for long-term creep test consisted of three electrical strain gauges of 4 mm gauge length. The first two strain gauges served to measure concrete strains in the compression and tension zones of the slab while the last to measure

steel strain inside the slab. This was in addition to two LVDT's used to measure the mid-span deflections of the inverted slab. This measuring system was done for each link slab bridge deck specimens as shown in Figure 3.10. Because of the long duration of the tests, permanently connecting the acquisition system to the specimens was not possible. This issue was remedied by using an indicator box (P-3500) to measure strains from time to time as deemed necessary as shown in Figure 3.11. Measurements were taken every day at the beginning of the test, then every three days for a period of almost two weeks. Finally, after the readings were stabilized, one reading per week was found reasonable.

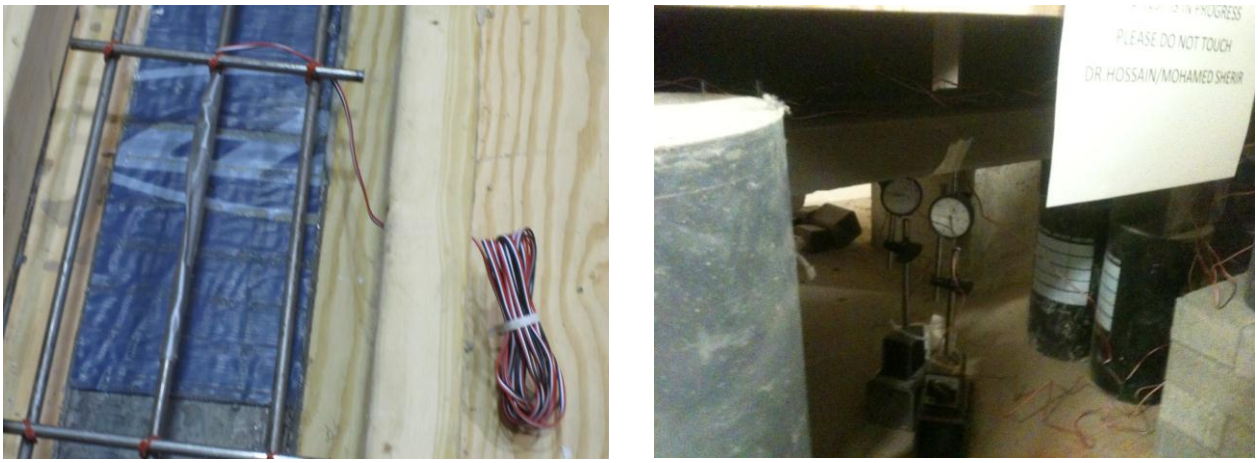

Figure 3.10 Instrumentation and measuring system for long-term creep test

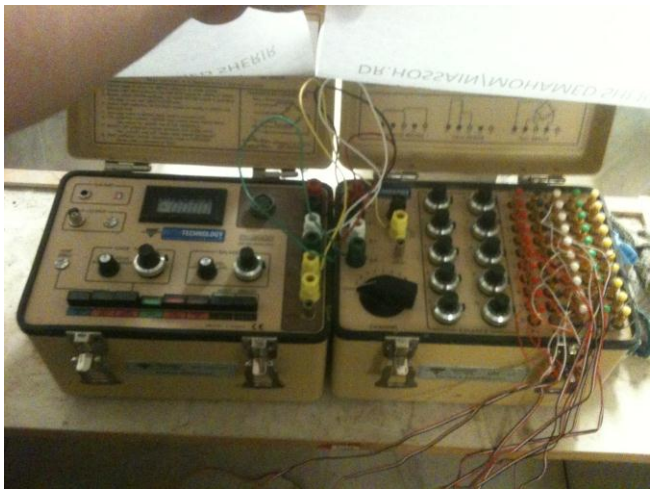

Figure 3.11 Indicator box (P-3500) to measure strains

3.6 Summary

Chapter 3 presented the mixing procedure for different ECC mixtures. All ECC mixtures have been cast at same casting procedure and kept in the same curing conditions. It should be noted that the author tried his best to ensure equal workability of all ECC mixtures. For this purpose, HRWRA was modified slightly in each mixture to achieve better fiber dispersion and workability.

In this chapter, the experimental program involved in the present research was also introduced. This experimental program involved five kinds of investigations (compressive strength, fracture energy, flexural strength, fatigue flexural loading and creep performance) to measure the performance of different ECC specimens. The result of these investigations will be introduced and discussed in the following chapter in details.

CHAPTER FOUR

RESULTS AND DISCUSSIONS

4.1 Introduction

Chapter 4 presents the results of the experimental studies of different ECC mixtures incorporating all SCMs i.e. fly ash class CI, F and slag on compressive/flexural strength and fracture energy.

In addition, this chapter also presents the results of the investigations on general fatigue loading test conducted on all ECC mixtures to assess their performance initially for choosing the best ECC mix design to be included in the special fatigue loading tests. This was done due to research time constraints which prevented the author to do fatigue loading tests for all 12 ECC mixtures studied in this research. As a consequence, slag ECC mixtures and fly ash ECC mixtures with SCMs/cement ratio of 1.2 were omitted from this investigation; a detailed discussion will be provided in this chapter. Special fatigue loading tests were applied to investigate the performance of chosen ECC mixtures. This type of tests adopted two kinds of approaches; the first was to apply different fatigue stress levels namely 40, 55 and 70% at 50,000 cycles and 4 Hz cyclic loading rate. The second approach was to apply different fatigue cycles of loading namely 200,000, 300,000 and 1,000,000 cycles at fixed fatigue stress level which was 55% and 4 Hz cyclic loading rate as well. As a consequence, fly ash class CI ECC mixtures were omitted from this investigation; again, further detailed discussion will be provided in this chapter.

At the end of extensive testing and evaluation mentioned above, the best ECC mixtures were used to cast three link slab bridge deck specimens to investigate the performance of ECC under long-term creep behaviour. For comparison purposes, one of these specimens was cast using self-consolidating concrete while the other two were cast using fly ash class F ECC mixtures incorporating silica and crushed sands, respectively.

4.2 Slump and workability of ECC mixtures

After mixing was completed, the workability was assessed at 3 different levels, ranging between "self-compacting" "moderated workability" and "hard to compact". Table 4.1 shows the slump flow for all mixtures, T_{50} time and state of workability.

Table 4.1 The slump flow and T50 time for ECCs mixtures

Mix No.	Mix Designation	Slump Flow mm	Flow Time (T_{50}) sec	State of workability
1	CI_1.2_SS	540	2.54	self-compacting
2	CI_2.2_SS	530	2.98	self-compacting
3	F_1.2_SS	535	4.13	moderate workability
4	F_2.2_ SS	530	2.93	self-compacting
5	SL_1.2_ SS	550	1.58	moderate workability
6	SL_2.2_ SS	485	N.A.*	hard to compact
7	CI_1.2_CS	520	3.43	moderate workability
8	CI_2.2_CS	500	3.11	moderate workability
9	F_1.2_CS	490	N.A.*	hard to compact
10	F_2.2_CS	515	3.09	moderate workability
11	SL_1.2_ CS	420	N.A.*	hard to compact
12	SL_2.2_ CS	415	N.A.*	hard to compact

∗ The author could not get values of T_{50} because of bleeding issue

Through laboratory observations and as shown in Table 4.1, ECC mixtures with FA class F/CI with silica sand exhibited self-consolidating property while Slag ECC mixtures incorporating both silica and crushed sands had hard to compact state of workability. Slag ECC mixtures required more mixing time led to further stiffness of the mix. To overcome the stiffness problem, additional HRWRA was needed to adjust their workability state which may lead to bleeding issues.

4.3 Compressive Strength

The compressive strength test results of ECC mixtures incorporating different aggregate sizes and types, and fly ash and slag contents are summarized in Table 4.2.

Table 4.2 Compressive strength of ECC mix

Mix No.	Mix Designation	Compressive Strength (MPa) 28 days
1	CI_1.2_SS	62
2	CI_2.2_SS	53
3	F_1.2_SS	61
4	F_2.2_SS	52
5	SL_1.2_SS	69
6	SL_2.2_SS	67
7	CI_1.2_CS	60
8	CI_2.2_CS	47
9	F_1.2_CS	59
10	F_2.2_CS	45
11	SL_1.2_CS	69
12	SL_2.2_CS	67

Compressive strength test were performed at age of 28 days. Three cubic specimens were tested at mentioned age. As seen from Table 4.2 and as expected, the compressive strength of ECC mixtures decreased with increasing both FA class CI or F content. The reason behind this observation was the slower reactivity of the FA compared with cement (Sahmaran et al., 2008). However, even at approximately 70% replacement of cement by (FA/C = 2.2), the compressive strength at 28 days of ECC can still exceed that of normal concrete, and fulfill engineering requirements in most projects.

At the same replacement level, the slag produced significantly greater compressive strengths than either fly ash class F or CI. This is because the high proportion of Calcium Oxide (CaO)

content which is quite close to Portland cement that leads to rapid hydrates and reactions of slag compared to those of FA-ECC mixtures. Alexander et al. (2003) verified that compressive strength of concrete systems with slag replacement level of 25%, 50% and 75% are equal or slightly higher than concrete itself without slag, at the age of 28 days (Alexander et al., 2003). Again, the CaO content is playing an effective role between FA-ECC mixtures themselves; class CI mixtures exhibited slightly higher compressive strength than class F mixtures. It is found that Calcium Oxide CaO content is directly proportional with the compressive strength for all ECC mixtures. However, all the mixtures, showed compressive strengths higher than 45 MPa at 28 days of age.

At each SCMs replacement level, ECC mixtures with microsilica sand yielded slightly higher compressive strengths than those with crushed sand. In the case of normal concrete, because the surface texture is partly responsible for the bond between paste and aggregate, the crushed sand is expected to produce a better bond between paste and aggregate, and therefore, higher compressive strength compared with silica sand. However, as seen from Table 4.2, crushed sand produced almost similar or slightly lower compressive strengths than ECC mixtures with microsilica sand. Therefore, unlike conventional concrete, aggregate characteristics, such as the surface texture and sand sizes, did not influence the compressive properties in the case of ECC. In general, everything else remaining the same, the larger the aggregate size the higher the local water-cement ratio in the interfacial transition zone and, consequently, the weaker and more permeable would be the concrete (Mehta and Monteiro, 2006).

4.4 Fracture Energy

Fracture energy tests were conducted on ECC specimens at 7, 28 and 90 days. Tests were performed in accordance with RILEM TC50-FMC. The test results in terms of fracture energy, maximum beam deflection and maximum load capacity of ECC mixtures are given in Table 4.3 incorporating different aggregate sizes, fly ash class F and CI, and slag contents. Figure 4.1 illustrates the effects of FA-ECC, slag-ECC and aggregate sizes on the fracture energy of ECC matrixes as a function of the age of the matrix. The figure showed that the fracture energy values of the ECC matrixes containing slag were

Table 4.3 Fracture Energy, Deflection and Load test results of ECC mixtures

Mix ID.	Fracture Energy, (N/mm)			Deflection, (mm)			Load, (kN)		
	7 d	28 d	90 d	7 d	28 d	90 d	7 d	28 d	90 d
CI_1.2_SS	1.24	1.71	1.74	2.41	2.09	1.84	1.97	3.19	3.87
CI_2.2_SS	1.20	1.39	1.62	2.94	2.39	1.89	1.59	2.23	2.62
F_1.2_SS	1.87	1.98	2.02	3.08	2.23	1.89	2.20	3.38	3.97
F_2.2_SS	1.69	1.83	1.86	3.79	2.61	2.07	1.58	2.63	3.25
SL_1.2_SS	2.30	2.39	2.41	2.28	1.94	1.95	3.86	5.11	5.52
SL_2.2_SS	2.07	2.30	2.29	2.68	2.12	2.03	3.69	4.48	5.18
CI_1.2_CS	1.47	1.82	1.90	2.18	1.74	1.54	2.67	3.94	4.41
CI_2.2_CS	1.32	1.74	1.78	2.31	1.90	1.82	2.34	3.40	4.08
F_1.2_CS	1.99	2.14	2.21	2.86	2.05	1.79	2.51	3.93	4.55
F_2.2_CS	1.99	2.10	2.13	3.14	2.31	1.98	2.06	3.31	4.01
SL_1.2_CS	2.57	2.65	2.68	2.11	1.55	1.51	4.58	5.94	5.98
SL_2.2_CS	2.46	2.61	2.72	2.26	1.69	1.79	4.53	5.56	5.74

consistently more than the fracture energy of the ECC matrixes containing both types of FA. This was mainly due to the enhanced matrix strength even at early ages caused by the presence of slag particles. Slag particles were most commonly activated by the hydration product of Portland cement, where calcium hydroxide CaO formed during hydration was the principal activator. Slag hydration products lead to decreased porosity in the matrix, resulting in enhanced matrix strength. Higher matrix strength could be detrimental for achieving the desired mechanical properties, and reducing the margin to develop multiple cracking behaviours (Li et al., 1995). Therefore, in order to satisfy the limits on the matrix strength in slag-ECC mixtures in terms of fracture energy, aggregate particle size had to be reduced or the amount of slag replacement had to be increased as shown in Figure 4.1.

Test results also indicated that the use of FA particles should be helpful for achieving strain-hardening behavior, as lower fracture energy values provided better opportunities for multiple cracking in the composite. Wong et al. (1999) mentioned that adding FA class F at replacement levels of 45 and 55% reduced the fracture energy values at 28 days in

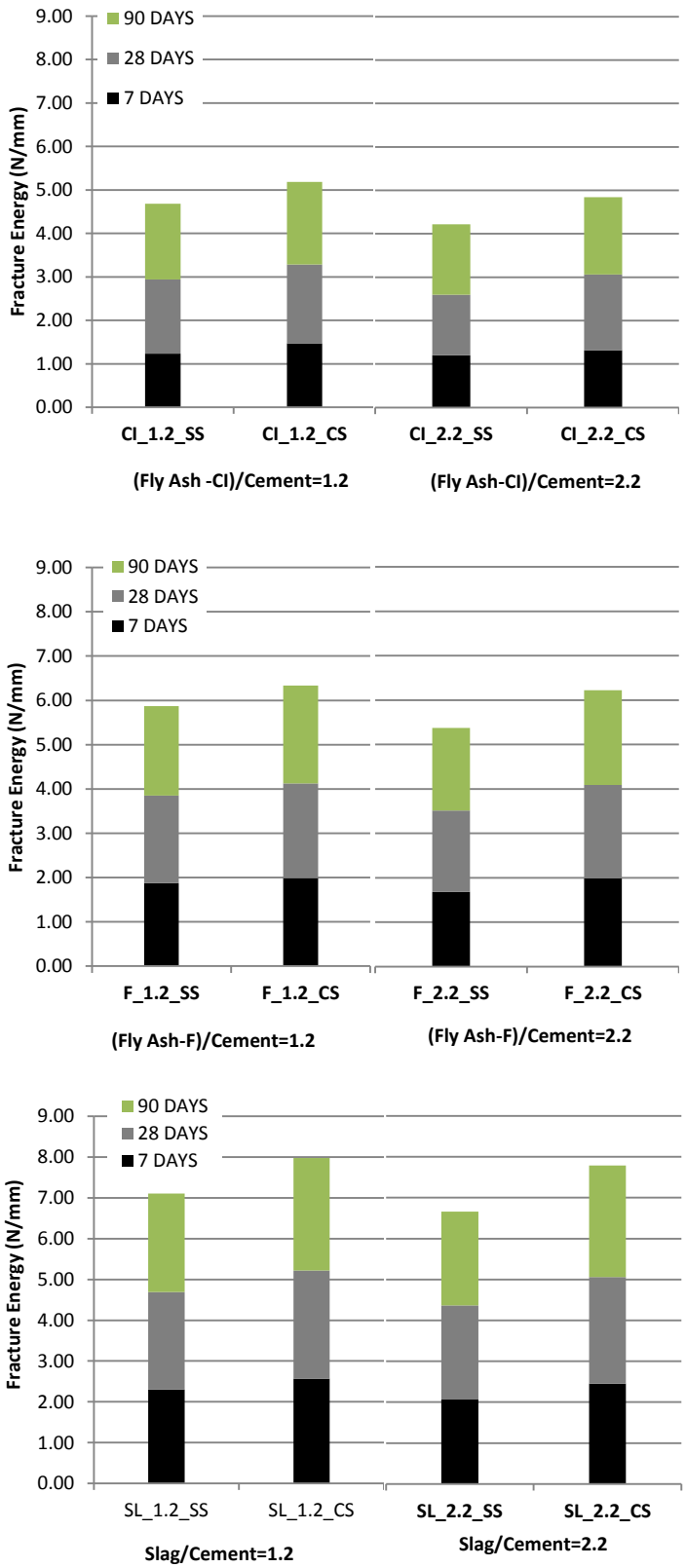

Figure 4.1 Fracture Energy and Deflection results as a function of the matrix age

conventional cement mortars (Wong et al., 1999). Consequently, fracture energy test results of ECC mixtures with the same aggregate sizes decreased as the replacement rate of SCMs increased as shown in Figure 4.1.

It is found that the fracture energy test results of ECC mixtures incorporating FA class F were slightly higher than those of ECC mixtures which were produced with FA class CI. This may be attributed to the fracture energy calculations adopted in the present study, see equation 3.1. From the equation, it can be seen that the value of the area under load deflection curves is playing a significant rule in increasing the fracture energy values. Accordingly, the mid span beam deflection values of fly ash class F ECC mixtures were much better than those of class CI; this will contribute to increasing the area under the curve values for these mixtures. However, fracture energy test results obtained with fly ash class F is still a way lower than the fracture energy test results obtained from slag-ECC mixtures which is helpful for achieving strain-hardening behavior.

It could be concluded that the relationship between the fracture energy and maximum beam deflection values is almost inversely proportional as shown in Figure 4.2.

The fracture energy of ECC matrixes with the same replacement rate of SCMs increased significantly as the aggregate size increased from SS =0.30mm to CS =1.18 mm. It is well known that when concrete is loaded, cracks prefer to propagate along the weaker interfacial zone or big larger pores in the matrix (Wu et al., 2000; Rao and Prasad, 2001; Chen and Liu, 2004; Bazant, 1979). As the crack meets an aggregate particle, it is forced either to propagate through the tougher aggregate or deflect and travel around the aggregate-mortar interface. For normal strength concrete, the cement paste is weaker than the aggregate. Cracks prefer to propagate along the cement paste, and then deflect and bridge cracks. Therefore, aggregate size increase results in more tortuous cracking path and more energy needed for cracking, and then higher values of fracture energy. The larger the maximum size of aggregate the more tortuous cracking path results in increased fracture energy.

Finally, Figure 4.3 shows the relationship between fracture energy and the compressive strength of ECC mixtures at 28 days. As in the case of high strength concrete (Rao and Prasad, 2001), fracture energy increases as the compressive strength increases.

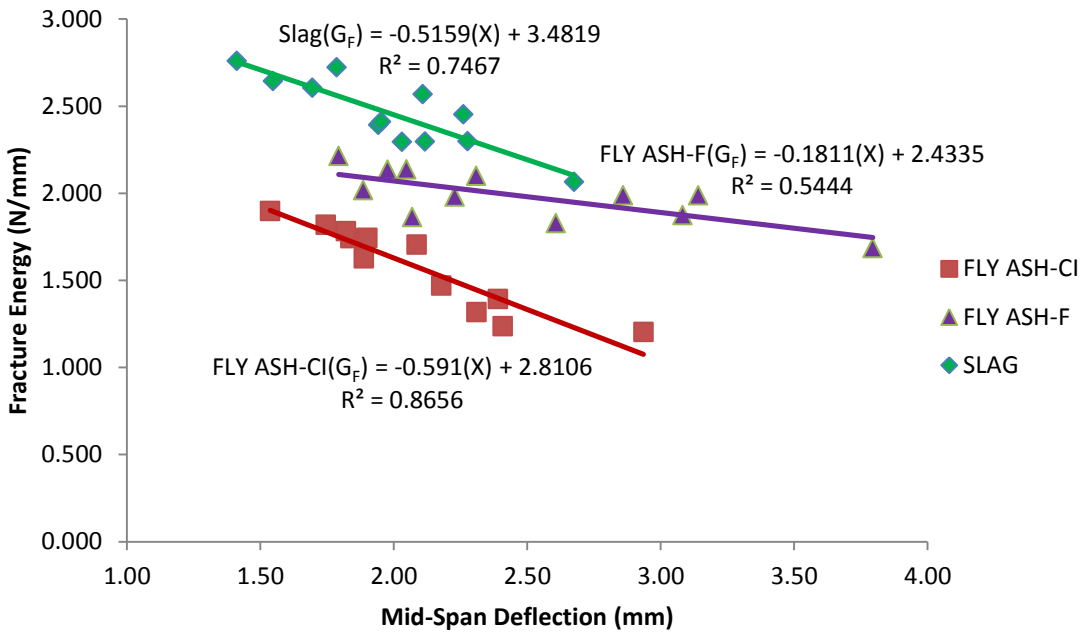

Figure 4.2 Relationship between mid-span beam deflections and fracture energy

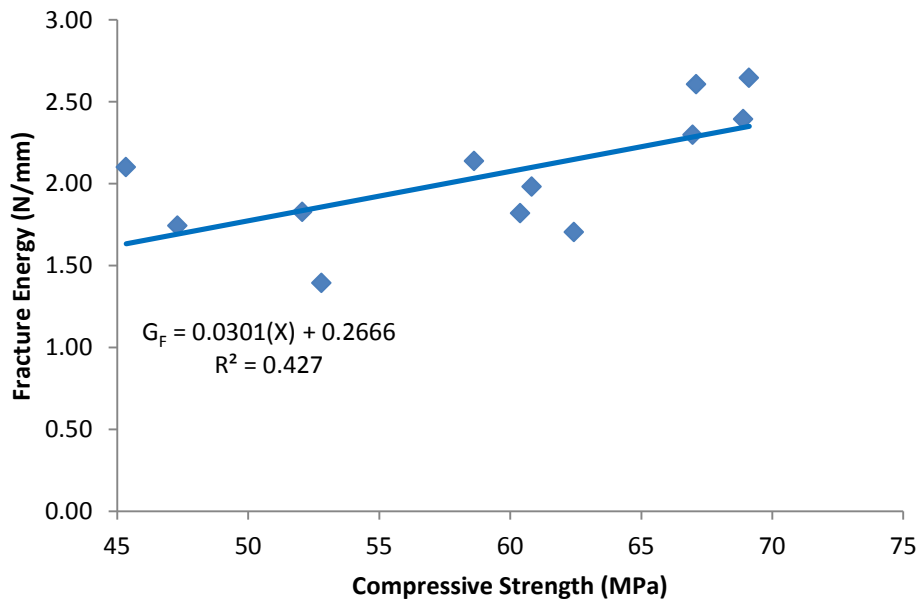

Figure 4.3 Relationship between fracture energy and compressive strength at 28 days

4.5 Flexural Strength

The test results in terms of flexural strength, modulus of rupture (MOR), and ultimate mid-span deflection are given in Table 4.4 at ages 28 and 56 days, and the typical flexural strength-mid span deflection curves of ECC mixtures at age of 28 days are shown in Fig. 4.4. To facilitate the comparison between the test results for different ECC mixtures, the same scales for both axes were used in these figures. Each result in Table 4.4 is the average of three measurements.

As seen from Table 4.4, the average ultimate flexural strengths vary from 10.48 to 15.81MPa and the bending capacity of the ECC beams vary from 1.61 to 4.45 mm depending on fly ash class CI, F and slag content.

Table 4.4 Flexural strength and ultimate deflection results at ages 28 and 56 days

Mix No.	Mix Designation	Flexural Strength			
		28 Days		56 Days	
		Stress (MPa)	Deflection (mm)	Stress (MPa)	Deflection (mm)
1	CI_1.2_SS	12.68	3.17	13.83	2.67
2	CI_2.2_SS	11.98	3.96	13.27	3.56
3	F_1.2_SS	11.80	3.91	12.38	3.75
4	F_2.2_SS	10.84	4.45	12.25	3.98
5	SL_1.2_SS	15.44	1.79	15.81	1.74
6	SL_2.2_SS	14.08	2.04	14.38	1.86
7	CI_1.2_CS	12.20	2.86	12.92	2.41
8	CI_2.2_CS	11.42	3.14	12.64	2.56
9	F_1.2_CS	11.20	3.66	12.12	3.26
10	F_2.2_CS	10.48	4.27	11.68	4.02
11	SL_1.2_CS	14.93	1.73	15.24	1.61
12	SL_2.2_CS	13.87	1.80	13.62	1.64

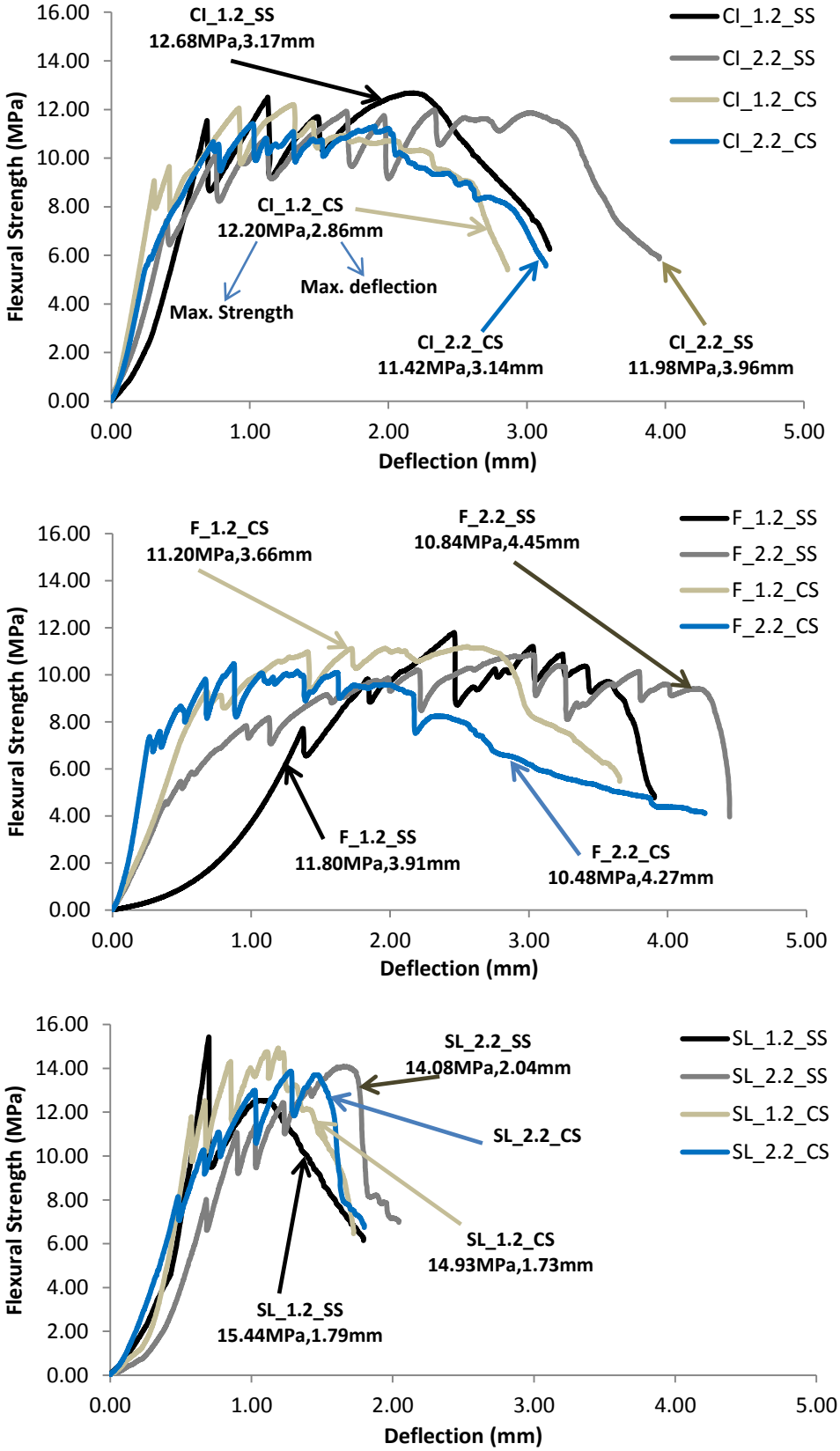

Figure 4.4 Typical flexural strength-mid span deflection curves of ECCs at 28 days

4.5.1 ECC's Deflection and Flexural Strength vs. SCMs Cement Replacement rate

Test results show that the increase of fly ash to cement ratio (FA/C) from 1.2 to 2.2 improved the bending capacity of ECC mixtures. The improvement in the bending capacity with the increase in the FA content can be attributed to the fact that the increase in the FA content tends to reduce the PVA fiber/matrix interface chemical bond and matrix toughness, while increasing the interface frictional bond, in favor of attaining high bending capacity (Wang and Li, 2007; Sahmaran et al., 2009). The slag-ECC mixes showed significantly lower deflection capacity when compared to the ductility of the FA-ECC mixes. The reduced ductility can possibly be caused by the higher fracture energy, bond strength and friction between the slag-ECC matrix and the fibers compared with FA-ECC mixes. The microstructural studies in macroscopic behavior of slag-ECC mixtures showed that there is no un-hydrated particles could be observed after the hydration process. This means that the fiber surfaces in slag-ECC have more attached matrix material compared to FA-ECC. For a fiber to be pulled out of the slag-ECC matrix, de-bonding at the fiber interface or fracture of the hydrate product is required to overcome interlocking of the hydrate product (Gao and Zijl, 2005). It should be noted that ECC mixtures incorporating with FA class CI were slightly higher than those of ECC mixtures which were produced with FA class F while mid-span beam deflection values of the former are lower than the later.

It is also apparent from the compressive strength test results that there is not a significant influence of the FA or slag replacement rate from 1.2 to 2.2 on the flexural strength values especially at the ages of 28 days or later in the tested range. However, even at about 70% replacement of cement by FA or slag, the flexural strength of ECC at 28 days was significantly higher than that of conventional concrete and fiber reinforced concrete.

4.5.2 ECC's Deflection and Flexural Strength vs. Aggregate Size

Adverse effect of increased size of aggregates on bending capacity performances of ECC mixtures was observed. The increase in aggregate size up to 1.18 mm slightly reduces the ductility characteristics and total mid-span beam deflection of ECC mixtures as shown in Table 4.4. The negative effects of increasing aggregate size on ductility may be attributed to

the adverse effect on the uniform dispersion of fibers. The balling of fibers encouraged by coarser sands at constant sand content prevents sufficient coating of fibers by the matrix, and thus reduces the fiber-to-matrix bonding, which is an important factor influencing ductility (Sahmaran et al., 2009). Moreover, for ECC with the larger aggregate size, a higher degree of aggregate interlock is expected, resulting in higher matrix toughness and work-of-fracture during crack propagation. According to the micromechanical model of steady state cracking, which is essential to achieving strain hardening behavior, high matrix fracture toughness reduces the margin to develop multiple cracking (Li et al., 1995). However, aggregates within the size range studied, as long as they do not interfere with the uniform dispersion of fibers, do not negatively influence the ductility of ECC (Sahmaran et al., 2009).

As in the case of compressive strength test results, the aggregate particle size had no or only a minor effect on the flexural strength test results. Simultaneously, flexural strength and mid-span deflection obtained with crushed sand is within the permissible limit of silica sand and might be similar or even better than the mechanical properties of ECC mixtures made with silica sand (Sahmaran et al., 2009).

It could be concluded that the most important feature of ECC, high ductility with multiple cracking behaviors, was protected and is not sacrificed by replacing cement with a maximum of 70% FA or by replacing silica sand with crushed sand.

4.5.3 Crack Characterization

For all ECC specimens, the first cracks to appear were flexural cracks starting at the surface of the tension face. After first cracking, the load continues to rise accompanied by multiple cracking, which contributes to the inelastic deformation as stress increases. Shortly after initial cracking, the crack width grows rapidly with an increase of deformation, and then stabilizes at a value between 25 to 100 μm while additional micro-cracks further developed. Micro cracks developed from the first cracking point and spread out in the mid-span of the flexural beam as shown in Figure 4.5. Bending failure in ECC occurred when the fiber bridging strength at one of the micro cracks was reached; resulting in localized deformation at this section (Figure 4.5) once the flexural strength is approached. After performing the

four-point bending test, the bending load was released and specimens were taken out the testing machine. A crack closure occurred on unloading position and it was observed in this study that the width of a loaded crack is approximately 30% more than the width of the unloaded one. All crack width measurements were conducted in the unloaded stage. The widths of the crack were measured on the tension surface of the specimens by using a crack microscope. Table 4.5 shows average crack widths and number of cracks on the span length of 102 mm at the center of prism specimen. Each data point in Table 4.5 is an average of at least three or more prism specimens and more than 10 μm crack widths were measured from each specimen. All of the ECC mixtures showed a crack width smaller than 100 μm.

Table 4.5 Average Crack Widths and Number of Cracks for ECC mixtures

Mix ID.	Crack No.		Crack width (μm)	
	28 d.	56 d.	28 d.	56 d.
CI_1.2_SS	11	7	63	50
CI_2.2_SS	49	20	50	25
F_1.2_SS	13	20	50	25
F_2.2_SS	105	40	50	50
SL_1.2_SS	5	2	100	100
SL_2.2_SS	13	6	75	63
CI_1.2_CS	17	18	50	50
CI_2.2_CS	33	19	50	50
F_1.2_CS	25	23	50	25
F_2.2_CS	119	30	25	25
SL_1.2_CS	10	8	75	50
SL_2.2_CS	15	6	75	63

As shown in Table 4.5, the number of crack increased and crack width reduced significantly as SCMs content increased at all ages. Adversely, the slag-ECC mixtures exhibited larger crack widths and less number of cracks than those of fly ash ECC mixtures. On the other hand, the use of aggregate up to 1.18 mm maximum aggregate size did not influence the average residual crack width for all ECC mixtures studied.

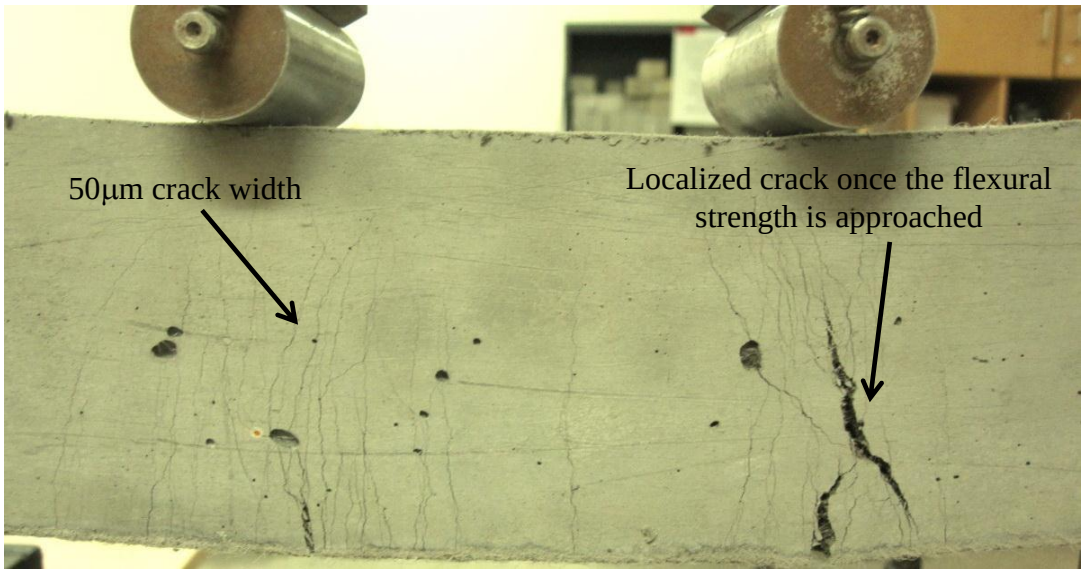

Figure 4.5 Typical cracking patterns of ECC beam specimen after flexure loading (Mix ID: F_2.2_SS)

Crack width control is of primary importance for many reinforced concrete applications because it is believed that there is a close relationship between the mean or maximum crack widths and the durability of the structure. Moreover, the lower magnitude of the crack width is expected to promote self-healing behavior and, thus, the transport properties in cracked composites (Sahmaran et al., 2007, Sahmaran et al., 2009). Consequently, in the serviceability limit state, a mean or maximum crack width less than approximately 0.1 mm (100 μm) is usually prescribed (Reinhardt and Jooss, 2003; Sahmaran et al., 2009).

4.5.4 Side Way Flexural Performance

Flexural strength test is an indirect measure of direct tensile performance (direct tensile strength) considered to be the most accurate and effective method to confirm the strain-hardening behavior of a composite depending on the specimen geometry. It is known that flexural performance of concrete is one of the principle concerns in designing concrete structures. Therefore, it is essential to give more interest to investigate the flexural strength and ductility performance of ECC mixtures.

To confirm the case of ECC mixtures with respect of flexural strength and mid-span deflection performance, the external loads were applied on ECC beams in the direction of the

short side of the specimen's cross sectional area (b = width) as shown in Figure 4.6. This kind of testing gives more capacity to resist more mid-span beam deflection due to the large area which might resists the external applied loads on the tested ECC beams. Moreover, in the case of ECC mixtures, more PVA fibers are to be involved in the load carrying capacity process due to large resistant area as well.

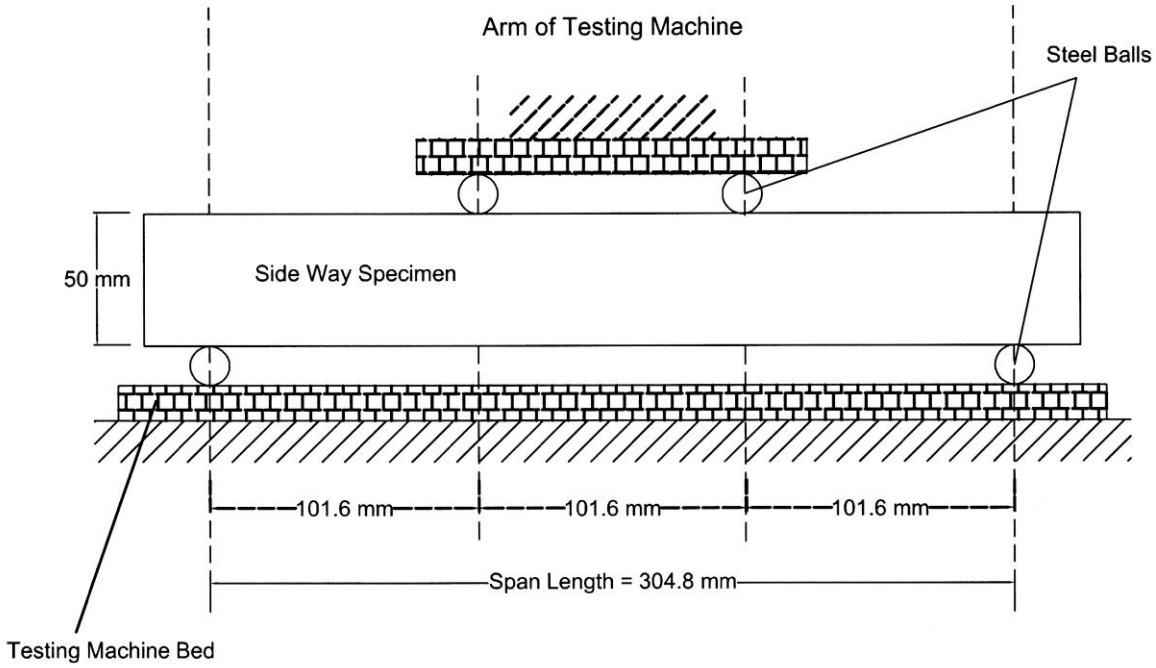

Figure 4.6 Four point bending test setup for Side way specimens

In this section, the author preferred to investigate ECC mixtures with 70% cement replacement (SCMs/C = 2.2) only. This was due to the fact that, as was found before, the increase of SCMs/C ratio from 1.2 (50% cement replacement) to 2.2 (70% cement replacement) improved the bending capacity of ECC mixtures.

The test results of side way in terms of flexural strength and ultimate mid-span deflection for ECC mixtures with cement replacement (SCMs/C = 2.2) at age of 28 days are presented in Table 4.6. Figure 4.7 shows the side way typical flexural strength-mid span deflection curves of ECC mixtures as well.

Table 4.6 Side way flexural strength and deflection performance of ECC mixtures

Mix ID.	Mix Designation	Side way test results at age of 28 days with (SCMs/C =2.2: 70% cement replacement)	
		Strength (MPa)	Deflection (mm)
2	CI_2.2_SS	12.70	5.90
4	F_2.2_SS	12.24	7.94
6	SL_2.2_SS	14.34	2.72
8	CI_2.2_CS	12.48	6.04
10	F_2.2_CS	12.11	7.85
12	SL_2.2_CS	14.30	2.85

As seen from Table 4.6, the average ultimate flexural strengths vary from 12.11 to 14.34 MPa and the bending capacity of the ECC beams vary from 2.72 to 7.94 mm depending on fly ash class CI, F and slag content.

It is found that F_2.2_SS and F_2.2_CS mixtures exhibited superior performance with respect of mid-span beam deflection capacity. It should be noted that both of them exhibited hairline crack widths, less than 50 μm, even with this extreme mid-span beam deflection performance as shown in Figure 4.8.

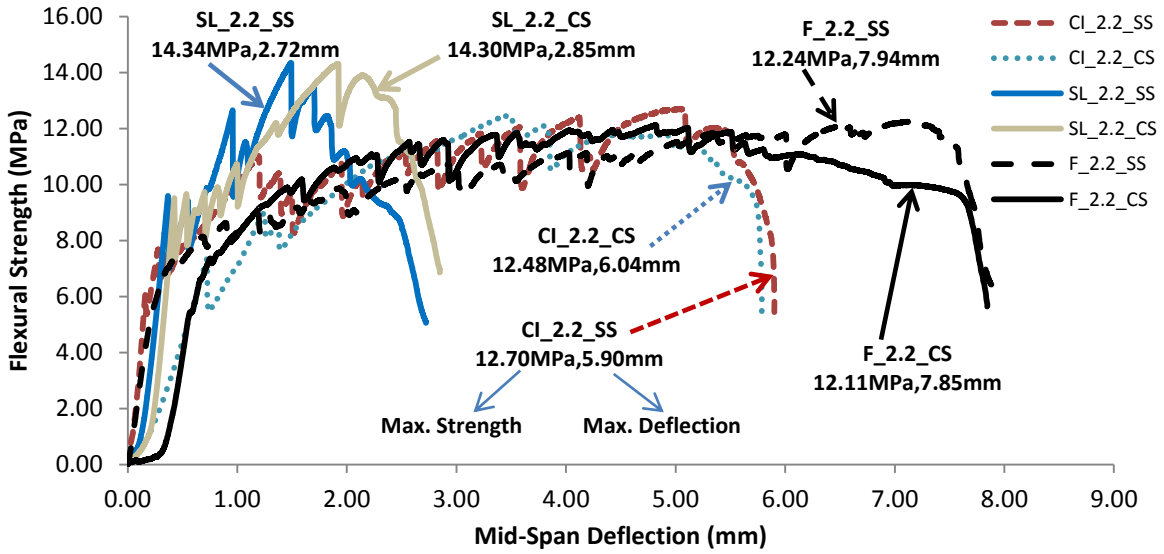

Figure 4.7 Typical side way flexural strength versus mid-span deflection curves of ECC mixtures, (SCMs/C=2.2), at age of 28 days

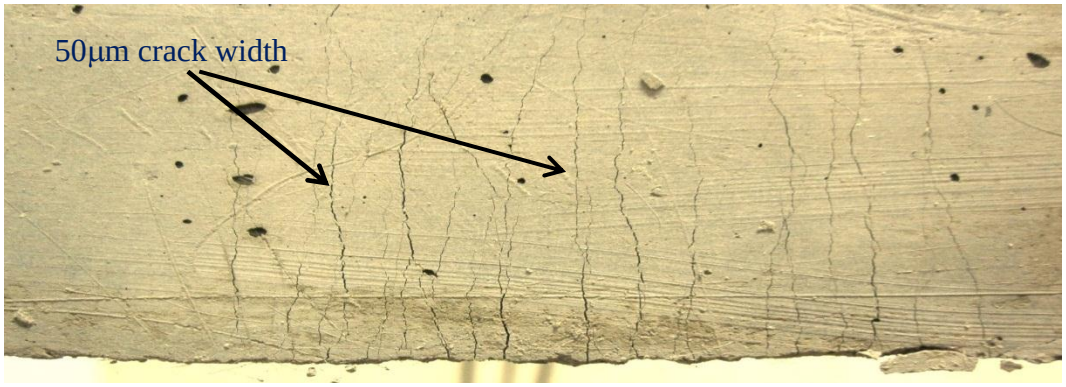

Figure 4.8 Typical side way cracking patterns of ECC beam specimen after flexure loading (Mix ID.: F_2.2_CS)

4.5.5 General Fatigue Flexure Performance

As mentioned before, the first part of the second phase in this study aims at investigating the flexural strength characteristics of the two ECC groups by applying flexural static testing at 28 and 56 days. The second part was flexural fatigue tests which were performed under load control conditions at 28 days only. Specimens were subjected to 4 Hz sinusoidal cyclic loading for 50,000 cycles. The maximum fatigue stress level was fixed at 55% of the averaged flexural strength results of ECC control specimens. At the end of the fatigue flexural tests, static flexural tests were applied on the fatigued ECC specimens to calculate the fatigue residual energy. The objective of this step was to assess the ECC mixtures initially to choose the best ECC mix designs to be included into the third phase. The fatigue test results of 12 specimens of the 12 ECC mixtures are presented in Table 4.7.

Table 4.7 shows the test result values of both flexural static testing without fatigue loading and after fatigue loading tests. By using these results, the percentage of fatigue residual energy of the fatigued ECC specimens for both residual stress and deflection could be calculated by the Equation (4.1):

$$\text{Residual Energy (\%)} = -1 \times \left\{ \left(\left(\frac{MOR_{without\,fatigue\,test} - MOR_{after\,fatigue\,test}}{MOR_{without\,fatigue\,test}} \right) \times 100 \right) - (100) \right\} \ldots (4.1)$$

As seen from Table 4.7, FA-ECC mixtures with 50% cement replacement (FA/C = 1.2) showed superior performance relative to high-volume fly ash mixtures with 70% cement replacement (FA/C = 2.2) with respect to both flexural fatigue strength and deflection. The flexural fatigue strength remains equal or slightly lower than flexural static strength.

Table 4.7 Fatigue Flexural Test Results

Mix ID.	Mix Designation	SCM/C (%)	Flexural Static Testing		Flexural Static After Fatigue Testing		Residual Energy (%)	
			Stress (MPa)	Deflection (mm)	Stress (MPa)	Deflection (mm)	Residual Stress (%)	Residual Deflection (%)
1	CI_1.2_SS	50%	12.68	3.17	11.77	3.92	92.82	123.66
3	F_1.2_SS		11.80	3.91	11.16	5.29	94.58	135.29
7	CI_1.2_CS		12.20	2.86	10.72	3.32	87.87	116.08
9	F_1.2_CS		11.20	3.66	10.75	4.81	95.98	131.42
2	CI_2.2_SS	70%	11.98	3.96	7.91	2.41	66.03	60.86
4	F_2.2_SS		10.84	4.45	7.04	3.09	64.94	69.44
8	CI_2.2_CS		11.42	3.14	8.13	2.58	71.19	82.13
10	F_2.2_CS		10.48	4.27	11.88	5.55	113.39	129.98
5	SL_1.2_SS	50%	15.44	1.79	8.91	0.94	57.73	52.57
11	SL_1.2_CS		14.93	1.73	11.12	1.17	74.45	67.80
6	SL_2.2_SS	70%	14.08	2.04	6.33	0.82	44.98	40.10
12	SL_2.2_CS		13.87	1.80	9.35	0.96	67.44	53.11

Naik et al. (1993) reported that conventional plain concrete with class C fly ash mixture having 15% cement replacement showed superior performance relative to high-volume fly ash mixture with 50% cement replacement with respect to compressive strength and flexural fatigue strength (Naik et al., 1993). Tse et al. (1986) indicated that concrete with equivalent or higher compressive and fatigue strength could be obtained with cement replacement of 25% by weight of low-calcium fly ash (class F) or 50% by weight of high-calcium fly ash (class C). The reason of ordinary performance of FA-ECC mixtures with 70% cement replacement relative to 50% cement replacement in both flexural fatigue strength and deflection can be attributed to the fixation of fatigue stress level at 55%. Suthiwarapirak et

al. (2004) indicated that the evolution of mid-span deflection depends on the fatigue stress level. Namely, the mid-span deflection increased to more than twice as much under high fatigue stress levels S=0.8–0.9 compared to that under low stress levels S=0.5–0.6 (Suthiwarapirak et al., 2004). However, as shown in the Table 4.7, fly ash concrete mixtures with cement replacement 50 and 70% showed almost the same results when flexural fatigue strength was expressed as percentage of the flexural static strength.

Surprisingly, fatigue test results showed that F_2.2_CS ECC mixture with conventional sand had a remarkable performance with respect to both flexural fatigue strength and deflection. The unique performance of F_2.2_CS ECC mixture is almost equal to the superior performance of FA-ECC mixtures with 50% cement replacement in fatigue deflection and even better than them in fatigue strength.

Slag-ECC mixtures with 50 and 70% cement replacement exhibited inferior performance with respect to both flexural fatigue strength and deflection. Ozaki and Sugata (1992) found out that the compressive fatigue limit ratios at two million cycles in water were 41% for the concrete with blast furnace, 44% for the silica fume concrete, and 31% for the plain cement concrete at 50% probability of survival fatigue life.

As a final consequence, Slag-ECC mixtures reached to the final point and should be omitted from this research according to many reasons. Higher fracture energy values could be positive for achieving the desired mechanical properties, but on the other hand reducing the margin to develop multiple cracking behaviour. High bond strength and friction between the slag-ECC matrix and the fibers compared with FA-ECC results in a significant lower deflection capacity. Further, larger crack widths produced by slag ECC-mixtures reduces crack width control which is expected to promote self-healing behavior and may lead to low durability for link slab applications. Finally, inferior performance with respect to both flexural fatigue strength and deflection resulting in omitting the slag-ECC mixtures from this research. Although slag-ECC mixtures exhibit smaller deformation capacity compared with FA-ECC, their flexural deflection capacity is around or more than 2 mm at 28 days of age.

The 2 mm deflection capacity remains almost 150 times higher than that in normal concrete and conventional fiber reinforced concrete.

Due to research time constraints, the author had to choose between the remaining two groups of FA-ECC mixtures (50 or 70% of cement replacement mixtures). So, he had chosen the 70% cement replacement group rather than 50% due to number of reasons. In general, fly ash has been used to replace cement in ECC mixture because of the absence of coarse aggregate in ECC results in higher cement content. Partial replacement using FA reduces the environmental burden. Further, it has been found that the addition of FA at high volumes improves the fresh and durability properties, reduces the drying shrinkage and matrix toughness, and improves the robustness of ECC in terms of tensile ductility (Wang and Li, 2007; Yang et al., 2007). Additionally, un-hydrated FA particles with a small particle size (<45 μm) and smooth spherical shape serve as filler particles resulting in higher compactness of the fiber/matrix interface transition zone that leads to a higher frictional bond, which aids in reducing the steady-state crack width beneficial for the long-term durability of the structure (Wang and Li, 2007; Yang et al., 2007).

Accordingly, fly ash-to-cement ratio (FA/C) of 2.2 was chosen in the following phase to satisfy the above requirements, while still maintaining adequate flexural and compressive strength properties similar to that of normal-strength concrete. The ECC mixtures selected to be involved in the third phase were CI_2.2_SS, F_2.2_SS, CI_2.2_CS and F_2.2_CS.

4.6 Special Fatigue Flexure Performance

In this phase, fatigue flexure tests were conducted in two different approaches; the first approach applied different fatigue flexural stress levels namely 40%, 55% and 70% of the average maximum static stress for 50,000 cycles at 4 Hz cyclic loading rate and the second approach applied different fatigue cycles namely 200,000, 300,000 and 1,000,000 cycles at 4 Hz cyclic loading and 55% fatigue stress level as well.

It should be noted that new samples of the selected ECC mixtures for this phase were cast following the same casting procedure and kept in same curing conditions to get fair results after testing them.

4.6.1 First Approach-Fatigue Stress Levels

4.6.1.1 Mid-span Deflection Evolution

The evolution of the average mid-span deflection as the number of cycles increased to 50000 cycles for ECC specimens with different fatigue stress levels of 40, 55 and 70% are plotted in Figure 4.9. Only a typical result at each fatigue stress level is shown in the figure.

The results showed that FA-ECC specimens with silica sand (CI_2.2_SS and F_2.2_SS) under fatigue loading developed much more damage than FA-ECC specimens with crushed sand (CI_2.2_CS and F_2.2_CS). The range of displacement evolution of ECC specimens between the maximum stress and minimum stress levels was very large except for F_2.2_CS specimen. Under high stress level 70%, the displacement at the maximum stress evolved up to about 2.1 mm mid-span deflection in silica sand ECC mixtures while the CI_2.2_CS specimen evolved up to 1.35 mm compared to 0.7 mm for the F_2.2_CS specimen. The evolution of the mid-span deflection was found to depend on the fatigue stress level. The mid-span deflection increased to around or more than twice at high fatigue stress level 70% compared to that under low fatigue stress level 55%. It should be noted that FA-ECC mixtures with silica sand exhibited slightly higher deformation capacity than FA-ECC mixtures with crushed sand under static loading while exhibited much higher deformation capacity under fatigue loading. It is also noticed that the CI_2.2_CS mixture exhibited higher deformation capacity than the F_2.2_CS mixture under fatigue loading. This is contrary to the fact that the former had lower deformation capacity than the latter under static loading.

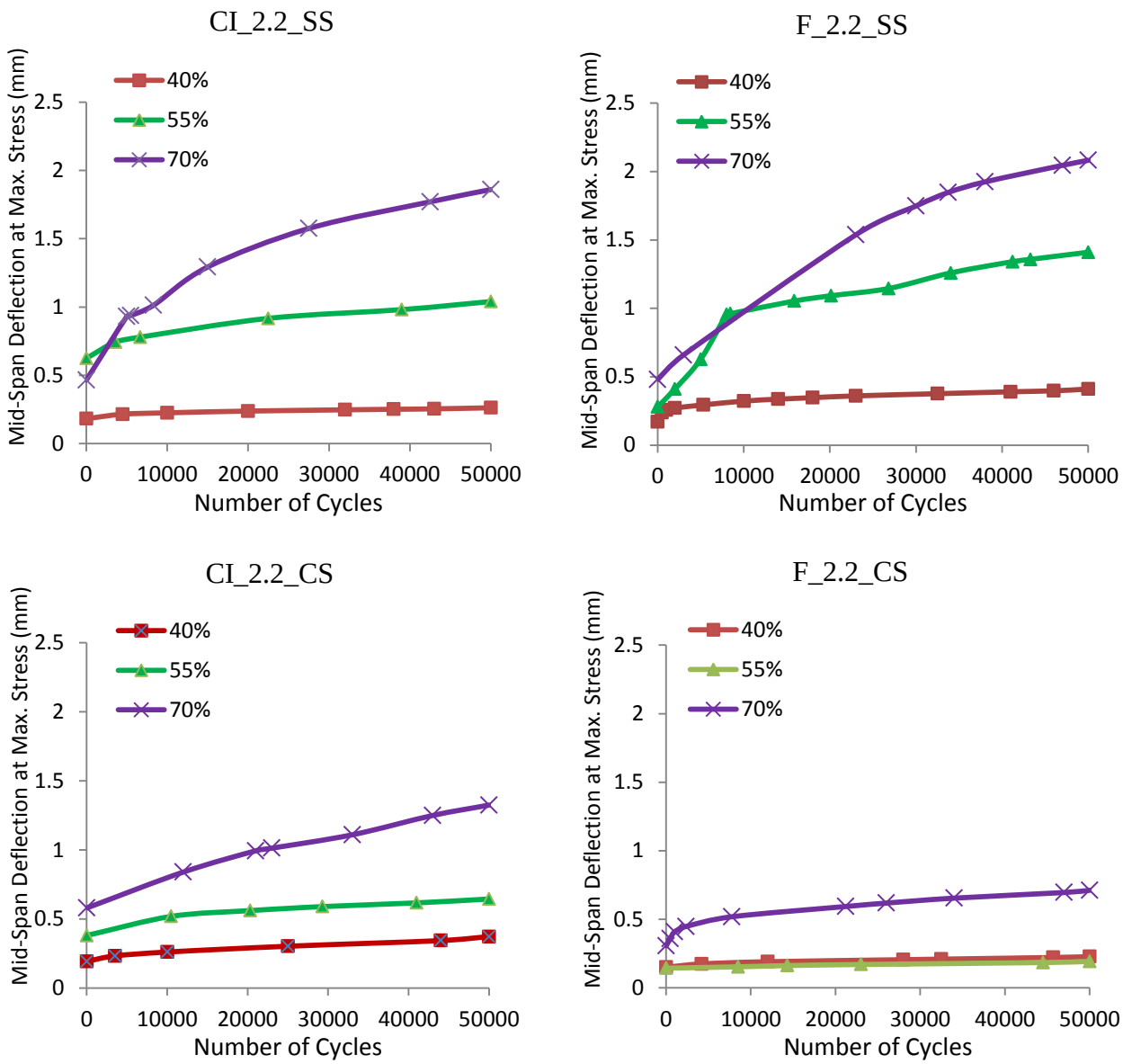

Figure 4.9 Evolution of mid-span deflection at different fatigue stress level

Table 4.8 Speed Rate of Mid-Span Deflection Evolution at Different Fatigue Stress Levels

Mix ID.	Mix Designation	Fatigue Stress Levels					
		Difference Between First and Last Values of Mid-Span Beam Deflection (μm)			Mid-Span Evolution Speed Rate (μm/208 min)		
		40%	55%	70%	40%	55%	70%
1	CI_2.2_SS	260-180= 80	1040-630=410	1860-465=1395	80/208 = 0.39	2.00	6.70
2	F_2.2_SS	410-170=240	1410-280=1130	2080-480=1600	1.15	5.43	7.70
3	CI_2.2_CS	373-193=180	645-381=264	1325-580=745	0.87	1.27	3.58
4	F_2.2_CS	227-150=77	192-143=47	711-306=405	0.37	0.24	1.95

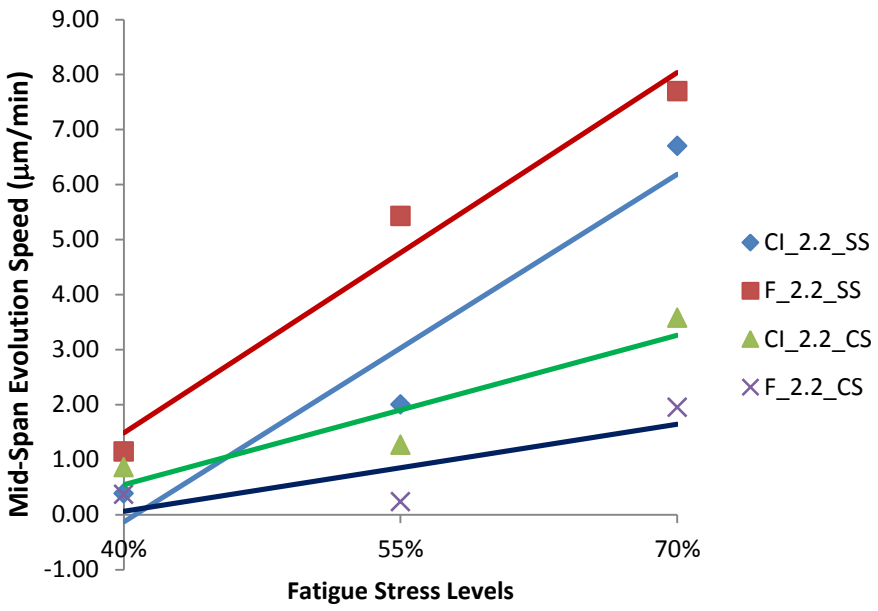

Figure 4.10 Speed Rate of Mid-Span Evolution at Different Fatigue Stress Levels

The fatigue flexural tests in this approach were applied for 50000 cycles at 4 Hz cyclic loading rate. 4 Hz means 4 cycles per second; therefore, the time required to finish 50000 cycles is 12500 seconds or 208 minutes. According to this, the mid-span evolution speed rate could be calculated at different fatigue stress levels, 40, 55 and 70% of maximum static stress as shown in Table 4.8. For example, as shown in Figure 4.9, at fatigue stress level 40% for CI_2.2_SS mixture, the mid-span evolution started at 180 µm and achieved at 260 µm when the 50,000 cycles were done. The difference between these two values is 80 µm; divided this value by 208 minutes resulted in 0.39 µm/min as shown in Table 4.8. Figure 4.10 shows the speed rate of mid-span evolution for all ECC mixtures. As seen from the Figure and as was expected, FA-ECC mixtures with silica sand have the highest speed rate of the evolution of mid-span deflection than FA-ECC mixtures with crushed sand while F_2.2_CS has the lowest speed rate in the two groups. This means that silica sand mixtures are developing much more damage under fatigue loading. The results of speed rate mid-span evolution of all ECC mixtures are consistent with the results of mid-span deflection evolution (Figure 4.9).

4.6.1.2 Number and Width of Cracks

Figures 4.11 and 4.12 illustrate the crack numbers and the crack widths of ECC mixtures respectively. It should be noted that the results in this section have been collected when the static loading was applied after the fatigue loading.

It was found that more cracks formed at higher fatigue stress levels and unexpectedly few cracks formed at lower fatigue stress levels. At 40% stress level, only a small number of cracks formed, meaning that ECCs tend to behave in a similar fashion to single cracking conventional normal concrete. The reason behind this is not clear but Qian and Li (2008) suggested that when the fatigue load level decreases, it is more difficult for ECC beams to reach saturated multiple cracking since the corresponding tensile stress at the bottom of the beam may be very close to the cracking strength.

It was noticed that the F_2.2_CS mixture had higher number of cracks and smaller value of crack widths than other ECC mixtures as shown in Figures 4.11 and 4.12, respectively. However, it has to be mentioned again, at least at the range of low number of cycles studied in the present approach, that the large number of cracks with small width did not increase the deformation capacity in the case of fatigue as in F_2.2_CS mixture (Figure 4.9). As was expected, the relation between crack widths and fatigue stress level was directly proportional as shown in Figure 4.12.

In general, it can be concluded that the final number of multiple cracks of ECC mixtures is depending on a maximum fatigue stress level and also that the multiple cracking behaviour terminates earlier at a lower stress level.

There is a need to confirm whether or not multiple cracks can be formed in ECC mixtures even under fatigue loading, since structural applications can't be realized when the multiple cracking ability of ECC is negated during fatigue loading. Especially when improved durability is expected with ECC, the formation of fine multiple cracks is a necessary condition to minimize the migration of aggressive substances and could be the key to assess the feasibility of the structural applications under fatigue loading (Matsumoto, 1998).

The results of the present study for fatigue testing confirmed that ECC mixtures showed multiple cracking under flexural fatigue loading as well as static loading. Figure 4.13 confirms this fact. As shown in the photograph, the colored cracks resulted under flexural fatigue loading while the new, un colored, cracks resulted under flexural static loading which applied after fatigue loading to get the residual energy in the tested ECC beam. To highlight even more on the performance of F_2.2_CS and F_2.2_SS ECC mixtures according to multiple cracking behaviour, the results of both mid-span deflection evolution as in Figure 4.8 and crack measurement data as in both Figures 4.11 and 4.12 could be used. It can be concluded that the F_2.2_SS mixture exhibited more damage under fatigue loading than the F_2.2_CS ECC mixture as the evolutions of mid-span deflection was higher, and the total number of cracks of the SS mixture was lower than the CS mixture at the same fatigue stress level. This was caused by the fact that ECC exhibited multiple cracks and that the number of cracks initiated depended on the fatigue stress level. The number of cracks was higher when the specimens underwent high fatigue stress levels.

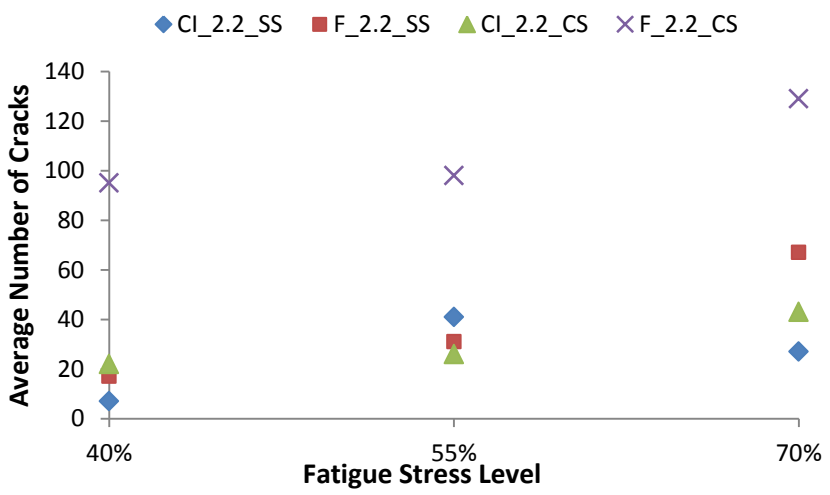

Figure 4.11 Average numbers of cracks at each fatigue stress level

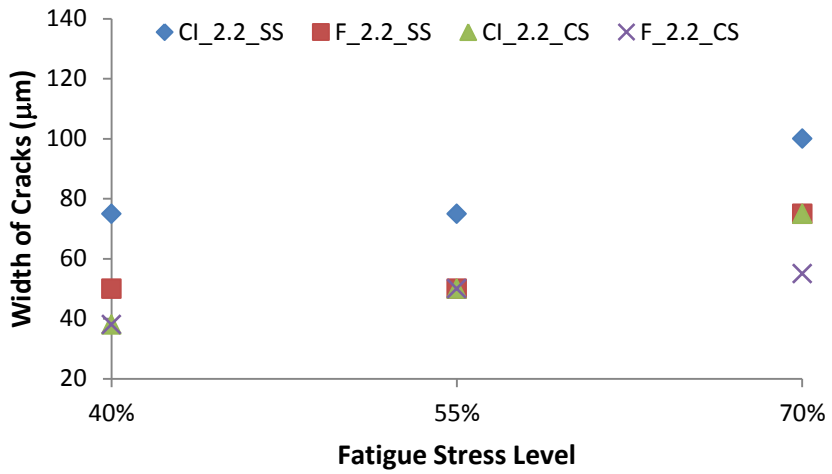

Figure 4.12 Crack Widths at each fatigue stress level

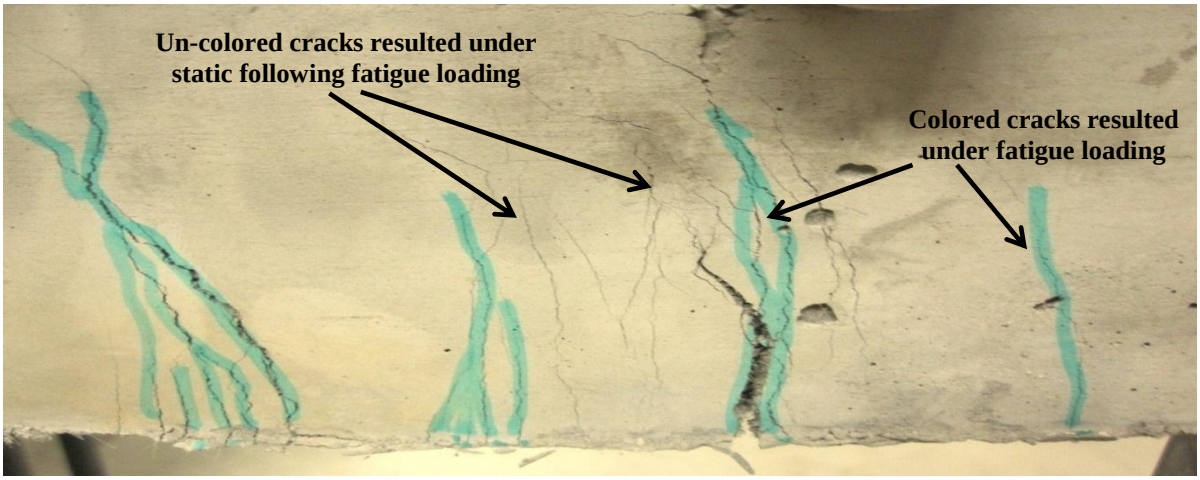

Figure 4.13 Multiple Cracking under Flexural Fatigue Loading

4.6.1.3 Static Tests after Fatigue Loading

At the end of the fatigue flexural tests as performed in the second phase, static flexural tests were applied on the exhausted and fatigued ECC specimens to calculate the fatigue residual energy for both strength and mid-span deflection. The fatigue flexural tests were expressed as percentages of static flexural tests and the residual strength and deflection are presented in Figures 4.14 and 4.15, respectively.

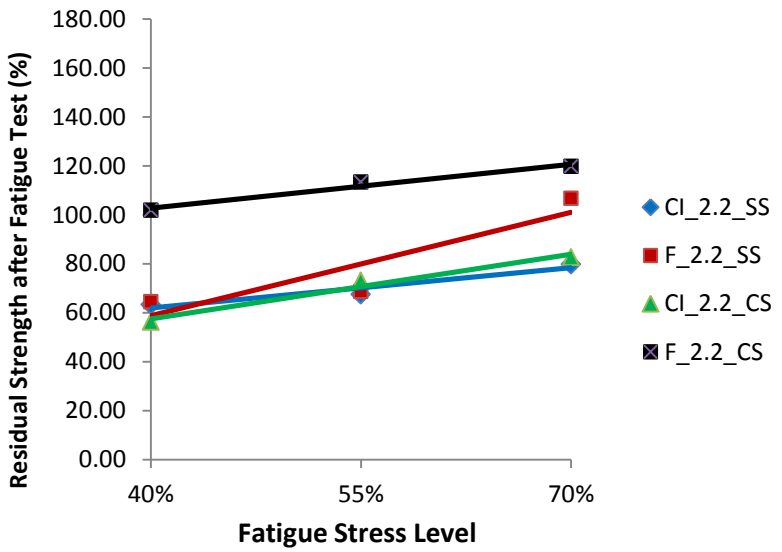

Figure 4.14 Percentages of Residual Strength after Fatigue Test

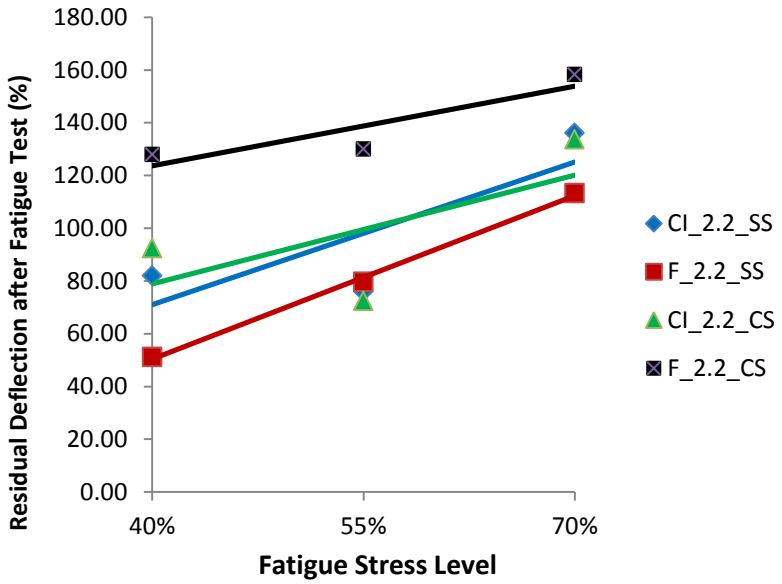

Figure 4.15 Percentages of Residual Mid-Span Deflection after Fatigue Test

Figures 4.14 and 4.15 show that at higher fatigue stress level (70%), all ECC mix designs exhibited higher strength and deformation capacity than lower fatigue stress levels (40 and 55%). Suthiwarapirak et al. (2004) indicated that when a high fatigue stress level was applied, ECCs exhibited a significantly prolonged fatigue life in comparison with other FRC due to their multiple crack characteristics. Their fatigue life tended to be equivalent to or become shorter than that of FRC at lower fatigue stress levels (Suthiwarapirak et al., 2004).

As mentioned in the second phase, at 55% of fatigue stress level, FA-ECC mixtures with 70% cement replacement exhibited ordinary performance relative to 50% cement replacement for both residual fatigue strength and deflection. It is found that when comparing ECC mixtures with 70% cement replacement under 70% of fatigue loading stress level to those 50% cement replacement under 55% of fatigue loading stress level with, the former showed equal or slightly higher superior performance of the latter with respect to both residual fatigue strength and deflection. For convenience, the second phase results of both fatigue strength and mid-span deflection are presented in Table 4.9 compared to present phase results. These results confirm that the selection for FA-ECC mixtures with 70% cement replacement to be included in the third phase was a good choice.

Table 4.9 Comparison between second and present Fatigue strength and deflection results

Mix ID.	Mix Designation	Residual Fatigue Energy at 55% of Stress Level (Second Phase)		Residual Fatigue Energy at 70% of Stress Level (Present Phase)	
		Residual Stress (%)	Residual Deflection (%)	Residual Stress (%)	Residual Deflection (%)
1	CI_1.2_SS	92.82	123.66	-	-
3	F_1.2_SS	94.58	135.29	-	-
7	CI_1.2_CS	87.87	116.08	-	-
9	F_1.2_CS	95.98	131.42	-	-
2	CI_2.2_SS	66.03	60.86	79.76	136.11
4	F_2.2_SS	64.94	69.44	106.71	113.26
8	CI_2.2_CS	71.19	82.13	82.69	133.69
10	F_2.2_CS	113.39	129.98	119.76	158.29

It is noticed that at 70% fatigue stress level, the F_2.2_SS mixture still shows high flexural strength capacity (106.71%) even with larger deflections during fatigue loading found in the results of the mid-span deflection evolution (2.082mm) (Figure 4.9). Again, it should be noted that the F_2.2_CS mixture shows the highest superior performance consistently at all fatigue stress levels with respect to residual fatigue stress and mid-span deflection as shown in Figures 4.14 and 4.15, respectively. In the case of F_2.2_CS, it is noticed that the mid-span deflection evolution is inversely proportional to the residual fatigue flexural strength

and mid-span deflection capacity. The lower the mid-span deflection evolution as in Figure 4.9 the higher the residual fatigue flexural strength and deflection capacity as in Figures 4.14 and 4.15, respectively. F_2.2_CS behaved as fiber reinforced concrete (FRC) under fatigue loading. Suthiwarapirak et al. (2004) mentioned that the evolution of mid-span deflection for FRC was very small. But unlike FRC behaviour when static loading was applied after fatigue loading at high fatigue stress levels, the residual energy for both stress and deflection was much larger than both FRC and even F_2.2_SS. To highlight the practical application of this finding; Li et al. (2004) confirmed that the most important properties required for link slab applications are tensile strain capacity (ductility) and crack width control for durability purposes. The minimum ductility required to withstand temperature and drying shrinkage stress, as well as live loads, was computed to be 1.4% using a factor of safety of two. Furthermore, it was confirmed that crack widths should be below 100 μm to minimize water/chloride penetration. These requirements are difficult, if not impossible, to attain for normal concrete, but are easily achievable with fly ash ECC mixtures with silica sand. The current study revealed that the performance of fly ash ECC mixtures with crushed sand was comparable with that of silica sand mixtures under static loading while they exhibited much better performance under fatigue loading in terms of both residual fatigue flexural strength and deflection capacity.

4.6.2 Second Approach-Fatigue Number of Cycles

The range of fatigue cycles studied in the first approach was somewhat low; only 50000 cycles. Therefore, further fatigue experiments were needed to be applied with higher range of fatigue cycles to confirm the case of FA-ECC mixtures. In the second approach, the fatigue tests were applied at different fatigue cycles, namely 200,000, 300,000 and 1,000,000 cycles. The specimens in the second approach were subjected to 4 Hz sinusoidal cyclic loading of 55% fatigue stress level.

4.6.2.1 Mid-span Deflection Evolution

The evolutions of mid-span deflection as function of the number of cycles are plotted in Figure 4.16 for each ECC specimens with 55% fixed fatigue stress level.

At 1,000,000 cycles and as in fatigue stress level results (first approach), FA-ECC specimens with silica sand (CI_2.2_SS and F_2.2_SS) under fatigue loading developed much more damage than FA-ECC specimens with crushed sand (CI_2.2_CS and F_2.2_CS). The range of displacement evolution of FA-ECC specimens with silica sand was very large compared to FA-ECC specimens with crushed sand. Under stress level of 55%, the displacement evolved up to about 1.10 mm mid-span deflection in silica sand ECC specimens compared to 0.53 mm crushed sand ECC specimens. The evolution of mid-span deflection was found to depend on the number of cycles in FA-ECC specimens with silica sand. The mid-span deflection increased to more than twice at high number of cycles (1,000,000 cycles) compared to low number of cycles (200,000 and 300,000 cycles) as shown in Figure 4.15.

Un-expectedly, the relationship between the number of cycles and the evolution of mid-span deflection in FA-ECC specimens with crushed sand is inversely proportional. Their behaviour for mid-span deflection evolution under high fatigue number of cycles was totally opposed to those with silica sand specimens. The more number of cycles in FA-ECC with crushed sand the lower evolution of mid-span deflection, at least in the range of number of cycles studied in present study, Figure 4.16 (d). The reason behind this is not completely clear, but is likely associated with many un-hydrated spherical FA particles in the interfacial zone of FA-ECC mixtures which will make FA particles difficult to connect with other cement product crystals (Gao and Zijl, 2005). This is consistent with the fact that around 25-30% in the paste with 50% replacement of fly ash did not hydrate and the unreacted fly ash may act like a micro-aggregate (Termkhajornkit et al., 2004). According to this, 70% of cement replacement was used in the present study which means around 30-40% of un-hydrated fly ash particles did not participate in the hydration process, but could be seen as mere filler material, or aggregate. Therefore, the use of crushed sand in FA-ECC mixtures facilitated to keep the un-hydrated fly ash particles as filler materials along with the PVA fibers due to its high porosity. FA-ECC mixtures with silica sand definitely reduced the chances for fly ash particles to act as a filler material because silica sand has extremely fineness than fly ash particles. Accordingly, when the fatigue tests applied on the crushed sand samples, the friction between cement crystals and the un-hydrated fly ash particles along with the confined PVA fibers in the zones of un-hydrated fly ash particles would be

increased due to the fatigue vibration and bouncing. Thus, enhanced friction may increase the chance to reactivate and accelerate the chemical reaction between the three mentioned above parties. Further experimental works are needed to confirm the case of FA-ECC with crushed sand.

Furthermore, Gao and Zijl (2005) indicated that the major phases of fly ash used in his study were glass phases containing mainly a SiO_2 with 60% content. Both the glass phase and the spherical shape of the FA may result in sluggish hydration and indicates that FA-ECC may have many un-hydrated binder particles with smooth surfaces, resulting in considerable interface between the matrix and the FA particles (Gao and Zijl, 2005). In the present study, SiO_2 proportion was around 60 and 40% of fly ash class F and CI respectively. This shows that class F fly ash mixture has more un-hydrated fly ash particles than class CI mixture which may enhance the composite performance under fatigue loading as mentioned above.

According to the fact that the un-hydrated fly ash particles do not participate in the hydration process and SiO_2 content, F_2.2_CS mixture exhibited much better performance than CI_2.2_CS mixture. This is signified in Figure 4.16 (a), (b) and (c), respectively. Figure shows that the mid-span deflection evolution of F_2.2_CS was consistently less than CI_2.2_CS mixture at fatigue cycles of 200,000, 300,000 and 1,000,000, respectively. Moreover, Figure 4.16(d) shows that the trend curve of F_2.2_CS mixture was more flat than CI_2.2_CS. This means that class F fly ash mixture has a material characteristic independent of the number of cycles than all ECC mixtures mentioned herein at least within the range of fatigue number of cycles studied.

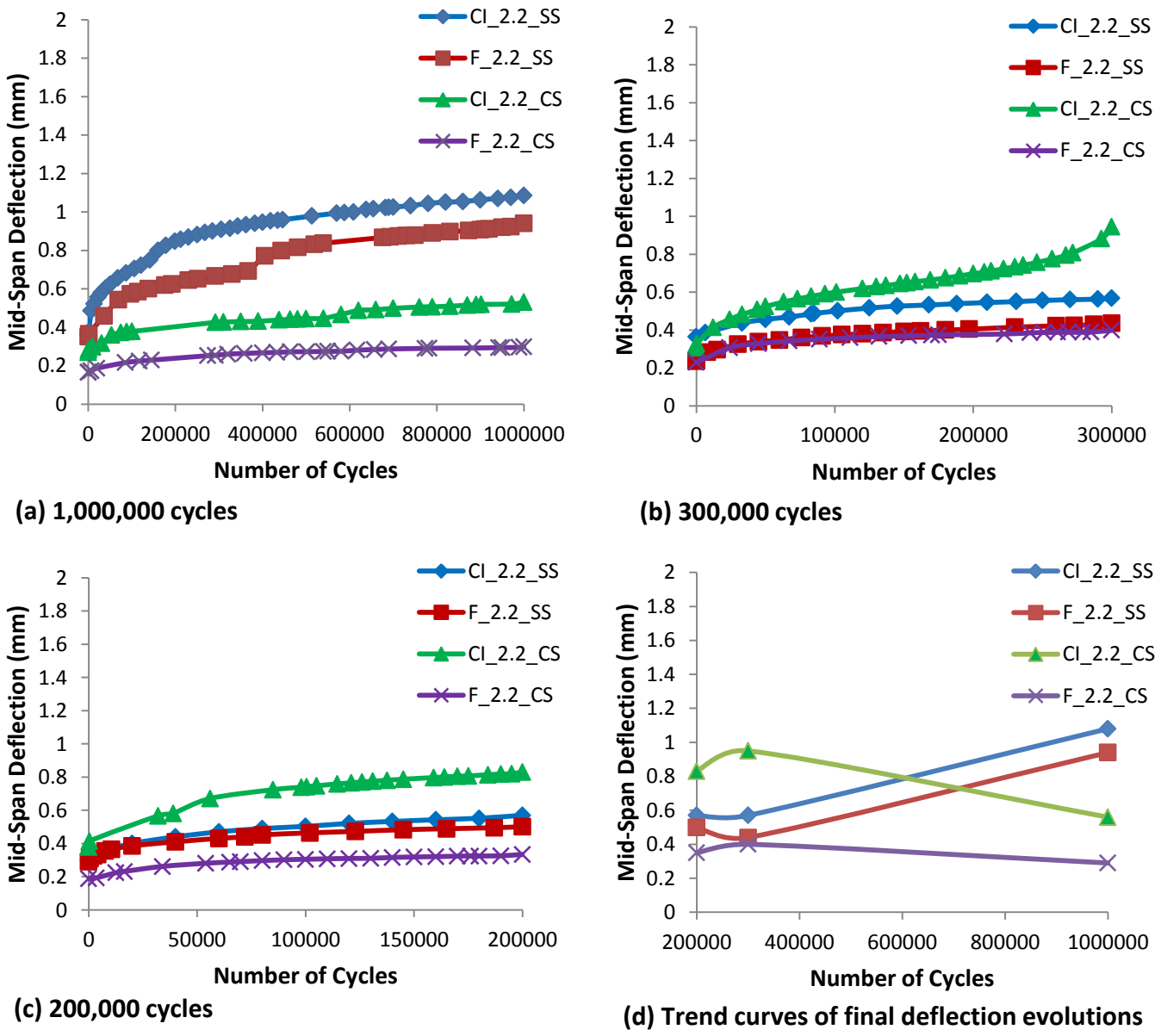

Figure 4.16 Evolution of mid-span deflection at 55% fatigue stress level and different fatigue number of cycles.

4.6.2.2 Number and Width of Cracks

To investigate the effect of fatigue loading on FA-ECC specimens, different fatigue number of cycles was applied on them namely 200,000, 300,000 and 1,000,000 cycles.

It should be noticed that the fatigue stress level was maintained at 55% for all of them. Again, it has to be mentioned that the results in this section had been collected when the

static loading was applied following the fatigue loading. Crack numbers and widths of FA-ECC specimens are presented in Figures 4.17 and 4.18, respectively.

It was found that more cracks formed at lower fatigue number of cycles in FA-ECC mixtures and unexpectedly, few cracks were formed at higher fatigue number of cycles. This might be attributed to the fact that the fiber/matrix interfacial bond stress degradation results in fiber pullout and fiber fatigue results in fiber rupture (Matsumoto et al. 2002). Furthermore, Suthiwarapirak et al. (2004) indicated that when comparing the fatigue specimens and static specimens, it was found that PVA fibers were severely ruptured under fatigue loading (Suthiwarapirak et al. 2004).

As in fatigue stress level results, first approach, F_2.2_CS mixture had higher number of cracks and smaller value of crack widths than other ECC mixtures as shown in Figures 4.16 and 4.18, respectively. It should be noted that F_2.2_CS and CI_2.2_CS mixtures exhibited the same value of crack width at all fatigue number of cycle tests, 50 μm and 75 μm, respectively.

Although the final number of multiple cracks of FA-ECC mixtures was inversely proportional to the number of cycles, FA-ECC mixtures still showed multiple cracking under flexural fatigue loading as well as static loading as shown in Figure 4.19. The photograph shows that the colored cracks resulted under flexural fatigue loading while the new, un-colored, cracks resulted under flexural static loading which applied after fatigue loading to get the residual energy in the tested ECC beam.

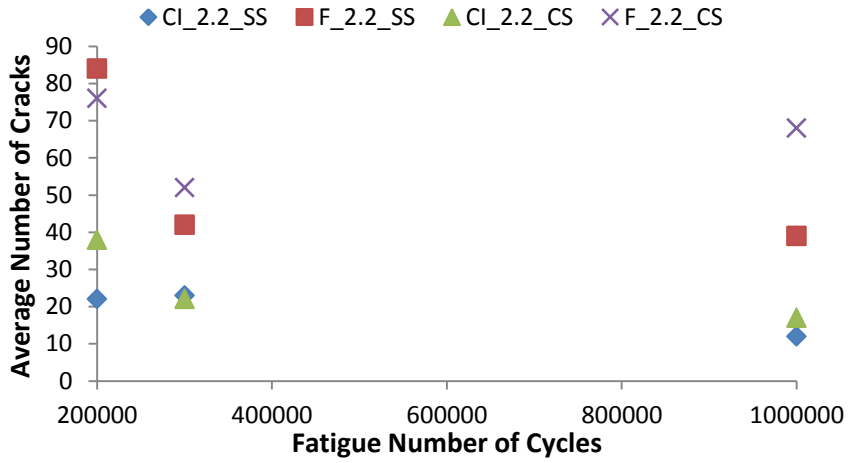

Figure 4.17 Average numbers of cracks at each fatigue number of cycles

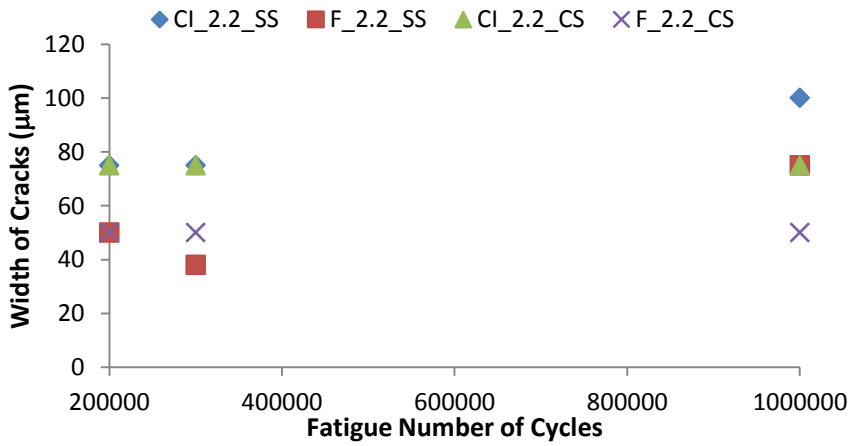

Figure 4.18 Crack Widths at each fatigue number of cycles

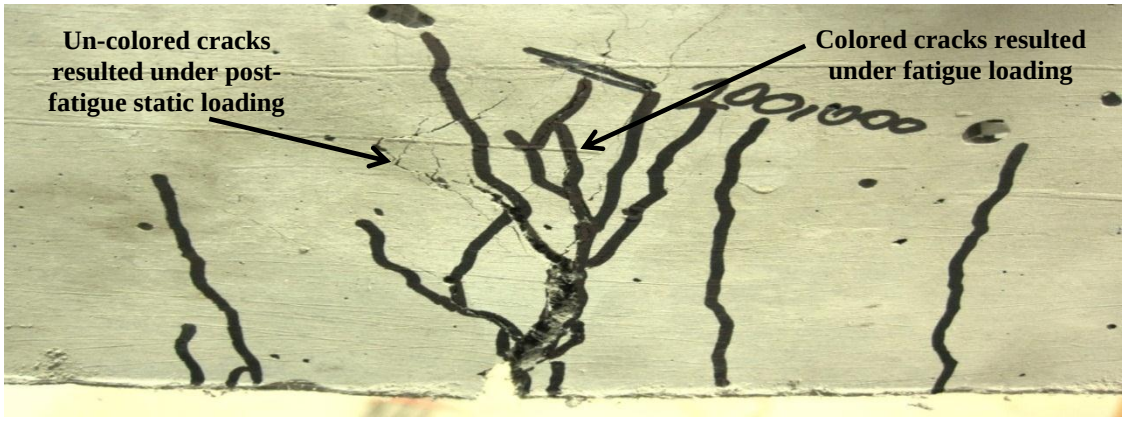

Figure 4.19 Multiple Cracking under Flexural Fatigue Loading

4.6.2.3 Static Loading Following Fatigue Loading

Static flexural tests were applied on the fatigued ECC specimens to calculate the fatigue residual energy in terms of strength and mid-span deflection at the end of the fatigue flexural tests. The fatigue flexural tests were expressed as percentages of static flexural tests (interms of residual strength and deflection) and are presented in Figures 4.20 and 4.21, respectively.

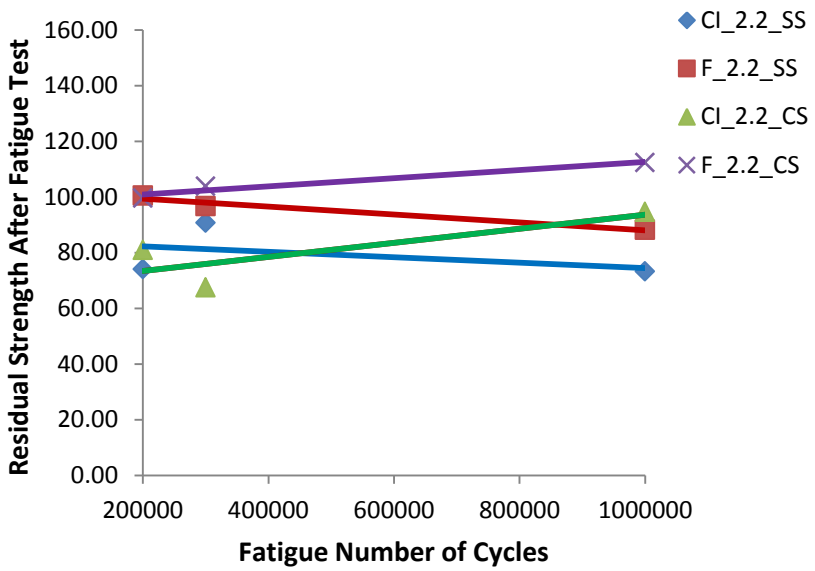

Figure 4.20 Percentages of Residual Strength after Fatigue Test

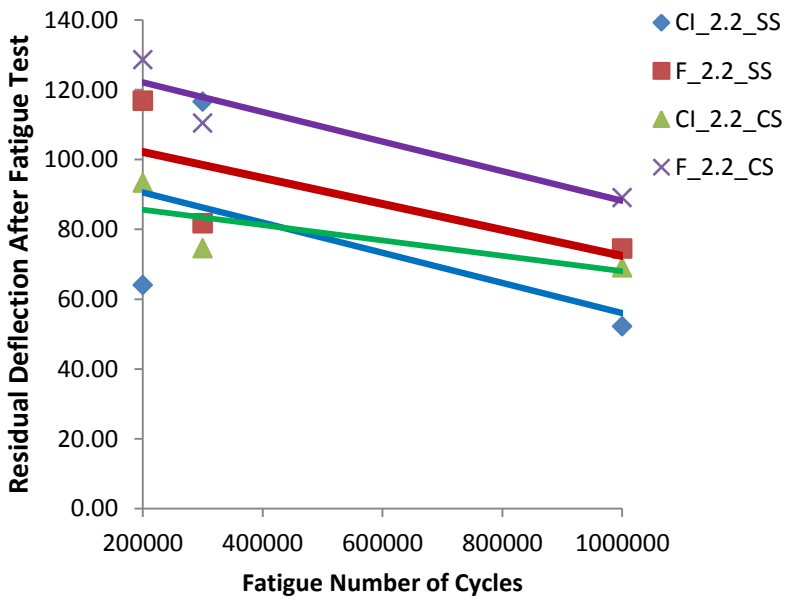

Figure 4.21 Percentages of Residual Mid-Span Deflection after Fatigue Test

Figures 4.20 and 4.21 show that at higher number of cycles, FA-ECC mixtures with crushed sand exhibited higher residual energy in terms of flexural strength capacity than ECC mixtures with silica sand, while all ECC mixtures exhibited lower residual energy in terms of deflection capacity. These results are consistent with the mid-span deflection evolution results, (Figure 4.16). It is found that the relation between the residual strength and the mid-span deflection evolution is inversely proportional. The lower the mid-span deflection evolution, the higher the residual fatigue flexural strength and vice versa. As in fatigue stress level results, F_2.2_CS mixture shows the highest superior performance consistently for all number of cycles with respect to fatigue stress and mid-span deflection as shown in Figures 4.20 and 4.21, respectively.

The superior performance in residual energy of crushed sand ECC mixtures even after applied 1,000,000 cycles could be attributed to the decrease in the maximum fatigue stress level. The stress level used herein was somewhat low, 55%. According to this, Awad (1971) reported that when normal concrete is subjected to high repeated stresses, a decrease of maximum stress level results in an increase of the number of cycles to failure. In addition to the decrease in fatigue stress level, high volume fly ash concrete subjected to high fatigue number of cycles at lower fatigue stress level as well would improve the performance of concrete. Tse et al. (1986) indicated that concrete with equivalent or higher compressive and fatigue strength of cylindrical concrete specimens incorporating large quantities of fly ash could be obtained with cement replacement of 25% by weight of low-calcium fly ash (class F) or 50% by weight of high-calcium fly ash (class C). Furthermore, Ramakrishnan et al. (1991) revealed that the high-volume fly ash concrete has slightly higher (7%) endurance limit when expressed as a ratio (ratio of flexural fatigue strength to static flexural strength) compared to plain Portland cement concrete. The results further indicated that there was an increase (15 to 30%) in static flexural strength for high-volume fly ash concrete which was previously subjected to four million cycles of fatigue stresses at their respective lower fatigue limit load (10%) (Ramakrishnan et al., 1991). In the present study, both the decrease in fatigue stress level which was 55% and the production of fly ash ECC mixtures with 70% cement replacement could be the reasons to the superior performance in residual fatigue energy of crushed sand ECC mixtures. In addition to these two reasons, most researchers

supported that during cyclic loading, fatigue of concrete occurs because of the propagation of the micro cracks and macro cracks present in the material, especially in the interface region as well as in the matrix. As an attempt to delay fatigue failure, Naik et al. (1993) reported the addition of fiber to concrete restrict crack formation and delays crack growth. Therefore, unstable cracks produced during loading are transformed into a slow and controlled growth. The overall tensile rupture strain of concrete is increased due to the introduction of fiber which will lead to the great improvement in the fatigue life of concrete.

4.6.2.4 Fatigue Stress Life Diagram, S-N Curve

The fatigue stress (S) to fatigue life versus the number of cycles (N) relationships for FA-ECC mixtures are plotted on a semi-logarithmic scale as shown in Figure 4.22. All 28 days specimens reached one million cycles without failure.

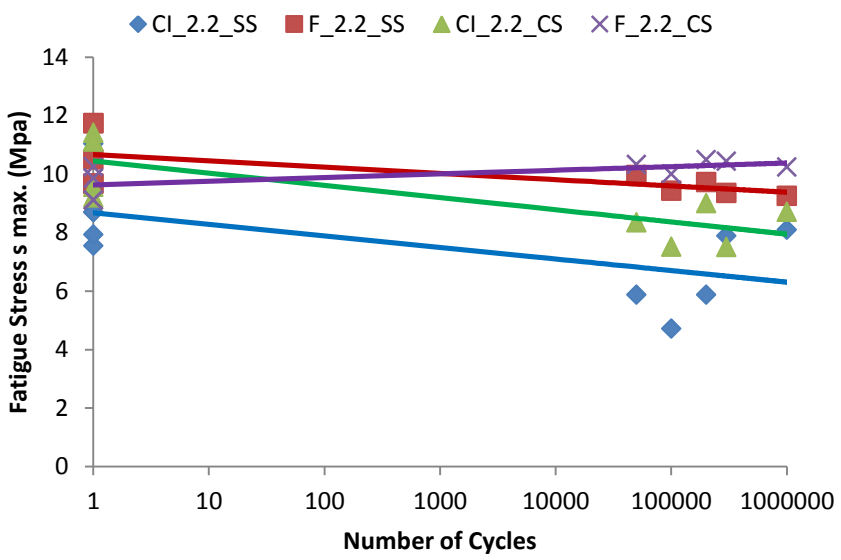

Figure 4.22 Fatigue Stress – Life Relationships

Figure 4.22 shows all average static and fatigue test results of all ECC mixtures. The fatigue number of cycle's axis was drawn by the logarithmic scale to the base 10 while stress axis was drawn in normal scale. It should be noted that further fatigue experiments were done for all ECC mixtures types at 50,000 and 100,000 fatigue cycles in addition to 200,000, 300,000 and 1,000,000 fatigue cycles to construct sufficient S-N curve for all fly ash ECC mixtures.

In this series of tests, two specimens at each static and fatigue loading were conducted except for the one million cycles; only one specimen was conducted for this purpose. As shown in Figure 4.22, it is found that F_2.2_CS and F_2.2_SS mixtures exhibited prolonged fatigue life compared with other CI-ECC mixtures at higher fatigue number of cycles.

The flexural fatigue stress–life relationships of the four ECC mixtures can be expressed as a function of the fatigue stress, *S*, and logarithmic values of the number of cycles, N. These equations developed in Excel are given bellow:

- CI_2.2_SS:
  $S = -0.172\ln(N) + 8.6844$, $R^2 = 0.38$ …… (4.1)
- F_2.2_SS:
  $S = -0.093\ln(N) + 10.674$, $R^2 = 0.42$ …… (4.2)
- CI_2.2_CS:
  $S = -0.181\ln(N) + 10.456$, $R^2 = 0.65$ …… (4.3)
- F_2.2_CS:
  $S = 0.054\ln(N) + 9.6397$, $R^2 = 0.48$ …… (4.4)

Unfortunately, on the S-N curve for ECC mixtures, the author could not determine whether ECC mixtures exhibit a bilinear relation on a semi-logarithmic scale or not when compared to S-N curve presented done by Suthiwarapirak et al. (2004), which is similar to the S–N relation of a metallic material. This is due to comparatively small number of fatigue cycles applied; one million cycles; compared to two million cycles done by Suthiwarapirak et al. (2004). The author could not have done more than one million cycles due to research time constraints.

In general, all ECC specimens showed superior fatigue strength compared to fatigue tests done by Zhang and Stang (1996). Table 4.10 shows fatigue strength results as a percentage of ultimate static strength of the present study along with Zhang and Stang results. Fatigue strength of plain concrete is 60%, and that of fiber reinforced concretes (FRCs) varies from 65% for hooked end (2% fiber content) to 90% for smooth steel (1%). Fatigue strength of polypropylene ECC (PE-ECC) is weaker than smooth steel (1%), but stronger than hooked

end (2%). The fatigue strength of PE-ECC reaches as high as 78% of the ultimate static strength and it fails within the observed range of fatigue strength of FRCs (Zhang and Stang, 1996). FA-ECC mixtures with silica and crushed sand showed better fatigue strength performance at 1000000 cycle than all plain, FRCs and PE-ECC mixture except CI_2.2_SS mixture, which showed lower fatigue strength than FRCs but still a way better than plain concrete performance.

Table 4.10 Comparison between fatigue strength of plain concrete, FRCs (Zhang and Stang, 1996), PE-ECC (Matsumoto, 1998) and present study FA-ECC specimens

Concrete type	Ultimate Static Strength (MPa)	Fatigue strength (MPa)	Fatigue Strength (%) of Ultimate Static Strength at 1 Million Cycles
Plain Concrete and FRCs (Zhang and Stang., 1996), and PE-ECC (Matsumoto., 1998)			
plain concrete	6.94	-	60%
smooth steel 1%	10.15	-	90%
hooked steel 1%	9.88	-	87%
hooked steel 2%	12.82	-	65%
hooked steel 1% + polypropylene 1%	9.46	-	87%
PE-ECC 1.5%	8.12	-	78% failed at 0.88 million
Present study fatigue strength			
CI_2.2_SS	11.04	8.095	73.32%
F_2.2_SS	10.50	9.26	88.19%
CI_2.2_CS	9.20	8.712	94.70%
F_2.2_CS	9.11	10.24	112.40%

4.6.2.5 The Case of F_2.2_CS ECC Mixture

As a conclusion to the high performance of ECC mixture incorporating fly ash class F with crushed sand, the mixture, F_2.2_CS, exhibited a unique performance which was equal to the superior performance of FA-ECC mixtures with 50% cement replacement in fatigue deflection and even better than them in fatigue strength. For 50,000 cycles and 70% higher fatigue stress level, the displacement evolution of F_2.2_CS mixture evolved up to 0.70 mm which was the lowest range of all other ECC mixtures. Accordingly, the speed rate of the mixture was 1.95 μm/min which is again the lowest fatigue speed rate. Higher number of cracks and lower crack widths of F_2.2_CS mixture at higher fatigue number of cycles, 70%, was remarkable. Test results showed that F_2.2_CS mixture exhibited 120 numbers of crack and 50 μm crack widths. The maximum numbers of crack and crack widths of all other ECC mixtures were 70 numbers of crack and 75 μm crack width, respectively.

At high fatigue number of cycles (1,000,000 cycles), F_2.2_CS mixture exhibited 0.30 mm displacement evolution range which was again the lowest value of all ECC mixtures. The average number of cracks of F_2.2_CS mixture at 1000000 cycles and at 55% stress level was around 70 whereas the crack width was consistently remained fixed for all fatigue number of cycles (started at 200,000 through 1,000,000 cycles). It can be said that the F_2.2_CS mixture has material characteristic independent of fatigue number of cycles than all FA-ECC mixtures which means the more this material is subjected to fatigue loading the more it gets stronger and more flexible in the same time at least within the range of number of cycles studied.

Both Suthiwarapirak et al. (2004) and Matsumoto et al. (2003) reported that the age of specimens at fatigue testing should be at least two months to alleviate the effect of initial hydration development. According to this, and due to the consistent superior performance in the case of F_2.2_CS mixture, the author preferred to conduct another flexural fatigue test for 1,000,000 cycles to the mentioned mixture at the age of 56 days to confirm this superiority. The mixture's specimen was subjected to similar fatigue loading conditions employed in the present study. It was subjected to 4 Hz sinusoidal cyclic loading rate at 55% fatigue stress level of the maximum static test result.

For comparison purposes, the evolution of mid-span deflection of this mixture was compared with all ECC mixtures mid-span deflection evolution. It can be found that the displacement evolved up to 0.6 mm mid-span deflection in F_2.2_CS_56 days compared to 0.3 mm in F_2.2_CS_28 days. The mid-span deflection increased to twice the value of 28 days mixture at high number of cycles (1,000,000 cycles) as shown in Figure 4.23. The figure shows that mid-span deflection evolution of F_2.2_CS_56days still exhibits less evolution than 28 days fly ash ECC mixtures with silica sand, even at the age of 56 days.

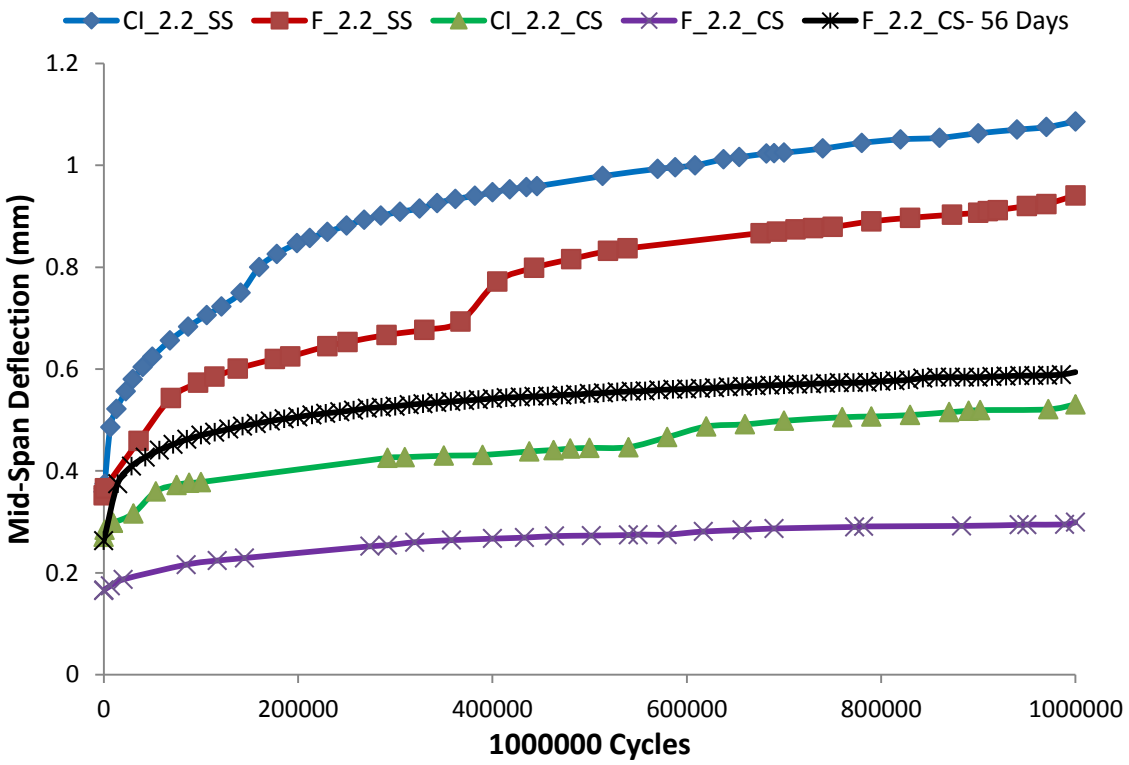

Figure 4.23 Evolution of mid-span deflection at 55% fatigue stress level and 1000000 cycles

Table 4.11 shows the fatigue loading characteristics of fly ash ECC mixtures studied in the second approach of fatigue performance including the characteristics of F_2.2_CS at the age of 56 days. The presented fatigue characteristics summarized in Table 4.11 are for fatigue loading test results at one million cycles only. It should be mentioned again that the results in this section had been collected when static loading was applied after fatigue loading. Crack

numbers, crack widths and residual fatigue energy expressed as percentages of static flexural tests (in terms of residual strength and deflection) of all FA-ECC mixtures mentioned above are presented in Table 4.11.

Table 4.11 Fatigue loading characteristics of fly ash ECC mixtures at one million cycles

Mix Designation	Age of Specimen	Static after Fatigue Loading		Residual Fatigue Energy at 55% Fatigue Stress Level	
		Crack Numbers	Crack Width (μm)	Residual Stress (%)	Residual Deflection (%)
CI_2.2_SS	28	12	100	73.32%	52.22%
F_2.2_SS	28	39	75	88.19%	74.46%
CI_2.2_CS	28	17	75	94.70%	69.09%
F_2.2_CS	28	68	50	112.40%	89.09%
F_2.2_CS	56	45	50	99.22%	81.20%

As shown in Table 4.11, the F_2.2_CS mixture at 56 days still has higher number of cracks and smaller value of crack widths than fly ash ECC mixtures with silica sand and CI_2.2_CS mixture. It should be noted that both F_2.2_CS at 28 and 56 days exhibited the same value of crack width at 1000000 fatigue cycles test which was around 50 μm. Furthermore, Table 4.11 shows that F_2.2_CS mixture at 56 days exhibited the best performance at 1,000,000 fatigue number of cycles with respect to residual fatigue stress and mid-span deflection of all fly ash ECC mixtures except obviously for the F_2.2_CS mixture at 28 days.

4.7 Long-term Creep Test

The best of ECC mixtures from the third phase was included in the fourth phase which was the long-term creep test. Only F_2.2_SS and F_2.2_CS mix designs were included in this phase with the SCC mix design as a control mix. It should be noted that long-term creep tests are still in progress. The creep test results mentioned herein indicate the drying creep which is the additional creep that occurs when the specimen under loading is allowed to dry. The total creep is the sum of both drying and basic creep. Basic creep is the creep measured in the sealed specimens (without drying). However, it is a common practice to ignore the distinction between the basic and the drying creep, and creep is simply considered as the deformation under load (Mehta and Monteiro, 2006).

The results of creep tests are shown in Figures 4.24 and 4.26 through 4.28. As expected, Figure 4.24 shows that SCC link slab specimen undergoes significantly less creep than the corresponding ECC specimens. This effect is attributed to aggregate characteristics. The creep of concrete can increase by 2.5 times when a high elastic modulus aggregate is substituted with a low elastic modulus aggregate (Mehta and Monteiro, 2006). Thus, the SCC mix has more modulus of elasticity than ECC mixtures due to their aggregate characteristics. The modulus of elasticity of SCC used herein was 33.59 GPa while in general ECC mixtures exhibit less modulus of elasticity which is around 21 GPa mentioned by (Quan and Li, 2008). Moreover, creep of concrete is inversely proportional to the strength of concrete at the time of application of load (Mehta and Monteiro, 2006). The compressive strength value of SCC used is in between 60~63 MPa while F_2.2_SS and F_2.2_CS mixtures showed 52 and 45 MPa, respectively. It can be concluded that the higher the modulus of elasticity and compressive strength the less is the creep. In general, creep is greatest in concretes with high cement paste content while concrete containing a large aggregate fraction creep less because only the paste creeps, and the creep is restrained by the aggregate (Macgregor and Bartlett, 2000). It is noticed that the creep behaviour of both ECC mixtures was almost the same but about 8 and 28 days after load application, F_2.2_CS mixture showed a sudden increase of deflection as shown in Figure 4.24. This could be caused by a crack forming in the specimen.

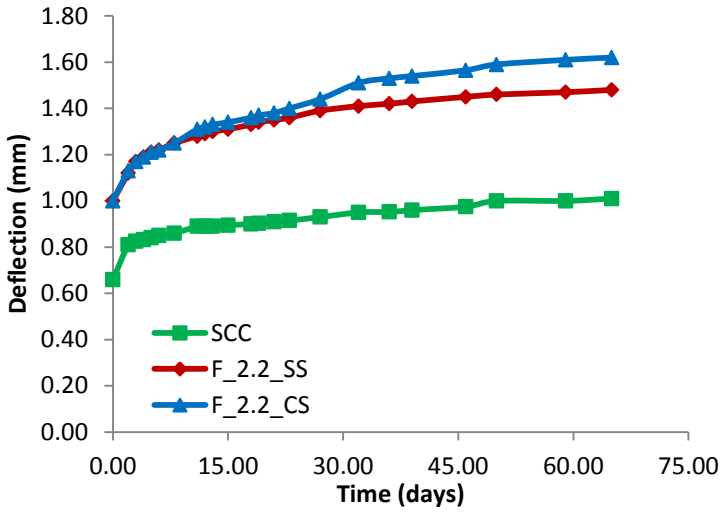

Figure 4.24 Long-term creep deflections of all test specimens

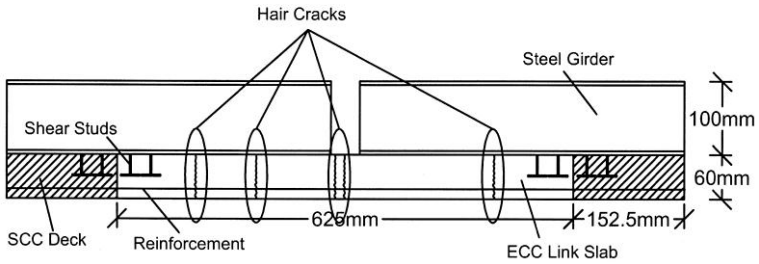

Fly ash ECC link slab specimen with crushed sand

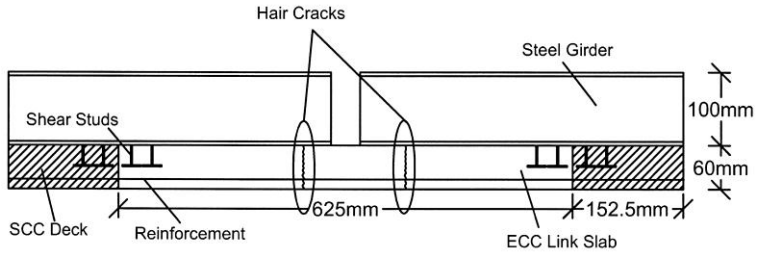

Fly ash ECC link slab specimen with silica sand

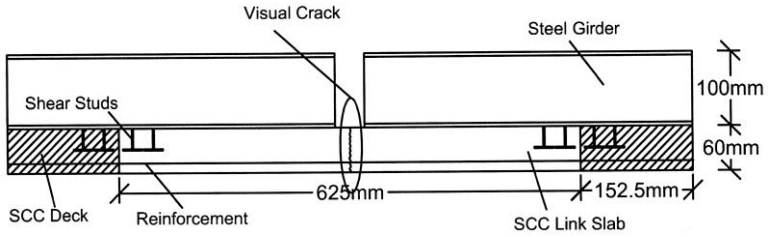

SCC link slab specimen with coarse aggregate

Figure 4.25 Crack formations of all link slab specimens. Dimensions in mm

Figure 4.25 shows the crack formations of all link slab specimens. As shown in Figure 4.25, 5 cracks were formed in fly ash ECC link slab specimen with crushed sand while only 2 cracks were formed in fly ash ECC link slab specimen with silica sand compared to one visual crack formed in SCC link slab specimen. All cracks in all link slab specimens were formed in link slab part. It should be noted that ECC specimens exhibited hair cracks compared to one visual macro crack in SCC specimen.

Figure 4.26 presents the strain development in gauges on the compression side of the link slab specimens. The figure shows that SCC mix exhibited less creep (signified by the less strain) than ECC mixtures due to aggregate characteristics as well. Mangat and Azari (1986) reported that steel fibers are effective in reducing both creep and shrinkage in concrete. They explained this result with a model in which the steel fibers aligned with the applied load act as compressive reinforcement for a cylinder of the idealized surrounding matrix. Conflicting results were found in the present study because ECC mixtures exhibited more creep in the compression side and did not act as compression reinforcement.

As shown in Figure 4.26, unfortunately the compression strain readings were lost around 28 days after loading application in the F_2.2_SS link slab specimen. This loss was due to equipment failure in the acquisition system device itself which was connected permanently to link slab specimens.

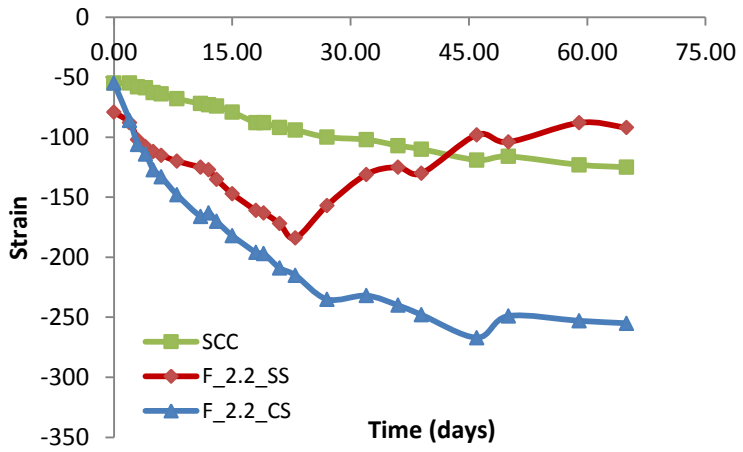

Figure 4.26 Strain evolution of the compression side of all test specimens

Figure 4.27 presents the strain development with time in gauges on the tension side of the link slab specimens. From the figure, link slabs with ECC mixtures tend to exhibit more ductile behaviour (signified by the higher tensile strain development) compared to SCC link slab specimen.

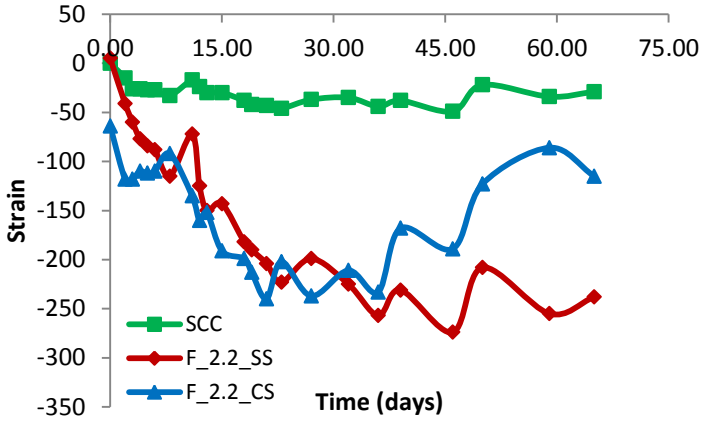

Figure 4.27 Strain evolution of the tension side of all test specimens

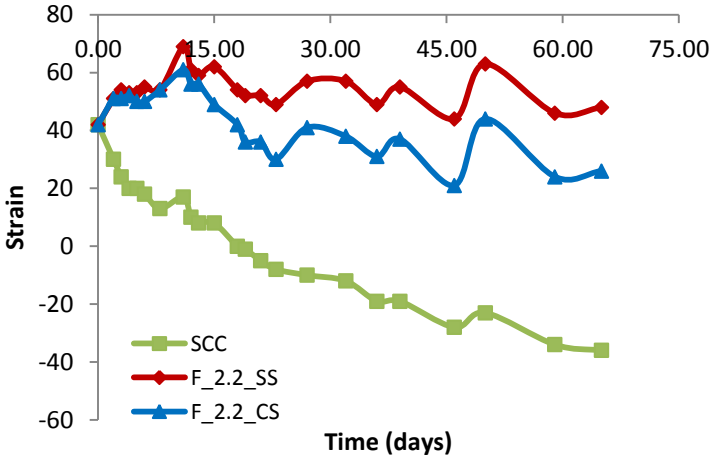

Figure 4.28 Strain evolution of steel reinforcement of all test specimens

Figure 4.28 shows the strain development in gauge installed on the tension steel reinforcement in link slab at the centre of the specimens. It is noticed that the steel is carrying more creep load in SCC (indicated by higher strain development) than ECC specimens.

As a summary, it can be concluded that ECC link slab specimens exhibited more creep deflection, compression and tensile strain development than SCC link slab specimen. Whereas, SCC link slab specimen exhibited more strain development in the steel reinforcement than ECC link slab specimens.

The creep development in ECC link slab specimens could be attributed to the presence of fibers. It is well known that one of the primary mechanisms of shrinkage and creep in cementitious materials is the loss of material's water to the environment. The higher the permeability, the more loss of water can occur. In concrete, a zone of higher porosity often exists at the interface between an aggregate and the surrounding matrix. The same zone is found around the fibers in an ECC material. Therefore, it is reasonable to expect a higher permeability in ECC materials because the porous zone may act as a conduit to promote moisture migration (Rouse and Billington, 2007). Because of this, ECC link slab specimens exhibited more creep than SCC link slab specimen. Moreover, to compare between ECC link slab specimens themselves, it is observed that ECC mixtures with crushed sand exhibited slightly more creep than ECC mixtures with silica sand due to the presence of crushed sand and fibers which may increase and accelerate the moister migration in the composite. As evidence to more moisture migration in F_2.2_CS specimen, Figure 4.25 indicates that there are more cracks formed in the specimen than F_2.2_SS and SCC link slab specimens which signified by sudden increases of long-term deflection curve of F_2.2_CS mixture as shown in Figure 4.24.

Although the presence of fibers in ECC link slab specimens is playing a significant rule in the creep behaviour, it is found that fibers delay the initiation of cracks and reduce the shrinkage crack openings (Rouse and Billington, 2007). This finding is acting as an evidence that ECC link slab specimens did not fail yet under long-term creep testing.

The more creep development in ECC rather than SCC link slab specimen does not mean that SCC resists more creep than ECC link slab specimens. The better creep resistance in SCC link slab specimen is due to the presence of steel reinforcement not from the SCC material itself. As shown in Figure 4.28, ECC link slab specimens exhibited less strain development

in steel reinforcement than SCC link slab specimen. This result is confirming the fact that ECC material has a material characteristic independent of steel reinforcement ratio. Therefore, steel reinforcement is very important to control crack width in SCC material. Once the crack occurs, the SCC no longer carries the loads and simultaneously, steel reinforcement's tensile stress increases substantially as it tries to hold the crack tight, such steel reinforcement can be completely eliminated in ECC. This result means that steel reinforcement and surrounding matrix share the loads ECC link slab specimens effectively and embedded reinforcements are less stressed. Furthermore, the stabilization of ECC readings in the long-term creep deflections curves as shown in the 4.24 means that ECC material can resist creep loads by itself without even any help of steel reinforcement. According to this, using ECC materials in link slab bridge deck applications definitely improve the long-term creep behaviour.

4.8 Summary

In this chapter, the experimental results of the present research are presented and discussed. The test results of five kinds of investigations (compressive strength, fracture energy, flexural strength, fatigue flexural loading and creep performance) were analyzed to evaluate the performance of different ECC mixtures. A full detailed conclusion of these analyses will be presented in the Chapter 5.

CHAPTER FIVE

CONCLUSIONS

5.1 General

This thesis describes the influence of aggregate size and type on the mechanical properties of ECC with different supplementary cementitious materials (SCMs). ECC mixtures containing SCMs (fly ash class CI, F and slag) with SCMs/cement ratio of 1.2 or 2.2, silica sand with maximum grain sizes of 0.30 and local crushed sand with maximum grain sizes of 1.18 mm were used. The aggregate/binder ratio of 0.36 was maintained and water/binder ratio was kept in the range of 0.27 for both class CI and F fly ash and 0.30 for slag. For comparison purpose, two main groups of 12 ECC mixtures have been designed and selected. The first group was composed of 6 ECC mixtures which were produced by using microsilica sand and SCMs. The second group was composed of the same first group ECC mixtures but was produced by using local crushed sand. A series of tests were carried out to study the compressive, flexure strength, fracture energy, fatigue performance and creep behaviour of ECC. The following conclusions can be drawn from this study.

- The fracture energy of SS-ECC mixtures, at 28 days of age, at 50% cement replacement ranges from 1.71 to 2.39 N/mm compared to 1.39 to 2.39 N/mm when the cement replacement increased up to 70%. The increase in SCMs replacement rate (FA and slag) up to 70% leads to a reduction in fracture energy of ECC mixtures. For a given SCMs type and content, higher results of fracture energy were achieved when aggregate size increased from 0.3mm up to 1.18mm. CS-ECC mixture's results exhibited an increase in fracture energy ranging between 1.82 and 2.61 N/mm compared to 1.71 to 2.39 N/mm at 50% cement replacement. Similar increment behaviour was found at 70% cement replacement rate. It can be concluded that in order to achieve strain-hardening behavior of ECC mixtures in terms of fracture energy,

aggregate particle size had to be reduced from 1.18 to 0.30 mm or the amount of SCMs replacement rate had to be increased from 50 up to 70%.

- Similar behaviour of fracture energy was found in terms of compressive strength performance of ECC mixtures when SCMs replacement rate increases. At 50% cement replacement rate, the compressive strength ranges between 61 and 69 MPa compared to 52 up to 67 MPa at 70% cement replacement. Unlike conventional concrete, aggregate characteristics, such as the surface texture and sand sizes, did not influence the compressive properties in the case of ECC. However, all the mixtures, showed compressive strengths higher than 45 MPa at 28 days of age.

- Slag-ECC mixtures consistently produced greater compressive strength than class CI and F fly ash mixtures. The compressive strength values of slag-ECC mixtures, whether incorporating silica sand or crushed sand, ranged between 67 to 69 MPa compared to 45 up to 62 MPa for FA-ECC mixtures. This is because the high proportion of Calcium Oxide (CaO) content which is quite close to Portland cement that leads to rapid hydrates and reactions of slag compared to those of FA-ECC mixtures.

- In general and as in the case of high strength concrete, there is a strong correlation between compressive strength and fracture energy of ECC mixtures. Fracture energy increases as the compressive strength increases.

- Both silica and crushed sands ECC mixtures exhibited multiple-cracking behaviour under static flexural loading. For all ECC mixtures, the average ultimate flexural strengths vary from 10.48 to 15.81MPa and the bending capacity of ECC beams vary from 1.61 to 4.45mm depending on class CI, F fly ash and slag content. It was found that the ductility of ECCs, by measuring mid-span beam deflection, improved when the cement replacement rate increased from 50 to 70% whereas no significant influence of the FA or slag replacement rate on the flexural strength values.

- Aggregates within the size range studied (0.30 to 1.18mm), as long as they do not interfere with the uniform dispersion of fibers, do not negatively influence the ductility of ECC. In general, the slag-ECC mixture showed significantly lower deflection capacity when compared to the ductility of the mixture of FA-ECC. The reduced ductility of slag mixtures can possibly be caused by the higher fracture energy, matrix and bond strength and friction between the slag-ECC matrix and the fibers compared with FA-ECC mixtures. The bending capacity of slag-ECC incorporating silica sand varies between 1.79 to 2.04 mm at the age of 28 days while varies between 1.73 to 1.80mm when the aggregate size increased up to 1.18mm. Again, and as in the case of compressive strength results, the aggregate particle size had no or only a minor effect on the flexural strength ECC performance.

- The relationship between the fracture energy and the maximum bending capacity is almost inversely proportional. Accordingly, the fracture energy of class F fly ash is slightly higher than those in class CI mixtures while both classes of fly ash had lower fracture energy than slag-ECC (SL) mixtures.

- The number of crack increases and crack width reduces significantly as SCMs content increased up to 70% at all ages. The average crack width was lower than 100 μm in average for slag-ECC mixtures and 60 μm in average for FA-ECC mixtures. On the other hand, the use of aggregate up to 1.18 mm did not influence the average residual crack width. Crack width control is of primary importance for many reinforced concrete applications, since it is believed that there is a close relationship between the mean or maximum crack widths and the durability of the structure.

- When the fatigue flexural value is expressed as percentage of static flexural value, the residual fatigue energy could be attained with respect to both residual fatigue strength and deflection. Accordingly, At 50,000 cycles, it was found that when a comparison is made between the residual fatigue energy of FA-ECC mixtures with 70% cement replacement under 70% of fatigue stress level and those 50% cement replacement under 55% of fatigue stress level, the former showed equal or slightly higher

performance than the latter with respect to both residual fatigue strength and deflection. The former's residual deflection capacity, 70% replacement rate at 70% stress level, ranges between 113.26 to 158.29% compared to 116.08 up to 135.29 % of the latter's residual deflection capacity, 50% cement replacement at 55% stress level. Moreover, at the same range of fatigue stress level (55%), F_2.2_CS had a remarkable performance compared to superior performance of FA-ECC mixtures with 50% cement replacement based fatigue deflection and even better than them in fatigue strength. Test results show that F_2.2_CS mixture had 113.39 and 129.98% of residual strength and deflection capacity respectively. Under stress level 70% and for 50,000 cycles, the residual strength of F_2.2_CS mixture was 120% which is the highest residual strength of all FA-ECC mixtures compared to 100% under 40% stress level which is again the highest residual strength ever. Under stress level 55% and for 1,000,000 cycles, the highest residual strength and deflection capacity was for F_2.2_CS mixture consistently.

- All FA-ECC mixtures with different types of aggregate (silica and crushed sand) exhibited multiple-cracking behaviour under flexural fatigue loading. Most of the multiple cracks occurred more at higher fatigue stress levels, 70%, and unexpectedly few cracks formed at lower fatigue stress levels, 40%. The maximum average number of cracks at 70% stress level for all FA-ECC mixtures was around 130 compared to around 100 at 40% stress level. It can be concluded that the final number of multiple cracks of FA-ECC mixtures is depending on fatigue stress level and also that the multiple-cracking behaviour terminates earlier at a lower stress level, 40%.

- More multiple-cracking behaviour was occurred at smaller number of loading cycles (200,000 and 300,000 cycles) while unexpectedly less cracks formed at higher number of loading cycles (1,000,000). This is in agreement with the widely acknowledged fact that PVA fibers are severely ruptured under fatigue loading than static loading. The maximum average number of cracks at the end of 1,000,000 cycles for all FA-ECC mixtures was around 70 compared to around 85 at the end of 200,000 fatigue cycles.

- Under high stress level (70%) and for 50,000 cycles, the mid-span deflection evolution of FA-ECC mixtures with silica sand evolved up to about 2.1mm compared to 1.35mm for FA-ECC with crushed sand. Under static loading, FA-ECC mixtures with silica sand exhibited slightly higher deformation capacity than FA-ECC mixtures with crushed sand while evolved much higher deflection evolution under fatigue loading. This means silica sand FA-ECC mixtures developed much more damage under fatigue loading.

- Under a stress level of 55% and for 1,000,000 cycles, the mid-span deflection evolved up to about 1.10 mm for silica sand FA-ECC mixtures compared to 0.53 mm for crushed sand FA-ECC mixtures. The relationship between the number of cycles and the evolution of mid-span deflection in silica sand FA-ECC mixtures was directly proportional. The higher the fatigue number of cycles means more deflection evolution and more damage development. By contrast, the higher number of cycles in crushed sand FA-ECC mixtures means lower deflection and less damage which means that this material characteristic is independent of fatigue number of cycles within the 1,000,000 cycles studied in this research.

- As expected, the relationship between crack widths and fatigue stress levels in all FA-ECC mixtures was directly proportional. As the fatigue stress level increases, the crack width of FA-ECC mixtures increases and vice versa. In the case of FA-ECC mixtures incorporating silica sand, the crack width increased as the number of cycles increased. Whereas in the case of mixtures incorporating crushed sand, the crack width was flat and fixed at all fatigue number of cycle with an average value of 60 μm.

- The fatigue stress (S) to fatigue life (N) relationship is called (S-N) curve. The S-N curve enables one to predict the mean fatigue life of concrete under given cyclic stress. The S–N relation of ECC mixtures did not exhibit a bilinear relationship on a semi-logarithmic scale, which is similar to the S–N relation of a metallic material. This is because of the number of fatigue cycles applied was only one million cycle. According to the S-N curve in this study, both fly ash class F ECC mixtures with both silica and

crushed sands exhibited a significantly prolonged fatigue life in comparison with fly ash class CI ECC mixtures.

- As a confirmation to the superiority in performance of F_2.2_CS mixture, flexural fatigue test for 1000000 cycles was conducted at the age of 56 days. F_2.2_CS mixture at 56 days exhibited higher number of cracks and smaller value of crack widths than fly ash ECC mixtures with silica sands and CI_2.2_CS mixture. This mixture has 45 cracks and 50μm of crack widths at 55% stress level for one million cycles which was equal to F_2.2_CS mixture at 28 days. It can be concluded that F_2.2_CS mixture has material characteristic independent of fatigue number of cycles than other FA-ECC mixtures at least within the range of number of cycles studied.

- Based on the experimental results for the creep behaviour of link slab specimens, it was found that FA-ECC link slab specimens developed greater creep strains than SCC link slab specimen. This is attributed to the presence of aggregate and the compressive strength of SCC which can significantly reduce creep of the material. It is also noticed that both FA-ECC mixtures with silica and crushed sands exhibited similar values of drying creep which means that they have same creep behaviour.

Finally, this study confirms the suitability of crushed sand in the production of cost-effective ECC mixtures, and indicates that crushed sand with relatively higher aggregate size can also be successfully used to produce an ECC mixture having similar or better mechanical properties than corresponding ECC made with microsilica sand. However, these conclusions should be valid for the ECC mixes developed in this study.

5.2 Recommendations for Future work

For a complete understanding of the mechanical performance of ECC containing crushed sand, further research will be needed to determine the mechanical characteristics of ECC under higher fatigue stress levels and higher fatigue number of cycles to evaluate the failure mechanism and mid-span deflection evolution under fatigue loading.

Furthermore, due to the prolonged pozzolanic reaction of fly ash, it would be necessary to investigate the long-term behavior (beyond the age of 56 days) of ECC with larger maximum aggregate size and high fly ash content and compare the results with ECC mixtures incorporating high volumes of combination of fly ash and slag at 28 days and later ages as well.

The results of the mentioned future study should be formulated (i) to develop guidelines for ECC mix design, (ii) to evaluate the performance of testing methods/protocol of ECC mixtures and (iii) to identify the critical ECC properties for contract specification.

Research should be conducted on link slabs under monotonic and cyclic/fatigue loading incorporating different ECC mix designs to evaluate the structural performance of ECC and to develop design guidelines for such structural elements. In addition, the research should be conducted under sustained loading to evaluate the creep behaviour for link slab applications using best ECC mix designs compared to self-consolidating concrete counterpart.

Finite element modelling should be carried out for better understanding of link slab behaviour in bridge deck applications.

REFERENCES

ACI Committee 215. (1997). Considerations For Design OF Concrete Structures Subjected TO Fatigue Loading. American Concrete Institute, Farmington Hills.

Alexander, M. G., Jaufeerally, H. and Mackechnie, J. R. (2003). Structural and Durability Properties of Concrete Made by Corex Slag. Research Monograph No. 6, Departments of Civil Engineering University of Cape Town, South Africa.

ASTM C1017. (2007). Standard Specification for Chemical Admixtures for Use in Producing Flowing Concrete. American Society for Testing and Materials, West Conshohocken, PA, USA.

ASTM C117. (2004). Standard Test Method for Materials Finer than 75-µm (No. 200) Sieve in Mineral Aggregates by Washing. American Society for Testing and Materials, West Conshohocken, PA, USA.

ASTM C136. (2005). Standard Test Method for Sieve Analysis of Fine and Coarse Aggregates. American Society for Testing and Materials, West Conshohocken, PA, USA.

ASTM C1611. (2009). Standard Test Method for Slump Flow of Self-Consolidating Concrete. American Society for Testing and Materials, West Conshohocken, PA, USA.

ASTM C39. (2003). Standard Test Method for Compressive Strength of Cylindrical Concrete Specimens. American Society for Testing and Materials, West Conshohocken, PA, USA.

ASTM C87. (2002). Standard Test Method for Flexural Strength of Concrete (Using Simple Beam with Third-Point Loading). American Society for Testing and Materials, West Conshohocken, PA, USA.

ASTM C 618. (2012). Standard Specification for Coal Fly Ash and Raw or Calcined Natural Pozzolan For Use In Concrete. American Society for Testing and Materials, West Conshohocken, PA, USA.

Awad, M.E. (1971). Strength and Deformation Characteristics of Plain Concrete Subjected to High Repeated and Sustained Loads, Ph.D. Thesis, University of Illinois at Urbana - Champaign, Illinois, Research Series 132, p, 266.

Balaguru, P. N. and Ramakrishnan, V. (1988). Properties of Fiber-Reinforced Concrete: Workability, Behavior under Long-Term Loading, Air-Void Characteristics. American Concrete Institute Materials Journal, Vol. 85, No. 3, 189-196.

Bazant, Z. P. (1979). Fracture Energy of Concrete: Method of Determination. Cement and Concrete Research, 10 (1), 78-89.

Caner, A. and Zia, P. (1998). Behavior and Design of Link Slabs for Jointless Bridge Decks. PCI Journal, 68-80

Chen, B. and Liu, J. (2004). Effect of Aggregate on The Fracture Behavior of High Strength Concrete. Construction and Building Materials, 18 (8), 585- 590.

Fischer, G. S. W. and Li, V. C. (2003). Design of Engineered Cementitios Composites (ECC) for Processing and Workability Requirement. In: BMC 7, Poland, 29-36.

Gao, and Zijl, V. (2005). Tailoring ECC for Commercial Application. In: M. di Prisco, R. Felicetti and G.A. Plizzari, Editors, Fiber Reinforced Concretes (BEFIB'2004), RILEM Pro039, 1391-1400.

Ho, E. and Lukashenko, J. (2011). Link Slab Deck Joints. MMM Group Limited, Paper prepared for presentation at the Session Bridges – Successes: Let's Build on them of the 2011 Annual Conference of the Transportation Association of Canada Edmonton, Alberta, p, 20.

Hassan, A. A. A. Lachemi, M. and Hossain, K. M. A. (2012). Effect of Metakaolin and Silica Fume on the Durability of Self-Consolidating Concrete. Cement and Concrete Composites, 34 (6), 801-807.

Hossain, K. M. A. (2003). Blended Cement Using Volcanic Ash and Pumice. Cement and Concrete Research - An international Journal, 33 (10), 1601-1605.

Hossain, K. M. A. (2004). Properties of Volcanic Pumice Based Cement and Lightweight Concrete. Cement and Concrete Research, 34 (2), 283-291.

Hossain, K. M. A. (2005). Volcanic Ash and Pumice as Cement Additives: Pozzolanic, Alkali-Silica Reaction and Autoclave Expansion Characteristics. Cement and Concrete Research, 35 (6) 1141-1144.

Hossain, K. M. A. (2011). Engineered Concrete Systems for Innovative Structural Design Applications. Report Submitted to Ministry of Transportation, Ontario, p, 10.

Hossain, K. M. A. (2012a). Lightweight Concrete with Volcanic Materials. Construction Materials Journal, ICE, 165 (CM2), 111-120.

Hossain, K. M. A., Mak, C. and Ametrano, D., Canadian Civil Engineer. (2012b) GFRP Reinforced UHPC Composites for Sustainable Bridge Construction, 12-15.

Houde, J., Prezeau, A. and Roux, R. (1987). Creep of Concrete Containing Fibers and Silica Fume. Fiber Reinforced Concrete Properties and Applications, American Concrete Institute, Detroit, Vol. 105, SP, 101-118.

Inaguma, H., Seki, M., Suka, K. and Rokugo, K. (2005). Experimental Study on Crack-Bridging Ability of ECC For Repair Under Train Loading. Workshop on HPFRCC in Structural Applications, Honolulu, Hawaii, USA, 499-508.

JCI-DFRCC Committee. (2003). DFRCC Terminology and Application Concepts. Journal of Advanced Concrete Technology Vol. 1, No. 3, 335-340, Copyright © 2003 Japan Concrete Institute.

Kanda, T. and Li, V. C. (1998). Multiple Cracking Sequence and Saturation in Fiber Reinforced Cementitious Composites. Concrete Research and Technology, JCI, Vol. 9, No. 2, 19-33.

Kaplan, M. F. (1961). Crack Propagation and the Fracture of Concrete. American Concrete Institute, Vol. 58, No. 11, 591-610.

Karahan, O., Hossain, K. M. A., Ozbay, E., Lachemi, M., Sancak, E. (2012). Effect of Metakaolin Content on the Properties Self-Consolidating Lightweight Concrete. Construction and Building Materials, 31(6), 320-325.

Kim, J. K., Kim, J. S., Ha, G. J. and Kim, Y. Y. (2007). Tensile and Fiber Dispersion Performance of ECC (Engineered Cementitious Composites) Produced With Ground Granulated Blast Furnace Slag. Cement and Concrete Research, 37 (7), 1096–1105.

Kim, Y.Y., Kim, J. S., Kim, H. S., Kim, J. K. and Ha, G. J. (2004a). Uniaxial Tensile Behavior of High Ductile Fiber Reinforced Mortar Designed with Ground Granulated Blast Furnace Slag. KSCE Conference, 1, 546-551.

Kim, Y. Y., Fischer, G. and Li, V. C. (2004b). Performance of Bridge Deck Link Slabs Designed with Ductile Engineered Cementitious Composite. American Concrete Institute Material Journal, Vol. 101, No. 6, 792-801.

Kim, Y. Y., Kong, H. J. and Li, V. C. (2003). Design of Engineered Cementitious Composite (ECC) suitable for wet-mix shotcreting. American Concrete Institute Materials Journal, Vol. 100, No.6, 511-518.

Kojima, S., Sakata, N., Kanda, T. and Hiraishi, T. (2004). Application of Direct Sprayed ECC for Retrofitting Dam Structure Surface -Application for Mitaka-Dam. Concrete Journal, 42(5), 135-139.

Kong, H. J., Bike, S. and Li, V. C. (2003a). Development of a Self-Consolidating Engineered Cementitious Composite Employing Electrosteric Dispersion/Stabilization. Journal of Cement and Concrete Composites, 25 (3), 301-309.

Kong, H. J., Bike, S. and Li, V. C. (2003b). Constitutive Rheological Control to Develop a Self-Consolidating Engineered Cementitious Composite Reinforce with Hydrophilic Poly (vinyl alcohol) Fibers. Journal of Cement and Concrete Composites, 25 (3), 333-341.

Kunieda, M. and Rokugo, K. (2006). Recent Progress on HPFRCC in Japan. Journal of Advanced Concrete Technology, 4**,** 19-33.

Lam, C., Lai, D., Au, J., Lim, L., Young, W. and Tharmabala, B. (2008). Development of Concrete Link Slabs to Eliminate Bridge Expansion Joints over Piers. Paper prepared for presentation at the Bridges - Links to a Sustainable Future (B) Session of the 2008 Annual Conference of the Transportation Association of Canada Toronto, Ontario, p, 20.

Lepech, M. and Li, V. C. (2007). Large Scale Processing of Engineered Cementitious Composites. Accepted for publication in American Concrete Institute Materials Journal. American Concrete Institute Materials Journal, 105(4), 358-366.

Lepech, M. and Li, V. C. (2005a). Water Permeability of Cracked Cementitious Composites. In: Proceeding of Eleventh International Conference on Fracture. Turin, Italy, CD-Paper 4539.

Lepech, M. and Li, V. C. (2005b). Durability and Long Term Performance of Engineered Cementitious Composites. In Proceedings of International RELIM Workshop on HPFRCC in Structural Applications, Honolulu, Hawaii, 165-174.

Lepech, M. D., Li, V.C., Robertson, R. E., and Keoleian, G. A. (2007b). Design of Ductile Engineered Cementitious Composites for Improved Sustainability. American Concrete Institute Material Journals, V. 105, No. 6, 567-575.

Li V.C. (1998). ECC Tailored Composites through Micromechanical Modeling. Fiber Reinforced Concrete: Present and the Future Edited by Banthia et al., CSCE. Montreal, 64-97.

Li, V. C. (2011). High-Ductility Concrete for Resilient Infrastructures. Journal of Advanced and High-Performance Materials. 16-21.

Li, V. C. (1997). Engineered Cementitious Composites Tailored Composites Through Micromechanical Modeling in Fiber Reinforced Concrete: Present and the Future, Banthia, N. A., Bentur, and Mufti, A. Editor. Canadian Society for Civil Engineering, 64-97.

Li, V. C. (2003). On Engineered Cementitious Composites (ECC) A Review of the Material and Its Applications. Journal of Advanced Concrete Technology, 1 (3), 215-230.

Li, V. C. and Yang, E. H. (2007). Self-Healing In Concrete Materials. In Self-Healing Materials: An Alternative Approach To 20 Centuries Of Materials Science. Van der Zwaag, S., Ed., 161–193., New York.

Li, V. C. and Lepech, M. (2004). Crack Resistant Concrete Material for Transportation Construction. In TRB 83rd Annual Meeting, Washington, D.C., Compendium of Papers CD ROM, 04-4680.

Li, V. C., and Kanda, T. (1998). Engineered Cementitious Composites for Structural Applications, ASCE Journal Materials in Civil Engineering, Vol. 10, No. 2, 66-69.

Li, V. C., Wu, C., Wang, S., Ogawa, A. and Saito, T. (2002) Interface Tailoring for Strain-Hardening PVA-ECC. American Concrete Institute Materials Journal. Vol. 99, No. 5, 463-472.

Li, V. C., Lepech, M., Wang, S., Weimann, M., and Keoleian, G. (2004). Development of Green ECC for Sustainable Infrastructure Systems. In Proceedings of the International Workshop on Sustainable Development and Concrete Technology, Beijing, China, Wang, K., Ed., 181–192.

Li, V. C., Mishra, D. K. and Wu, H. C. (1995). Matrix Design for Pseudo Strain-Hardening Fiber Reinforced Cementitious Composites. RILEM Journal of Materialsand Structures, 28, 586-595.

Li, V. C., Wang, S. and Wu, C. (2001). Tensile Strain-hardening Behavior of PVAECC. American Concrete Institute Materials Journal, Vol. 98, No. 6, 483-492.

Lin, Z. and Li, V. C. (1997). Crack Bridging in Fiber Reinforced Cementitious Composites with Slip-Hardening Interfaces. Journal of Mechanics and Physics of Solids, Vol. 45, No. 5, 763-787.

Lin, Z., Kanda, T. and Li, V. C. (1999). On Interface Property Characterization and Performance of Fiber Reinforced Cementitious Composites. Concrete Science and Engineering, RILEM, 1, 173-184.

Maalej, M., and V. C. Li. (1994). Flexural Strength of Fiber Cementitious Composites. ASCE Journal of Civil Engineering Materials, Vol. 6, No. 3, 390-406.

MacGregor, J. G., and Bartlett, F. M. (2000). Reinforced Concrete: Mechanisms and Design (Canadian Edition). Prentice-Hall Canada Inc., Toronto, Ontario, Canada.

Mangat, P. S., and Azari, M. M. (1986). Compression Creep Behavior of Steel Fiber Reinforced Cement Composites. Materiaux et Constructions, Vol. 19, No. 113, 361-370.

Maruta, M., Kanda, T., Nagai, S. and Yamamoto, Y. (2005). New High-Rise RC Structure Using Pre-Cast ECC Coupling Beam. Concrete Journal, 43**,** 18-26.

Matsumoto, T. (1998). Fracture Mechanics Approach to Fatigue Life of Discontinuous Fiber Reinforced Composites. PhD thesis, Dept. of Civil and Environmental Engineering, University of Michigan, Ann Arbor, Michigan, p, 274

Matsumoto, T., Suthiwarapirak, P., and Asamoto, S. (2002). Model development of ECC fatigue analysis. Proc., Japan Concrete Institute, JCI, Japan, Vol. 24, No.1, 237-242.

Matsumoto, T., Suthiwarapirak, P., Kanda, T. (2003). Mechanism of Multiple Cracking and Fracture of DFRCC under Fatigue Flexure. Journal of Advanced Concrete Technology, Vol. 1, No. 3, 299-306.

Mehta, P. K., and Monteiro, P. J. M. (2006). Concrete: Structure, Properties, and Materials, Third Edition, McGraw Hill, New York, p, 659.

Mehta, P. K. (1985). Influence of Fly ash Characteristics on The Strength of Portland-Fly ash Mixtures. Cement and Concrete Research, 15 (4), 669-674.

Mitamura, H., Sakata, N., Shakushiro, K., Suda, K. and Hiraishi, T. (2005). Application of Overlay Reinforcement Method on Steel Deck Utilizing Engineered Cementitious Composites – Mihara Bridge. Bridge and Foundation Engineering, Vol. 39, No. 8, 88-91.

Naik, T. R., Singh, S. S., and Ye, C. (1993). Fatigue Behavior of Plain Concrete Made With or Without Fly Ash. A Technical Report Submitted to (Electric Power Research Institute) EPRI, California, USA.

Nawy, E. G. (2008). Concrete Construction Engineering Handbook. Second Edition, Taylor & Francis Group, LLC, p, 1584.

Neville, A.M. (2002). Properties of Concrete. Fourth and Final Edition, John Wiley & Sons, New York, p, 884.

Ozaki, S., and Sugata, N. (1992). Fatigue of Concrete Composed of Blast Furnace Slag or Silica Fume Under Submerged Conditions", Proceedings of the Fourth International Conference, Istanbul, Turkey, Vol. II, American Concrete Institute Special Publication No. SP-132, 1509-1524.

Peled, A. and Shah, P. S. (2003). Processing Effect in Cementitious Composites: Extrusion and Casting, Journal of Materials In Civil Engineering. Vol. 15, No.2, 192-199.

Qian, S. and Li, V. C. (2008). Durable Pavement with ECC. First International Conference on Microstructure Related Durability of Cementitious Composites, Nanjing, China, Vol. 61, 535-543.

Ramakrishnan, V., Malhotra, V. M., and Longley, W. S. (1991). Comparative Evaluation of Flexural Fatigue Behavior of High Volume Fly Ash and Plain Concrete. Presented at the 70th Annual Meeting of the Transportation Research Board, Washington, D.C.

Rao, G. A., and Prasad, B. K. R. (2001). Fracture Energy and Softening Behavior of High-Strength Concrete. Cement and Concrete Research, 32 (2), 247-252.

Reinhardt, H. W. and Jooss, M. (2003). Permeability and Self-Healing of Cracked Concrete as a Function of Temperature and Crack Width. Cement and Concrete Research, 33 (7), 981-985.

Rokugo, K., Kunieda, M. and Lim, S. C. (2005). Patching repair with ECC on cracked concrete surface. Vancouver, Canada.

Rouse, J. M., and Billington, S. L. (2007). Creep and Shrinkage of High-Performance Fiber-Reinforced Cementitious Composites. American Concrete Institute Materials Journal, Vol. 104, No. 2, 129-136.

Ruskulis and Otto., (2005). Pozzolanas an Introduction, Practical Action/Technology Challenging Poverty, UK, p, 6.

Sahmaran, M., Lachemi, M., Hossain, K. M. A., Ranade, R., and Li, V.C. (2009). Influence of Aggregate Type and Size on the Ductility and Mechanical Properties of ECC, American Concrete Institute Materials Journal, Vol. 106, No.3, 308-316.

Sahmaran, M., Lachemi, M., Hossain, K. M. A., Ranade, R. and Li, V. C. (2010). Internal Curing of ECCs for Prevention of Early Age Autogenous Shrinkage Cracking, Cement Concrete Research, Vol. 39, No. 10, 893-901.

Sahmaran, M., Yaman, I., Tokyay, M. (2008). Transport and Mechanical Properties of Self-Consolidating Concrete with High Volume Fly Ash. Cement and Concrete Composites, Vol. 31, No. 2, 99-106.

Sahmaran, M., Li, V. C., and Li, M. (2007). Transport Properties of Engineered Cementitious Composites under Chloride Exposure. American Concrete Institute Materials Journal, Vol. 104, No. 6, 604-611.

Schutter, G. (2005). Guidelines for Testing Fresh Self-Compacting Concrete. University College London Civil, Environmental & Geomatic Engineering, p, 23.

Suthiwarapirak, P., Matsumoto, T., Kanda, T. (2004). Multiple Cracking and Fiber Bridging Characteristics of Engineered Cementitious Composites under Fatigue Flexure. Journal of Materials in Civil Engineering © ASCE, Vol. 16, No.5, 433-443.

Suthiwarapirak, P., Matsumoto, T., Kanda, T. (2002). Flexural Fatigue Failure Characteristics of an Engineered Cementitious Composite and Polymer Cement Mortars. JSCE, Tokyo, Vol. 718, No. 57, 121-134.

Termkhajornkit, P., Nawa, T., Nakai, M., Saito, T. (2005). Effect of fly Ash on Autogenous Shrinkage. Cement and Concrete Research, Vol. 35, No. 3, 473-482.

Tse, E.W., Lee, D. Y., and Klaiber, F. W. (1986). Fatigue Behavior of Concrete Containing Fly Ash. Proceedings of the Second International Conference on the Use of Fly Ash, Silica Fume, Slag and Natural Pozzolans in Concrete, Madrid, Spain, V.M. Malhotra, Vol. 1, American Concrete Institute Special Publication No. SP-9, 273-289.

Wang, S. and Li, V.C. (2007). Engineered Cementitious Composites With High Volume Fly Ash. American Concrete Institute Materials Journal, Vol. 104, No. 3, 233–241.

Wang, S. and Li, V.C. 2006. High Early Strength Engineered Cementitious Composites. American Concrete Institute Material Journal, Vol. 103, No. 2, 97–105.

Wang, S. and Li, V. C. 2003. Materials Design of Lightweight PVA-ECC. In Proceedings of the Fourth International RILEM Workshop on High-Performance Fiber-Reinforced Cement Composites (HPFRCC 4), Naaman, A. E. and Reinhardt, H. W., Eds., 379–390. RILEM, Paris.

Weimann, M.B.and Li, V. C. (2003). Hygral behavior of engineered cementitious composites (ECC). International Journal for Restoration of Buildings and Monuments, Vol. 9, No. 5, 513-534.

Wong, Y. L., Lam, L., Poon, C. S., Zhou, F. P. (1999). Properties of fly Ash-Modified Cement Mortar-Aggregate Interfaces. Cement and Concrete Research 29 (12), 1905–1913.

Wu, K.R., Chen, B., Yao, W., Zhang, D. (2000). Effect of Coarse Aggregate Type on Mechanical Properties of High-Performance Concrete. Cement and Concrete Research, 31 (10), 1421–1425.

Yang, E. and Li, V. C. (2006). A Micromechanical Model for Fiber Cement Optimization and Component Tailoring. In: Proceedings of 10th International Inorganic-Bonded Fiber Composites Conference, San Paulo, Brazil, CD-Paper K4.

Yang, E. H., Yang, Y. and Li, V. C. (2007). Use of High Volumes of Fly Ash to Improve ECC Mechanical Properties and Material Greenness. American Concrete Institute Materials Journal, Vol. 104, No. 6, 620-628.

Yang, Y., Lepech, M., and Li, V. C. (2005). Self-Healing of Engineered Cementitious Composites under Cyclic Wetting and Drying. In Proceedings of The International Workshop on The Durability of Reinforced Concrete under Combined Mechanical and Climatic Loads (CMCL), Qingdao, China, 231–242.

Zhang, J. and Li, V. C. (2002). Monotonic and Fatigue Performance In Bending of Fiber Reinforced Engineered Cementitious Composite In Overlay System. Cement and Concrete Research, 32, 415-423.

Zhang, J., and Stang, H. (1996). Fatigue Performance in Flexure of Fiber Reinforced Concrete. American Concrete Institute Material Journal, Vol. 95, No. 1, 58-67.

Zhou, J., Qian, S., Beltran, M. G. M., Ye, G., VanBreugel, K. and Li, V. C. (2009). Development of Engineered Cementitious Composites with Limestone Powder and Blast Furnance Slag. Rilem Journal of Materials and Structures, 43, 803-814.